

# Triggering Mechanisms in Control Systems Design

BY

Azhar Mehmood Memon

A Dissertation Presented to the  
DEANSHIP OF GRADUATE STUDIES

**KING FAHD UNIVERSITY OF PETROLEUM & MINERALS**

DHAHRAN, SAUDI ARABIA

In Partial Fulfillment of the  
Requirements for the Degree of

**DOCTOR OF PHILOSOPHY**

In

**SYSTEMS ENGINEERING**


December 2015

KING FAHD UNIVERSITY OF PETROLEUM & MINERALS  
DHAHRAN 31261, SAUDI ARABIA


DEANSHIP OF GRADUATE STUDIES

This thesis, written by **AZHAR MEHMOOD MEMON** under the direction of his thesis adviser and approved by his thesis committee, has been presented to and accepted by the Dean of Graduate Studies, in partial fulfillment of the requirements for the degree of **DOCTOR OF PHILOSOPHY IN SYSTEMS ENGINEERING**.

Dissertation Committee


  
Dr. Magdi S. Mahmoud (Adviser)


  
Dr. Fouad M. Al-Sunni (Member)

  
Dr. Mohammed Ali Y. Abido  
(Member)

  
Dr. Lahouari Cheded (Member)

  
Dr. Luai Al-Hadhrami (Member)

  
Dr. Hesham K. Al-Fares  
Department Chairman

  
Dr. Salam A. Zummo  
Dean of Graduate Studies



29/12/15  
Date

©Azhar Mehmood Memon  
2015

*To my wife...*

# ACKNOWLEDGMENTS

*In the name of ALLAH (SWT), the Entirely Merciful, the Especially Merciful. All praise and thanks belongs to ALLAH (SWT), the LORD of the entire existence.*

*It is HIM alone we worship and submit, and HIM alone we ask for help.*

*Peace and blessings be upon the beloved Prophet Muhammad (SAW), the mercy unto the worlds.*

*First of all, I would like to thank all the committee members, Dr. Magdi S. Mahmoud, Dr. Luai M. Al-Hadhrami, Dr. Fouad M. Al-Sunni, Dr. Mohammed Ali Y. Abido and Dr. Lahouari Cheded, for their time and valuable comments on my thesis. I would like to express special gratitude to my adviser Dr. Magdi and Dr. Luai. During my four years stay at KFUPM I enjoyed the mentoring of Dr. Magdi at every step during my course-work and research, and benefited from the advice of Dr. Luai who always facilitated me.*

*I also feel grateful to Dr. Moustafa Elshafei and Dr. Uthman Baroudi for their valuable advice and support. I owe thanks to my colleagues Dr. Muhammad Sabih and Mr. Nezar Al-Yazidi for their assistance and guidance through out my stay. It is a great pleasure to acknowledge the funding granted by DSR through project **RG-1316**, and I am thankful to KFUPM for providing me with both the*

*resources and an excellent research-conducive environment.*

*Lastly, I express deepest gratitude to my parents, because of whom I have reached to this point of success, and the whole family for their prayers – especially my wife.*

# TABLE OF CONTENTS

|   |             |
|---|-------------|
| <b>ACKNOWLEDGEMENTS</b>                       | <b>iii</b>  |
| <b>LIST OF TABLES</b>                         | <b>ix</b>   |
| <b>LIST OF FIGURES</b>                        | <b>x</b>    |
| <b>LIST OF ABBREVIATIONS</b>                  | <b>xiv</b>  |
| <b>ABSTRACT (ENGLISH)</b>                     | <b>xvii</b> |
| <b>ABSTRACT (ARABIC)</b>                      | <b>xix</b>  |
| <b>CHAPTER 1 INTRODUCTION</b>                 | <b>1</b>    |
| 1.1 Overview . . . . .                        | 1           |
| 1.2 Objectives . . . . .                      | 5           |
| 1.3 Contributions . . . . .                   | 5           |
| 1.4 Organization . . . . .                    | 6           |
| <b>CHAPTER 2 LITERATURE REVIEW</b>            | <b>7</b>    |
| 2.1 Preliminaries and Notations . . . . .     | 8           |
| 2.2 Event-Triggered Network Control . . . . . | 10          |
| 2.2.1 Stability . . . . .                     | 11          |
| 2.2.2 Scheduling and event design . . . . .   | 19          |
| 2.2.3 Co-design . . . . .                     | 20          |
| 2.2.4 State Feedback-based ETC . . . . .      | 29          |

|        |  |    |
|--------|--|----|
| 2.2.5  | Output Feedback-based ETC and Event-based estimation . . . . . | 33 |
| 2.2.6  | Periodic Event-Triggered Control (PETC) . . . . .              | 41 |
| 2.2.7  | Quantized Systems . . . . .                                    | 46 |
| 2.2.8  | ETC of Decentralized and Distributed systems . . . . .         | 49 |
| 2.2.9  | Adaptive Control . . . . .                                     | 59 |
| 2.2.10 | Model-based ETC . . . . .                                      | 60 |
| 2.2.11 | Event-based Model Predictive Control (MPC) . . . . .           | 61 |
| 2.2.12 | Event-based PID controller and actuator saturation . . . . .   | 63 |
| 2.2.13 | Miscellaneous Results . . . . .                                | 64 |
| 2.3    | Self-Triggered Network Control . . . . .                       | 66 |
| 2.3.1  | Stability . . . . .  | 66 |
| 2.3.2  | Self-triggered control of linear systems . . . . .             | 71 |
| 2.3.3  | Self-triggered control of nonlinear systems . . . . .          | 74 |
| 2.3.4  | Minimum attention and anytime attention control . . . . .      | 78 |
| 2.3.5  | Miscellaneous results . . . . .                                | 79 |
| 2.4    | Conclusion . . . . .   | 80 |

**CHAPTER 3 EVENT-BASED CONTROL OVER IEEE 802.15.4**

|                |   |     |
|----------------|---|-----|
| <b>NETWORK</b> | <b>86</b>                                     |     |
| 3.1            | Introduction . . . . .                        | 86  |
| 3.2            | Problem definition and overview . . . . .     | 91  |
| 3.3            | ET LQG controller . . . . .                   | 95  |
| 3.4            | Event condition . . . . .                     | 100 |
| 3.5            | IEEE 802.15.4 Network . . . . .               | 101 |
| 3.6            | Simulation results and discussion . . . . .   | 103 |
| 3.6.1          | Robustness against packet-dropouts: . . . . . | 106 |
| 3.7            | Conclusion . . . . .                          | 108 |

**CHAPTER 4 SELF-TRIGGERED (ST) CONTROL OVER IEEE**

|                         |                        |     |
|-------------------------|------------------------|-----|
| <b>802.15.4 NETWORK</b> | <b>110</b>             |     |
| 4.1                     | Introduction . . . . . | 110 |



|  |   |            |
|--|---|------------|
| 4.2  | Problem Definition and Overview . . . . .                 | 112        |
| 4.3  | First Level: Controller Module . . . . .                  | 114        |
| 4.3.1  | Asynchronous LQG controller . . . . .                     | 115        |
| 4.3.2  | ST Sampler . . . . .                                      | 121        |
| 4.4  | Second Level: Network Manager . . . . .                   | 127        |
| 4.4.1  | Superframe (SF) . . . . .                                 | 127        |
| 4.4.2  | Network Manager . . . . .                                 | 129        |
| 4.5  | Simulation Results and Discussion . . . . .               | 133        |
| 4.6  | Conclusion . . . . .                                      | 137        |
| <br>   |   |            |
| <b>CHAPTER 5 AN EVALUATION OF SELF-TRIGGERING</b>                                  |   |            |
| <b>METHODS</b>   |   | <b>139</b> |
| 5.1  | Introduction . . . . .                                    | 139        |
| 5.2  | Problem Definition . . . . .                              | 140        |
| 5.3  | ST Linear Quadratic Regulator [1] . . . . .               | 141        |
| 5.4  | Comparison . . . . .                                      | 144        |
| 5.4.1  | Controller design . . . . .                               | 145        |
| 5.4.2  | ST sampling . . . . .                                     | 145        |
| 5.4.3  | Computational requirements . . . . .                      | 146        |
| 5.4.4  | Case Studies . . . . .                                    | 146        |
| 5.5  | Conclusion . . . . .                                      | 152        |
| <br>   |   |            |
| <b>CHAPTER 6 <math>\mathcal{H}_\infty</math>-BASED SELF-TRIGGERED CONTROL OVER</b> |   |            |
| <b>IEEE 802.15.4 NETWORK</b>   |   | <b>154</b> |
| 6.1  | Introduction . . . . .                                    | 154        |
| 6.2  | Problem Definition and Overview . . . . .                 | 156        |
| 6.3  | Comparison . . . . .                                      | 158        |
| 6.3.1  | Simulation . . . . .                                      | 163        |
| 6.3.2  | Results . . . . .   | 164        |
| 6.4  | First Level: ST $\mathcal{H}_\infty$ controller . . . . . | 167        |
| 6.4.1  | Triggering time computation . . . . .                     | 182        |

|   |   |            |
|---|---|------------|
| 6.4.2                                       | System's Overall State Indicator (SOSI) . . . . . | 184        |
| 6.5   | Second Level: Network Manager . . . . .           | 186        |
| 6.5.1                                       | Superframe . . . . .                              | 186        |
| 6.5.2                                       | Network Manager . . . . .                         | 188        |
| 6.5.3                                       | Modified Protocol . . . . .                       | 190        |
| 6.6   | Simulation Results and Discussion . . . . .       | 196        |
| 6.7   | Conclusion . . . . .                              | 202        |
| <b>CHAPTER 7 CONCLUSION AND FUTURE WORK</b> |   | <b>203</b> |
| <b>REFERENCES</b>                           |   | <b>206</b> |
| <b>VITAE</b>                                |   | <b>228</b> |

# LIST OF TABLES

|     |   |     |
|-----|---|-----|
| 2.1 | List of papers which consider time-delays in aperiodically triggered NCSs. . . . .  | 85  |
| 3.1 | System parameters. . . . .  | 103 |
| 3.2 | Parameters of ZigBee protocol. . . . .  | 104 |
| 4.1 | Parameters for simulation. . . . .  | 133 |
| 5.1 | Parameters of the four-tank system. . . . .   | 149 |
| 6.1 | Parameters for simulation. . . . .  | 197 |
| 6.2 | Comparison of three implementations for simulation time of 30sec. The periodic scheme uses $BO = 4$ and $\tau = 0.192$ . Tx $j$ : number of transmissions from $j$ -th system; SF: number of superframes. . . . . | 201 |

# LIST OF FIGURES

|      |   |     |
|------|---|-----|
| 2.1  | Block diagram of event-triggered system. Solid lines denote continuous signal transmission and dotted lines show the event-based signals. . . . .                     | 10  |
| 2.2  | Timing diagram for an event-triggered implementation. . . . .   | 11  |
| 3.1  | Wireless networked control system with $N$ control loops. Solid line: wired connection; dashed line: wireless link. . . . .   | 92  |
| 3.2  | Timing diagram illustrating sampling times for ET systems with random transmission delays. . . . .  | 93  |
| 3.3  | Superframe structure of IEEE 802.15.4 protocol. . . . .   | 94  |
| 3.4  | State norms of System 1 (Top), System 2 (Middle), and System 3 (Bottom). . . . .  | 105 |
| 3.5  | Sampling times of System 1 (Top), 2 (Middle), and 3 (Bottom). . . . .   | 105 |
| 3.6  | Network usage of aperiodic (Top) and periodic (Bottom) implementation. Used slot: 1, free slot: 0. . . . .  | 106 |
| 3.7  | Estimation error $ x(t)  -  \hat{x}(t) $ of System 1 (Top), 2 (Middle), and 3 (Bottom). . . . .   | 106 |
| 3.8  | Error between state trajectories with and without packet-drop, $ x_{drop}(t)  -  x(t) $ of System 1 (Top), 2 (Middle), and 3 (Bottom). . . . .                        | 107 |
| 3.9  | Estimation error between state trajectories with and without packet-drop, $ \hat{x}_{drop}(t)  -  \hat{x}(t) $ of System 1 (Top), 2 (Middle), and 3 (Bottom). . . . . | 107 |
| 3.10 | Timing diagram illustrating packet-dropouts. . . . .  | 108 |

|     |  |     |
|-----|--|-----|
| 4.1 | Wireless networked control system with $N$ control loops. Solid line: wired connection; dashed line: wireless link. . . . .  | 113 |
| 4.2 | Timing diagram illustrating sampling ( $\delta$ ), reception ( $\rho$ ), and control application ( $\eta$ ) times with transmission and computation delays. . . . .  | 116 |
| 4.3 | ST sampler synthesis. . . . .  | 124 |
| 4.4 | Modified SF structure. The duration is denoted as $BI_{sf+1}$ . Active period includes a beacon packet and three slots for transmission; remaining time constitutes the inactive period. Each slot is of duration $\Delta_s$ . . . . . | 128 |
| 4.5 | Modified structure of the Network Manager. Solid line: wired connections; dotted line: wireless link. . . . .  | 129 |
| 4.6 | State norm, solid: $\ x_{ST}(t)\ $ , dashed: $\ x _{\alpha}(t)\ $ . Top: System 1, middle: System 2, bottom: System 3. . . . .   | 135 |
| 4.7 | Event times of systems 1 (first), 2 (second), and 3 (third). Length of beacon intervals (BIs) (fourth). . . . .  | 136 |
| 4.8 | Estimation error $\ x_{ST}(t)\  - \ \hat{x}_{ST}(t)\ $ . . . . .   | 137 |
| 5.1 | ST sampler synthesis for mass-spring system. . . . .   | 147 |
| 5.2 | State norm. . . . .  | 148 |
| 5.3 | Sampling times for mass-spring system. Top: [1]; bottom: novel ST scheme. . . . .  | 148 |
| 5.4 | (a) State norm. Top: [1]; bottom: novel ST scheme. (b) Inputs. Top: [1]; bottom: novel ST scheme. . . . .  | 150 |
| 5.5 | Sampling times for the four-tank system. Top: [1]; bottom: novel ST scheme. . . . .  | 151 |
| 5.6 | Top: sampling times; bottom: state norm. . . . .   | 152 |
| 6.1 | NCS with two-level control. Solid lines: wired connection; dashed lines: wireless link. . . . .  | 156 |
| 6.2 | Normalized state errors for event- and self-triggered control schemes for $w(t) = 0$ , $\delta = 1$ and $\epsilon = 0$ . . . . .   | 164 |

|      |   |     |
|------|---|-----|
| 6.3  | Normalized state errors for event- and self-triggered control schemes for $w(t)$ as given in (6.21), $\delta = 1$ and $\epsilon = 0$ . . . . .  | 165 |
| 6.4  | Sampling period versus time for event-triggered control scheme for $w(t) = 0$ , $\delta = 1$ and $\epsilon = 0$ . . . . .   | 165 |
| 6.5  | Sampling period versus time for self-triggered control scheme for $w(t) = 0$ , $\delta = 1$ and $\epsilon = 0$ . . . . .  | 166 |
| 6.6  | Sampling period versus time for event-triggered control scheme for $w(t)$ as given in (6.21), $\delta = 1$ and $\epsilon = 0$ . . . . .   | 167 |
| 6.7  | Sampling period versus time for self-triggered control scheme for $w(t)$ as given in (6.21), $\delta = 1$ and $\epsilon = 0$ . . . . .  | 167 |
| 6.8  | Timing diagram. Controller module performs two sets of computations; first set: $\Delta_{k,1}$ , second set: $\Delta_{k,2}$ . . . . .   | 168 |
| 6.9  | When the computed triggering time is less than the assigned one. . . . .  | 171 |
| 6.10 | Modified superframe structure. The duration is denoted as $BI_{i+1}$ . Active period includes a beacon packet and three slots for transmission; remaining time constitutes the inactive period. Each slot is of duration $\Delta_s$ . . . . . | 187 |
| 6.11 | Modified structure of the Network Manager. Solid line: wired connections; dotted line: wireless link. . . . .   | 188 |
| 6.12 | System states. Top: $\ x_{ST}(t)\ $ for Algorithm 2; bottom: $\ x_p(t)\  - \ x_{ST}(t)\ $ , where $x_p(t)$ denotes states for periodic implementation. . . . .  | 198 |
| 6.13 | ST events. Top: System 1, middle: System 2, bottom: System 3. . . . .   | 199 |
| 6.14 | Snapshot of transmissions, $N_{max} = 4$ . Top: beacon packets and transmissions for systems 1, 2, and 3 are scaled as 5, 1, 2, and 3, respectively; bottom: duty cycle of the scheduler. . . . .   | 199 |
| 6.15 | System states. Top: $\ x_{PBS,ST}(t)\ $ for Algorithm 3; bottom: $\ x_{PBS,ST}(t)\  - \ x_{ST}(t)\ $ , where $\ x_{PBS,ST}(t)\ $ denotes the states due to PBS algorithm. . . . .   | 200 |
| 6.16 | ST events. Top: System 1, middle: System 2, bottom: System 3. . . . .   | 200 |

6.17 Snapshot of transmissions,  $N_{max} = 2$ . Top: beacon packets and transmissions for systems 1, 2 and 3 are scaled as 5, 1, 2, and 3, respectively, bottom: duty cycle of the scheduler. . . . . 201

## LIST OF ABBREVIATIONS

The alphabetically ordered list of abbreviations used in the thesis is presented as follows:

ARE: Algebraic Riccati Equation

ASDS: Asynchronous Sampled-Data System

BI: Beacon Interval

CA: Controller-to-Actuator

CAP: Contention Access Period

CFP: Contention Free Period

CLF: Control Lyapunov Function

CPS: Cyber-Physical System

CT: Continuous Time

DOFC: Dynamic Output-Feedback Controller

DT: Discrete-Time

EBSE: Event-Based State Estimator

ET: Event-Triggered

GAS: Global Asymptotic Stability

GTS: Guaranteed Time Slot



IaP: Inactive Period

IFS: Inter-Frame Spacing

ISS: Input-to-State Stable

LMI: Linear Matrix Inequality

LQG: Linear Quadratic Gaussian

LQR: Linear Quadratic Regulator

LTI: Linear Time-Invariant

MPC: Model-Predictive Control

MSE: Mean Squared Error

N-MPC: Nonlinear Model Predictive Control

NCS: Networked Control System

NM: Network Manager

NN: Neural Network

NUM: Network Utility Maximization

PAN: Personal Area Network

PBS: Priority-Based Scheduling

PETC: Periodic Event-Triggered Control

PWL: Piecewise Linear

PWQ: Piecewise Quadratic

RPI: Robustly Positively Invariant

S-GAS: Semi-Global Asymptotic Stability

SC: Sensor-to-Controller

SF: Superframe

SOSI: System's Overall State Indicator

ST: Self-Triggered

U-ISS: Uniformly Input-to-State Stable

UB: Ultimate Boundedness

UUB: Uniform Ultimate Boundedness

WNCS: Wireless Networked Control System

WSAN: Wireless Sensor and Actuator Network

WSN: Wireless Sensor Network

ZOH: Zero-Order Hold

# THESIS ABSTRACT

**NAME:** Azhar Mehmood Memon  
**TITLE OF STUDY:** Triggering Mechanisms in Control Systems Design  
**MAJOR FIELD:** Systems Engineering  
**DATE OF DEGREE:** December 2015

*A networked control system (NCS) is a type of feedback control system where at least one of the sensor-controller or controller-actuator links is based on a communication network. The work presented in this thesis considers wireless NCS with multiple control loops sharing a common communication network based on IEEE 802.15.4 protocol to close the feedback loop. The main objective is to optimize the control cost, communication bandwidth, computational resources, and energy consumption without compromising the control performance.*

*In this spirit, a hierarchical framework is presented in the context of event- and self-triggered linear quadratic (ET/ST LQ) and ST  $\mathcal{H}_\infty$  controllers, and to enhance the energy efficiency in IEEE 802.15.4 protocol, some modifications are proposed. In addition to this, communication and computational delays are considered.*

*The results demonstrate satisfactory performance against the conventional periodic triggering scheme, and the ST LQ controller is shown to outperform the existing controller in the literature. In the context of ST  $\mathcal{H}_\infty$  controller, the scheme gives satisfactory control performance while being computationally efficient as compared with the results in the literature. In addition to this, due to the modifications introduced in the said protocol, significant battery power is saved.*



# CHAPTER 1

## INTRODUCTION

### 1.1 Overview

A networked control system (NCS) is a special type of regular feedback control system, whereby either sensor-controller or controller-actuator or both connections are completed using a communication network, instead of a traditional point-to-point link. The communication network can be wired or wireless depending upon the specific application. The necessity for this kind of setting arises mainly from the geographical distribution of various components of the control systems. Recently, the availability of low-cost wireless networked platforms with sensing and actuation capabilities has further encouraged the use of networked feedback loops and plant monitoring for industrial applications. The reason for this high demand can be attributed to the advantages of wireless networks over the traditional communication, such as the ease of maintenance and the provision of distributed control over large geographical areas.

However, the usage of communication network also poses certain challenges such as optimization of control, communication and computational costs, network imperfections, low bandwidth, decoupling control and communication designs, and energy economy at the wireless sensor nodes. Moreover, during the past few years, some practical issues of NCSs arising from the thrust towards cyber-physical systems (CPSs), have been highlighted [2]. Some of the crucial points are:

- Joint design of communication, control, and computation ( $C^3$ ) forms the basis of efficient CPSs.
- Modularity, which permits independent design of each module without affecting the logical correctness of the overall system.
- Opposing requirements of each module.

In order to meet these challenges and requirements, several strategies can be followed, such as designing controllers which are robust to network imperfections, installing high-bandwidth network, using intelligent techniques for balancing the communication load especially when the network is shared [3], or implementing aperiodic transmission schemes which sample the plant state only when required, unlike periodic scheme.

The standard implementations of feedback control over a network or an embedded platform use periodic triggering, whereby sensing and/or actuation is done at equidistant samples of time. Although it decouples communication from control and a mature systems theory exists which eases the design and implementation, it causes an enormous waste of energy and communication capabilities, especially

when there is no need for a corrective feedback signal. In contrast, the aperiodic transmission schemes (event- and self-triggered (ET and ST)), while saving considerable amount of energy and communication resources, introduce correlation between the states of participating control loops in networked control systems (NCSs), which complicates the interaction between control and communication. This correlation results from the opposing requirements of control performance and communication bandwidth economy, i.e., if high performance is required, one needs to sample the system more frequently, hence compromising on the bandwidth usage.

Both ET and ST schemes comprise two elements, a controller, and a triggering mechanism. This mechanism determines the next update time of the control law based on the previously sampled state information. Particularly, in ET [4, 5, 6], the sensor (or controller) node determines on the basis of a comparison between the present state and a threshold, if the information to the controller (or actuator) should be sent. As compared with the periodic setting, ET significantly reduces the amount of required communication. However, implementation of event-triggering mechanism on the sensor node increases the computational load due to continuous (or periodic) monitoring of the plant state. This is not well-suited for the battery powered wireless sensor nodes. Furthermore, ET requires a dedicated hardware to check the event condition. ST mechanism was introduced as a remedy to this problem [7]. This scheme does not require continuous checking of the state, rather it predicts update time on the basis of previously sampled



state and plant dynamics. Hence, ET mechanism is reactive and ST is proactive. The literature on aperiodic triggering mechanisms also contains hybrid triggering technique which combines the advantages of both ET and ST methodologies [8]. Specifically, the hybrid technique employs ST in normal operation, and an ET mechanism is only activated if the system encounters disturbance.

The low-rate wireless communication protocol IEEE 802.15.4, which forms the basis of industrial standards like WirelessHART and ISA100, has been the center of attention since its availability as the low data-rate and energy-efficient protocol [9]–[10]. With the use of aperiodic triggering schemes, the energy-efficiency of this protocol can be enhanced.

It can be concluded from above discussion that the economic and environmental constraints on wireless NCSs (WNCSs) necessitate efficient use of the available resources, i.e.,  $C^3$ , while incorporating the constraints of network artifacts, and low power consumption. Satisfying all of these requirements at the same time is a very difficult task, if not impossible. Hence, the designer must set appropriate priorities and trade-offs according to the performance requirement of the WNCS. Also, the proactive nature of ST scheme saves considerable amount of energy at the sensor node, which enhances energy economy in the applications based on IEEE 802.15.4 wireless protocol. Additionally, ST scheme can avoid contention and congestion in the network because of the transmission schedule being provided in advance.

## 1.2 Objectives

The objectives of this work are now presented:

1. ET optimal control of multiple LTI systems sharing common communication network based on the said protocol with computational and network-induced time delays.
2. ST optimal control of multiple LTI systems sharing common communication network based on the said protocol with computational and network-induced time delays.
3. ST  $\mathcal{H}_\infty$  control of multiple LTI systems sharing common communication network based on the said protocol.

## 1.3 Contributions

Following these objectives, our work has following main contributions:

- A novel ST LQR scheme which results in better performance, in terms of control cost economy, communication bandwidth saving and computational load reduction, as compared with the ST LQR presented in the literature [1],
- Modifications for IEEE 802.15.4 protocol which take maximum benefit from the predictive nature of the ST methodology, consequently saving significant amount of battery power of the wireless sensor nodes,

- Integration of priority-based scheduling algorithm in the modified protocol, to accommodate more systems as compared with the number of maximum number of allowed transmission slots,
- ST  $\mathcal{H}_\infty$  controller which ensures control performance in the presence of disturbance and a shared communication network.

## 1.4 Organization

Chapter 2 presents a comprehensive literature review on the subject of aperiodic triggering mechanisms for NCSs. Chapter 3 reports on the ET implementation and Chapter 4 presents its ST counterpart. The ST scheme is then compared with an existing ST LQR technique in Chapter 5 and three case studies are reported. The results of implementation of  $\mathcal{H}_\infty$  controller are presented in Chapter 6. Finally, Chapter 7 concludes the thesis and points out some potential research directions.

The notations used in each chapter are mentioned in the respective introduction. Furthermore, in the context of aperiodic state transmission, the terminology *co-design* is used for simultaneous design and/or optimization of control and event condition, however, in subsequent chapters the simultaneous optimization of both of these designs will be referred to as *co-optimization*.

## CHAPTER 2

# LITERATURE REVIEW

In this chapter, the reader will find a survey on the aperiodic triggering mechanisms in Networked Control Systems (NCSs), which can be classified into event- and self-triggered schemes. We have tried to cover most of the work done with an emphasis on the theoretical results. The motivating factors behind reporting a detailed survey were to provide us with a concrete base for the work presented in this thesis, and the need to organize the scattered results on the subject, which will facilitate the interested researchers to visualize open problems. The part of literature which discusses application of aperiodic triggering over IEEE 802.15.4 protocol is reported in the forthcoming chapters.

In the literature, ET scheme is referred to using various terminologies such as, event-based sampling, event-driven sampling, Lebesgue sampling, dead-band sampling, send-on-delta sampling, level-crossing sampling, and state-triggered sampling.

The chapter is organized as follows. Section 2.1 gives some mathematical pre-

liminaries and notations used in the chapter. The literature for ET methodology is presented in Section 2.2, while that for ST scheme is given in Section 2.3. The conclusion is presented in Section 2.4. For the reader's ease, possible future directions are given as remarks, the advantages and disadvantages are pointed out in the discussion at the end of each subsection, and the table given at the end of this chapter lists the works which consider time-delay.

## 2.1 Preliminaries and Notations

For this chapter, a continuous function  $\alpha : [0, a) \rightarrow [0, \infty)$  is said to belong to class  $\mathcal{K}$  if it is strictly increasing and  $\alpha(0) = 0$ . It belongs to class  $\mathcal{K}_\infty$ , if  $a = \infty$  and  $\alpha(r) \rightarrow \infty$  as  $r \rightarrow \infty$ . Similarly,  $\beta$  is of class  $\mathcal{L}$  if it is continuous and decreasing to zero. A function  $\zeta : [0, \infty) \rightarrow [0, \infty)$  is said to be of class  $\mathcal{G}$  if it is continuous and non-decreasing and  $\zeta(0) = 0$ . A continuous function  $\gamma : [0, a) \times [0, \infty) \rightarrow [0, \infty)$  is said to belong to class  $\mathcal{KL}$  if, for each fixed  $s$ , the mapping  $\gamma(r, s)$  belongs to class  $\mathcal{K}$  with respect to  $r$  and, for each fixed  $r$ , the mapping  $\gamma(r, s)$  is decreasing with respect to  $s$  and  $\gamma(r, s) \rightarrow 0$  as  $s \rightarrow \infty$ . Class  $\mathcal{KK}$  functions are defined in the same fashion.

Local stability is defined when the initial state of the system lies close to the equilibrium point. When it can lie anywhere in the state space then the stability is defined as global. A system is said to be uniformly stable if its stability is independent of the initial time  $t_0 \geq 0$ . A system is said to be stable if for each  $\epsilon > 0$ , there exists a  $\delta = \delta(\epsilon) > 0$  such that if  $\|x(t_0)\| < \delta$  then  $\|x(t)\| < \epsilon, \forall t \geq 0$ .

It is said to be asymptotically stable if it is stable and  $\delta$  can be chosen such that if  $\|x(t_0)\| < \delta$  then  $\lim_{t \rightarrow \infty} x(t) = 0$ . A system is said to be exponentially stable if there exists  $\sigma, \lambda \in \mathbb{R}^+$  such that  $\forall t \geq 0 \ \|x(t)\| \leq \sigma \|x(t_0)\| e^{-\lambda t}$ . The state of a system is said to be ultimately bounded if there exist constants  $\varepsilon, \rho \in \mathbb{R}^+$  ( $\varepsilon$  defined as the bound) and for every  $\eta \in (0, \rho)$  there is a constant  $T = T(\eta, \varepsilon) \in \mathbb{R}^+$  such that if  $\|x(t_0)\| < \eta$  then  $\|x(t)\| \leq \varepsilon, \forall t \geq t_0 + T$ . A system is said to be Input-to-State Stable (ISS) if there exist a class  $\mathcal{KL}$  function  $\gamma$  and a class  $\mathcal{K}$  function  $\alpha$  such that for any initial state  $x(t_0)$  and any bounded input  $u(t)$ , the state of the system satisfies  $\forall t \geq t_0 \geq 0$  the following inequality,

$$\|x(t)\| \leq \gamma(\|x(t_0)\|, t - t_0) + \alpha\left(\sup_{t_0 \leq \tau \leq t} \|u(\tau)\|\right)$$

Consider a system with input-output relation given as  $y = Hu$  for some mapping  $H$ . This mapping is said to be  $\mathcal{L}_p$  stable if there exist a class  $\mathcal{K}$  function  $\alpha$ , defined on  $[0, \infty)$  and a nonnegative constant  $\mu$  such that,

$$\|(Hu)_\tau\|_{\mathcal{L}_p} \leq \alpha(\|u_\tau\|_{\mathcal{L}_p}) + \mu, \quad \forall \tau \in [0, \infty).$$

It is finite-gain  $\mathcal{L}_p$  stable if there exist nonnegative constants  $\zeta$  and  $\mu$  such that,

$$\|(Hu)_\tau\|_{\mathcal{L}_p} \leq \zeta \|u_\tau\|_{\mathcal{L}_p} + \mu, \quad \forall \tau \in [0, \infty).$$

Here  $\mathcal{L}_p$  denotes the  $p$  norm where  $1 \leq p \leq \infty$ .

Expectation operator and conditional expectation are denoted as  $E[\cdot]$  and  $E[\cdot|\cdot]$ ,

respectively.

## 2.2 Event-Triggered Network Control

ET networked control (ETNC) or ET control (ETC) caught a great deal of attention by the end of last decade and plenty of work was done focusing on the development of systems theory. A classification of this large number of control methods was presented in [11] where an appropriate generic model was introduced.

The general structure of ETNC system for sensor-controller communication is shown in Fig. 2.1. It consists of the plant, an event detector, an observer, and a control signal generator. When an event occurs, the event detector sends the plant output to the observer. Here, an event refers to a situation whereby the output crosses a predefined threshold. The observer then computes state estimates and passes information to the control signal generator which generates the input signal for the process. The observer and control generator operate in open-loop between the events, therefore, the design of the generator is a central issue. In case all the states are available, full state vector is transmitted with the occurrence of an event [12]. Also, controller and actuator can be connected over the network.

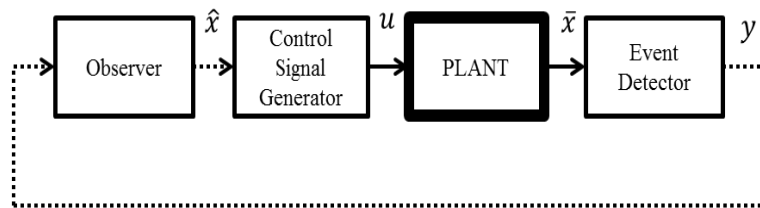


Figure 2.1: Block diagram of event-triggered system. Solid lines denote continuous signal transmission and dotted lines show the event-based signals.

Fig. 2.2 shows the timing relationships for an ET scheme. The black rectangles on the timeline indicate when the control task is being executed. The time  $T_j = r_{j+1} - r_j$  is called the task period and it is the interval between any two consecutive invocations of the control task.  $D_j$  is the delay in  $j$ th job and it is the time between finishing and release time, i.e.,  $D_j = f_j - r_j$ .

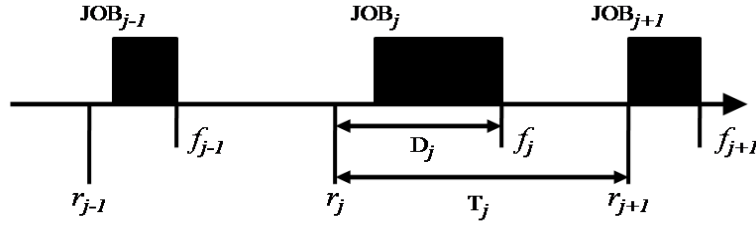


Figure 2.2: Timing diagram for an event-triggered implementation.

We now present the survey for ETNC.

### 2.2.1 Stability

Stability in terms of ultimate boundedness (UB) was studied in [13] for continuous-time (CT) linear systems with additive disturbances, on embedded systems. The authors provided the first step of a proper analysis of these kind of loops and focused on the trade-off between performance and computational load to show the obtainable ultimate bounds and how they depend on the parameters of the control strategy. By using these results, the event-driven controller can be tuned to get satisfactory transient behavior and desirable ultimate bounds, while reducing the required average processor load. The theory is based on inferring properties of the ETC system from discrete-time (DT) linear systems (in case of uniform sampling) or piecewise linear (PWL) systems (in case of nonuniform sampling).



The paper showed that even for a simple system, the complexity and challenge for analysis and synthesis is significant.

Before the stability results are given, we briefly define the concepts of uniform and non-uniform sampling in the context of ETC. Consider the LTI CT system given by,

$$\dot{x}(t) = A_c x(t) + B_c u(t) + E_c w(t), \quad (2.1)$$

where,  $x(t) \in \mathbb{R}^n$  is the state,  $u(t) \in \mathbb{R}^m$  is the control input and  $w(t) \in \mathcal{W}_c$  is the unknown disturbance. The set  $\mathcal{W}_c \subset \mathbb{R}^p$  is convex and compact and contains the origin. Let  $\mathcal{B}$  be an open bounded set containing the origin, such that the control value is not updated until the state  $x(t) \in \mathcal{B}$ . In uniform sampling, it is checked every  $T_s$  time unit, if the state lies in  $\mathcal{B}$ , i.e.,

$$\tau_{k+1} = \inf\{jT_s > \tau_k | j \in \mathbb{N}, x(jT_s) \notin \mathcal{B}\}, \quad (2.2)$$

where  $\tau_k, k \in \mathbb{N}$  are the control update times. Nonuniform sampling, which is hard to implement in practice, does not require constant checking, rather it updates control whenever state reaches the boundary of  $\mathcal{B}$ , i.e.,

$$\begin{aligned} \tau_1 &= \inf\{t \geq \tau_o | x(t) \notin \mathcal{B}\}, \quad \text{and} \\ \tau_{k+1} &= \inf\{t \geq \tau_k + T_s | x(t) \notin \mathcal{B}\}, \quad k > 0, \end{aligned} \quad (2.3)$$

where  $\tau_o = 0$  is the first control update time, irrespective of whether the initial

state lies in  $\mathcal{B}$  or not.

A discrete-time state feedback controller with gain  $F \in \mathbb{R}^{m \times n}$  is defined as

$$u_k = Fx_k, \quad (2.4)$$

where  $x_k = x(\tau_k)$  and  $u_k = u(\tau_k)$ . Using a zero-order hold (ZOH),  $u(t) = u_k$  for all  $t \in [\tau_k, \tau_{k+1})$ . Hence, the system is given by

$$\begin{aligned} \dot{x}(t) &= A_c x(t) + B_c u(t) + E_c w(t), \\ u(t) &= Fx(\tau_k), \quad \forall t \in [\tau_k, \tau_{k+1}). \end{aligned} \quad (2.5)$$

The control update times  $\tau_k$  are equally spaced in time for periodic triggering mechanism and depend on state dependent condition for aperiodic schemes.

In the stability analysis of ETC scheme, the discretized version of (2.1) and (2.4) for a fixed sampling time  $T_s$  is defined as,

$$x_{k+1}^d = (A + BF)x_k^d + w_k^d = A_{cl}x_k^d + w_k^d, \quad (2.6)$$

with

$$\begin{aligned} A &:= e^{A_c T_s}, \\ B &:= \int_0^{T_s} e^{A_c \theta} d\theta B_c, \\ w_k^d &:= \int_{\tau_k}^{\tau_{k+1}} e^{A_c(\tau_{k+1}-\theta)} E_c w(\theta) d\theta. \end{aligned}$$

Moreover, for both uniform and nonuniform cases, system (2.5) behaves as (2.6) away from set  $\mathcal{B}$ .

The theorem given below, states UB for nonuniform sampling case.

**Theorem 2.1** *For Nonuniform sampling:*

Consider system (2.5) and (2.3) with  $\mathcal{W}_c$  a closed and convex set containing the origin. Let  $\mathcal{W}_d$  be given as

$$\mathcal{W}_d := \left\{ \int_0^{T_s} e^{A_c(T_s-\theta)} E_c w(\theta) d\theta \mid w \in \mathcal{L}_1^{loc}([0, T_s] \rightarrow \mathcal{W}_c) \right\}$$

1. If  $\Omega$  is a robustly-positively invariant (RPI) set for the linear discrete-time system (2.6) with disturbances in  $\mathcal{W}_d$  and  $cl\mathcal{B} \subseteq \Omega$ , then  $\Omega$  is RPI set for the event-driven system (2.5) and (2.3) on the control update times for disturbances  $\mathcal{W}_c$ .
2. If system (2.6) with disturbances in  $\mathcal{W}_d$  is UB to the RPI set  $\Omega$  and  $cl\mathcal{B} \subseteq \Omega$ , then event-driven system (2.5) and (2.3) is UB to  $\Omega$  for the disturbances in  $\mathcal{W}_c$  on control update times.

For uniform sampling, the ETC is termed as periodic event-triggered control (PETC) ([14]) and the reader is referred to Section 2.2.6 for the stability theorem.

Two conjoint methods to guarantee UB of the ETC system were proposed by [15]. First method, the global approach aims at bringing the system from any initial state to a target set in the state space, and second, the local approach, keeps the system state within the target set. The methods were experimentally validated on a thermofluid process.

By modeling ETC of nonlinear systems as hybrid systems, [16] provided

Lyapunov-based conditions to guarantee semi-global asymptotic stability (S-GAS) of the closed-loop system and explained how they can be utilized to synthesize ET rules. Specifically, the fact that monotonic decrease of Lyapunov function is not necessary to guarantee stability, was used to develop a family of triggering rules which gives larger inter-event times at the expense of some performance degradation.

*Remark 1 The authors assumed no transport delay in communication from sensor to controller and from controller to actuator, and left the study of the effects of the eventual induced delays for future work.*

Asymptotic stabilization of linear systems with time-varying transmission delays was investigated by [17]. The sensor, controller and event-detector were considered to be collocated at a node. This allowed the event-generation to be control-error dependent rather than state-error, as was the case in [18]. The authors provided the criteria to design feedback gain and the ET mechanism which were driven to guarantee stability and performance.

*Remark 2 The authors indicated discrete detection methodology (supervision of the event condition at discrete sampling instants), and joint design of event-detector parameter and the controller gain, as future works.*

The problems of exponential stability,  $\mathcal{L}_2$ -gain analysis and  $\mathcal{L}_2$ -gain based controller design, along with network-induced delays and parameter uncertainties were studied in [19], using a unified model of NCSs with hybrid ET schemes.

Sufficient conditions for exponential stability and  $\mathcal{L}_2$ -gain analysis were developed in the form of LMIs by using a discontinuous Lyapunov-Krasovskii functional approach. Moreover, two novel ET conditions were proposed: first on the sensor side, where an event-detector is placed between sensor and controller, which periodically (instead of continuously) checks the state to trigger an event, and second on the controller side, which decides when to send the control signal to the actuator.

*Remark 3 The following topics deserve further investigation:*

1. *To take into account the random communication delays and data packet dropouts and/or quantization, stochastic systems, and fault-tolerant control of NCSs with the proposed ET scheme,*
2.  *$\mathcal{H}_\infty$  controller analysis and synthesis for DT NCSs can be studied in the proposed framework, and*
3. *Extension to  $\mathcal{H}_\infty$  filtering.*

A universal formula for event-based stabilization of general nonlinear systems affine in control, was proposed by [20]. It was proved that an event-based static feedback, smooth everywhere except at the origin, can be designed to ensure GAS of the origin. Also, for any initial condition within any given closed set, the minimal inter-sampling time is bounded from below, avoiding infinitely fast sampling phenomena, called Zeno behavior (occurrence of infinitely fast sampling).

A framework to analyze stability and stabilization of ETC was proposed by [21], along with the tradeoff between communication and the desired performance. Lyapunov–Krasovskii functional approach was used for this purpose and sufficient criteria were obtained in terms of LMIs. The main feature of the scheme is that the released sampled data is not only determined by the current state and the error between the current and the latest transmitted state, but also by the current state of the network dynamics. Moreover, an information-dispatching middleware was constructed which implemented a novel ET scheme.

The exponential practical stabilization of event-driven LTI systems with bounded disturbances and bit-rates is considered in [22]. The authors also consider the practical limitations of real-time NCSs namely, quantization and encoding. It was pointed out that the characterization of necessary or sufficient conditions on the average bit-rates is necessary to measure the performance improvement of ET systems over the periodic ones. Specifically, a necessary condition on the required average bit-rate was identified for the exponential convergence of state trajectories with prescribed rate of convergence. Also, controller design was presented which guarantees exponential convergence and performance, by adjusting the communication rate in accordance with the state information. The presented approach guarantees bounded bit-rates.

*Remark 4 The following topics deserve further investigations:*

1. *Characterization of data rates under disturbances,*
2. *Suppression of the synchronization requirement between encoder and decoder*

*to maintain a synchronized quantization domain,*

*3. Extension of the results to stochastic time-varying communication channels,*

*and*

*4. Understanding of the trade-offs between system performance and timeliness*

*and size of transmissions.*

## **Discussion**

For S-GAS, the approach in [16] is general because it encompasses several existing ET policies and new strategies which further reduce the resources needed for control of nonlinear systems. In contrast, the authors in [17] provided GAS guarantee, but for linear systems only. Moreover, two limitations of this scheme are,

1. Requirement of a delicate hardware for the event detector to monitor control signal and test the condition continuously, and
2. The parameter of event detector was chosen with an assumption that the controller guarantees GAS without considering transmission delays.

The results of [20] for GAS of a class of nonlinear systems are based on the assumption of existence of a smooth control Lyapunov function (CLF). However, this assumption may limit the applicability of the results to a number of scenarios.

For exponential stability, the methodology used in [19] can be extended to the case of parameter uncertainties. The approach presented in [22] considered

exponential stability from an information-theoretic perspective, in contrast to ISS point of view.

The methodology of [21] considered network dynamics along with the control performance. In addition, the middleware allowed masking of the complex details of communication network, and easing the control design.

### **2.2.2 Scheduling and event design**

The idea of “control under communication constraints” was applied to the problem of scheduling stabilizing control tasks on embedded processors by [18]. In the context of real-time scheduling, CPU’s load is reduced by reducing the number of control tasks being executed, which depends on the state dependent feedback mechanism. The real-time scheduler could be regarded as a feedback controller, which decides on the task execution priority at a given instant, while guaranteeing S-GAS of the plant by control related tasks, and on-time execution of control unrelated tasks. Investigation of a simple event-based scheduler showed that the performance and lower bounds on the task release times are guaranteed.

An ET scheme was presented in [23] which ensures exponential stability of the closed-loop system, and exploits the fact that the monotonic decrease of storage function is not necessary for stability of switched systems. An exponential function is properly chosen; during the operation, when the storage function intersects with the chosen exponential function, the state is sampled. The inter-sampling periods were reported to be large as compared with the previous works. The ISS



guarantee of CT system with respect to the measurement errors ensures that the inter-sampling periods and deadlines are bounded strictly away from zero.

A novel choice of the event function that only requires the computation of control and is independent of Lyapunov function, to ensure stability and non-zero inter-execution time for control-affine nonlinear systems was proposed in [24]. Furthermore, the strategy was used to stabilize an inverted pendulum by [25] which experimentally demonstrated a reduction of about 50% in the number of samples as compared with the periodic scheme.

### **Discussion**

The event-design schemes in [18] and [23] were presented in the context of embedded-systems. The framework given by [18] is applicable to both linear and nonlinear systems with conservative results for the later, while the methodology of [23] was presented for nonlinear systems. The problems with ETC of nonlinear systems are the heavy computational demand of event function as compared with the control computation, and the use of Lyapunov function which is not necessarily available. For a class of nonlinear systems, [24] gave solution to both problems. However, the control-based event functions did not consider delays.

### **2.2.3 Co-design**

Simultaneous design of control and communication is referred to as co-design in the context of NCSs. There are two methodologies in the literature to achieve co-design of ETNC: Lyapunov approach ([26, 27]), and cost function minimization

which penalizes the inter-event times besides state and control variable ([28]–[29]). Also, [30] discusses Lyapunov based co-design with state and input signal quantization and is mentioned in Section 2.2.7.

ET  $\mathcal{H}_\infty$  control for the NCSs with uncertainties and transmission delays was considered in [26]. A delay system model was used which modeled delays and the event-driven system. Then, based on the model and Lyapunov functional method, and by using LMIs, the criteria for stability with an  $\mathcal{H}_\infty$  norm bound and co-design, was given.

The scheme proposed in [27] maintains the desired  $\mathcal{H}_\infty$  performance against disturbances, and takes into account the delays and packet loss. The main novelty was that the algorithm gives a *one-step* approach to co-design, as opposed to the previous methodologies which first design the controller with perfect signal transmission assumption, and then consider ET scheme.

Event-driven strategy, implementing one-step finite horizon boundary while considering network induced delays, was considered by [28]. At each task execution the appropriated controller gain, and the next task execution time are computed in order to achieve co-design. The computation of both parameters is constrained by the periodic LQR control cost under same network utilization. Simulation results showed better control performance than periodic scheme and robustness against time delays.

*Remark 5 Possible extension of the scheme is to investigate the optimization of a finite-horizon cost function for more than one step.*

A theoretical framework to analyze the trade-off between control performance and communication cost for transmission over a lossy network was presented in [31], where a controller-actuator network was considered. A multi-dimensional Markov chain model was used to represent packet retransmissions in case of packet loss. By combining this communication model with an analytical model of the closed-loop performance, a systematic way was provided to analyze the trade-off by appropriately selecting an event-threshold.

Co-design problem in a linear stochastic CT setting was considered in [32] by formulating the problem as the minimization of cost function which also penalizes the transmissions between sensor and controller,

$$J = \mathbb{E} \left[ \int_0^T x_t' Q x_t + u_t' R u_t dt + x_T' Q_T x_T + \lambda k_T \right], \quad (2.7)$$

where  $Q$ ,  $Q_T$  and  $R$  are standard matrices defined for optimal control problems, and the weighting factor  $\lambda > 0$  penalizes  $\mathbb{E}[k_T]$  which is the average number of transmissions in a finite interval of time  $[0, T]$ . The key innovation of this paper was to show that the underlying optimization problem is similar to two sub-problems, LQG regulator and optimal stopping time problems, hence enabling the use of standard techniques for optimal stochastic control to yield optimal ET policy. The optimization problem was reformulated in a way such that the separation principle is still valid. Numerical examples showed the effectiveness of the proposed scheme as compared to optimal time-triggered controllers.

*Remark 6 Following topics deserve further investigations:*

1. *The case of infinite horizon with discounted cost, and*
2. *Extension to partial observations at the sensor-side, non-ideal communications and multi-terminal settings.*

Now we present the results of [32] briefly. Consider the system given by,

$$dx_t = Ax_t dt + Bu_t + dw_t, \quad (2.8)$$

where  $A \in \mathbb{R}^{n \times n}$ ,  $B \in \mathbb{R}^{n \times d}$ . The initial state  $x_0$  is given a priori at scheduler and controller. The vector-valued Brownian motion process in  $\mathbb{R}^n$  with zero mean and normalized variance is represented by  $w_t$ . Let  $k$  be the counting process with  $k_0 = 0$ , the value of which is incremented by one with every state transmission. The goal is to find the control policy  $u_t$ , and counting process  $k$  that minimize (2.7). The structure of optimal time-variant control law is given by,

$$u_t = \gamma^*(x_{\tau_k}, \tau_k, t) = -L_t \mathbb{E}[x_t | \mathcal{I}_t], \quad \tau_k \leq t < \tau_{k+1}, \quad (2.9)$$

where  $\mathbb{E}[x_t | \mathcal{I}_t]$  denotes the expected value of the state given  $\mathcal{I}_t = \{x_{\tau_k}, \tau_k\}$ , the available information at the controller at time  $t$ .  $\tau_k$  represent the stopping or transmission times and  $\tau_0 = 0$ . If  $\tau_k$  is not defined, its upper bound is replaced by  $T$ , i.e., the time horizon.  $L_t$  is defined as,

$$\begin{aligned} L_t &= -R^{-1} B^T S_t, \\ -\frac{dS_t}{dt} &= A^T S_t + S_t A + Q - S_t B R^{-1} B^T S_t, \quad t \in [0, T], \end{aligned} \quad (2.10)$$

with initial condition  $S_T = Q_T$ . The estimation error is given as  $\Delta_t = x_t - \mathbb{E}[x_t|\mathcal{I}_t]$  and at  $\tau_k$  this error is zero, i.e.,  $\Delta_{\tau_k} = 0$ . The complete design procedure is summarized in the following theorem.

**Theorem 2.2** *The optimal ET controller minimizing (2.7) is given by,*

1. control policy (2.9) with  $L_T$  defined in (2.10),
2. estimator,

$$\mathbb{E}[x_t|\mathcal{I}_t] = e^{(A-BL_t)(t-\tau_k)}x_{\tau_k}, \text{ and} \quad (2.11)$$

3. scheduling policy  $k^*$  which minimizes,

$$J^E(k) = \min_k \mathbb{E} \left[ \int_0^T \Delta_t^T L_t^T R L_t \Delta_t + \lambda k_T \right], \quad (2.12)$$

where  $\Delta_t$  is a jump-diffusion process given as,

$$\begin{aligned} d\Delta_t &= A\Delta_t dt + dw_t, \\ \Delta_{\tau_k} &= 0, \end{aligned} \quad (2.13)$$

with initial condition  $\Delta_0 = 0$ .

The work presented in [32] was extended by [33] for the systems with large number of states. A novel approximation method was thus developed, whereby the number of state variables of the process was reduced to the number of control

inputs, as the processes often consist of only few inputs compared with the number of state variables. It was shown that the proposed approximate ET preserves the asymptotic behavior of the closed-loop system, while reducing the computational complexity significantly. Moreover, a condition for the reduced ET law and the optimal solution to be equal, was given and a measure to evaluate the approximation accuracy was proposed, which reflects the performance decrease very accurately. Numerical simulations showed the effectiveness of the proposed model reduction method compared to the optimal solution.

*Remark 7 Following topics can be considered for further research:*

1. *To study advanced order reduction schemes that increase the approximation accuracy,*
2. *Consideration of real-time network imperfections, and*
3. *To Investigate the bounds on performance decrease of the approximate scheme.*

The co-design problem for multiple control systems closed over a common network was considered by [34]. Individual subsystems were modeled as DT stochastic linear systems with a quadratic control cost. The adaptation ability of event-based systems was exploited to develop a distributed algorithm, whereby each subsystem adjusts its ET mechanism to optimally meet the global communication network constraint, which was given by limiting the total average transmission rate of all subsystems. Numerical examples showed the effectiveness of the

algorithm.

*Remark 8 A few topics which deserve further investigations are:*

- 1. Convergence analysis of the overall adaptive system based on stochastic approximation, and*
- 2. Consideration of hard communication constraints rather than an average rate constraint with a limited number of transmission slots.*

The certainty equivalence controller was reported to be optimal for an ET control system with resource constraints in [35]. The system model was an extension of the stochastic linear quadratic system framework. Three different types of resource constraints were considered: first one penalized every controller update with additional cost, second considered a limitation on the number of resource acquisitions, and third imposed a constraint on the average number of resource acquisitions. The obtained result is also valid in the presence of noisy measurements and for communication with delays and dropouts if an instantaneous error-free acknowledgment channel exists.

Two suboptimal design strategies for ETC of linear DT stochastic systems in the presence of time-delays and packet-dropouts were presented in [29]. These strategies were based on certain design assumptions which made the separate design of controller and ET possible; due to these assumptions the strategies were regarded as suboptimal. Drift criteria, which is used to analyze asymptotic properties of Markov chains, was used for closed-loop stability analysis, which

showed that sufficient conditions exist to guarantee bounded moment stability for both design strategies.

*Remark 9 To analyze these algorithms for multiple control loops sharing a common communication network, where time-delays are varying and packet-dropouts have complex statistical models, can be considered for future research.*

To decouple communication from control, [36] limited the usage of communication channel in terms of maximum allowable transmission rate, which depended upon the maximum number of transmission slots offered by the channel. The authors used the solution of stochastic optimal control problem in order to determine the optimal transmission rate for each system while optimizing the control cost.

*Remark 10 Some avenues for further exploration are:*

- 1. To prove the chaoticity in equilibrium assumption for the underlying system,*
- 2. Realization of the centralized schedulers without gathering the state information of all heterogeneous multidimensional subsystems,*
- 3. Investigation on the online adjustment of the event-trigger according to the network traffic that also leads to a decentralization of the global resource allocation problem, and*
- 4. Studying more complicated models for the communication network.*



## Discussion

The proposed schemes in [26] and [27] use robust control with the former being superior in terms of average release times compared with some other ET schemes in the literature, and later giving *one-step* approach for co-design. The co-design scheme given in [28] is robust against time-delays.

The curse of dimensionality problem in dynamic programming framework for ETC was addressed in [33] by presenting the model order reduction methodology. In [35] it was indicated that the results cannot be extended to the case of ZOH control waveforms. In [29] numerical simulations indicated that the suboptimal procedures outperform time-triggered control systems, while marginally deviating from a lower bound on the system performance.

Decoupling of control from communication is a major issue in co-design methodology which was addressed by [36]. The framework thus provided determines the Pareto frontier for each subsystem offline, without the consideration of communication network parameters. Also, due to the consideration of a slotted protocol the approach can also be applied over a real-time slotted communication network. However, the authors did not consider rejection of the packets by the network controller, containing state information. As the methodology considered multiple control systems, [36] is also discussed in the context of ET-based decentralized systems in Section 2.2.8.

Pareto optimality is a concept defined in welfare economics, which is a state of allocation of available resources among individuals whereby it is impossible to

make any one individual better off without making at least one individual worse off. Pareto frontier is the set of allocations that are all Pareto optimal. In the context of co-design of control and communication strategy, the individuals are control cost and sampling-interval and the objective is to improve either control performance or communication bandwidth usage.

### 2.2.4 State Feedback-based ETC

A review of recent progress in utilization of ET scheme for state-feedback control was given in [37]. A state-feedback ETC scheme for which the performance of the closed-loop system approximates the behavior of a continuous state-feedback system with a focus on robustness against disturbance was proposed by [38]. The event based control policy was designed in such a way that the state of the closed-loop system remains in a bounded set around the state of the corresponding continuous time system. The extent of this bounded set, called the *approximation precision*, can be varied by changing the threshold of the event generator. Moreover, between two consecutive event times the unknown disturbance is estimated and a new event is only generated if the effect of the estimation error exceeds a given sensitivity bound. Hence, if the disturbance is small enough, no further event is generated.

This work was extended by [39] for situations in which the communication network induces time-delay in the control loop. It was shown that for bounded delays and appropriate pre-processing of the delayed information, the event-based

control loop is stable such that its state remains in a bounded set around the state of CT state-feedback loop without delays. Moreover, conditions were given which can be used to determine the maximum delay for which a stable behavior of the event-based control loop is guaranteed.

The main result of [39] is given in the following. The LTI plant is given as,

$$\dot{x}(t) = Ax(t) + Bu(t) + Ed(t), \quad x(0) = x_0, \quad (2.14)$$

where the state  $x \in \mathbb{R}^n$  and the time  $t$  are assumed to be measurable,  $u(t) \in \mathbb{R}^m$  denotes the input and disturbance  $d(t) \in \mathbb{R}^l$  is bounded according to  $\|d(t)\| \leq d_{max}$ . The bounded communication delay is represented by  $\tau_k \leq \bar{\tau} \in \mathbb{R}_+$ , which is assumed to be less than the interval between two consecutive events. The CT closed-loop reference system is given as,

$$\dot{x}_{CT}(t) = \bar{A}x_{CT}(t) + Ed(t), \quad x_{CT}(0) = x_0, \quad (2.15)$$

with  $\bar{A} = A - BK$ , where the controller  $K$  is assumed to stabilize the plant. The event-generator consists of a copy of the model (2.15), which it executes between two consecutive events,

$$\dot{x}_e(t) = \bar{A}x_e(t), \quad x_e(t_k^+) = x_k, \quad t_k \leq t < t_{k+1}, \quad (2.16)$$

where  $x_e(t)$  represents the state of the event generator. The instant  $t_k^+$  represents the time after update of the model state  $x_e$  with the measured state  $x_k$ .

An event is generated when the difference between the states of plant event generator reaches a threshold, i.e.,

$$\|x(t_k) - x_e(t_k^-)\| = \bar{e}, \quad (2.17)$$

where  $x_e(t_k^-)$  and  $t_k^-$  denote the state and instant before the update of the model, respectively.

Similar to the event-generator, the control input generator also uses a copy of (2.15) to compute the control input in the time interval  $t \in [t_k + \tau_k, t_{k+1} + \tau_{k+1})$ ,

$$\begin{aligned} \dot{x}_s(t) &= \bar{A}x_s(t), \quad x_s(t_k + \tau_k^+) = x_{sk}^+, \\ u(t) &= -Kx_s(t), \end{aligned} \quad (2.18)$$

where,  $x_s(t)$  denotes the state of the control input generator. The control generator has  $x_k$  and  $\tau_k$  at the time  $t_k + \tau_k$ , which implies that the relation  $x_s(t) = x_e(t)$  holds for  $t_k + \tau_k \leq t < t_{k+1}$ , if  $x_{sk}^+$  is taken as,

$$x_{sk}^+ = e^{\bar{A}\tau_k} x_k. \quad (2.19)$$

Let  $x_\Delta(t) = x(t) - x_s(t)$  be the difference state, then

$$\|x_\Delta(t)\| \leq x_{\Delta_{max}} = \bar{c}\bar{e} + \bar{d}_{xd}d_{max}, \quad t \geq 0, \quad (2.20)$$

with

$$\bar{c} = \min_{\tau \in [0, \bar{\tau}]} \|e^{A\tau}\|; \quad \bar{d}_{xd} = \int_0^{\bar{\tau}} \|e^{A\alpha} E\| d\alpha.$$

The following theorem gives the main result,

**Theorem 2.3** *Consider the event-based control system given by, (2.14), (2.16), (2.17) and (2.18) with communication delay and state update given by (2.19). Assume that the maximum time delay due to the communication network is upper-bounded by  $\bar{\tau} \leq \tau^*$ , where  $\tau^*$  is given by,*

$$\begin{aligned} \tau^* &= \arg \min_{\tau \in [0, \bar{\tau}]} \left\{ \frac{\int_0^{\tau} \|e^{A\alpha} E\| d\alpha \cdot d_{max}}{1 - \|e^{A\tau} - e^{\bar{A}\tau}\|} = \bar{c} \right\}, \\ \tilde{\tau} &= \arg \min_{\tau \geq 0} \{ \|e^{A\tau} - e^{\bar{A}\tau}\| = 1 \}. \end{aligned} \quad (2.21)$$

Then the difference  $e(t) = x(t) - x_{CT}(t)$  is upper bounded by,

$$\|e(t)\| \leq e_{maxd}, \quad (2.22)$$

with

$$e_{maxd} = x_{\Delta_{max}} \cdot \int_0^{\infty} \|e^{\bar{A}\alpha} BK\| d\alpha, \quad (2.23)$$

where  $x_{\Delta_{max}}$  is defined in (2.20).

Another extension of [38] was reported in [40] which improves the behavior of event-based control loop with respect to reference tracking and disturbance attenuation. It was shown that for a plant affected by a bounded, constant or

time-varying disturbance, the scheme guarantees set-point tracking or holds the output in a bounded region around a prescribed reference signal, respectively. The experimental results demonstrated a considerable reduction in communication.

## **Discussion**

The limiting assumptions of [38] are consideration of stable plant without uncertainties, delay-free communication channel, and no restriction on the computational complexity. Although [39] addressed and solved the issue of delayed information, and [40] considered reference tracking and disturbance attenuation, the overall approach is still not able to completely compensate for model uncertainties.

### **2.2.5 Output Feedback-based ETC and Event-based estimation**

In many control systems all states of the plant are not available for measurement which motivates the study of ET systems with output feedback, and event-based estimation. In former, the plant output is either used to estimate the state on sensor side and then this estimate is transmitted to the controller, or the output is transmitted directly to the controller. In event-based estimation, sensor transmits the output to a *remote-observer* based on the occurrence of an event.

#### **Output feedback control**

First result presenting dynamical output based ET control is due to [41]. However, an exhaustive analysis of the minimum inter-event time was not provided, which

was addressed by [42], besides studying stability and  $\mathcal{L}_\infty$  performance. Minimum inter-event time is guaranteed by choosing a triggering mechanism that depends on the difference between the output of plant or controller, and its previously-sampled value plus a threshold. Furthermore, by modeling the ET system as impulsive system, closed-loop stability is guaranteed in terms of LMIs with larger minimum inter-event times than the existing results. The authors extended the same work for decentralized setting in [43] (see Section 2.2.8).

A computationally-tractable approach for determining suboptimal event-triggers in finite-horizon output-feedback problem for *multidimensional* DT linear systems, was presented in [44]. The proposed approximate solution, which uses families of quadratic forms to characterize the value functions in the optimal dynamic program, has a computational complexity that is polynomial in state-space dimension and horizon length. The numerical example showed that the proposed sub-optimal triggering sets perform similar to the optimal ones.

The results for state feedback based ETC reported in [38] were extended to output feedback control in [45] by including a Luenberger observer in the event generator which *continuously* estimates the state. As opposed to [41] and [42], all the states are transmitted instead of output when an event occurs. The observation error was shown to be bounded and the event condition, based on the observed state, guaranteed stability in the presence of disturbances and measurement noise. Additionally, minimum inter-event time was guaranteed to be bounded from below.

*Remark 11* As indicated by the authors, the observer can be extended to a disturbance estimator to give an estimate of the actual disturbance to both the event generator and the control input generator, to reduce the information exchange.

Tracking of an external reference for MIMO sampled plants with non accessible state, and their internal stability conditions were presented in [46]. Internal stability of the output feedback ET system was studied for the first time and the effectiveness of the method was shown, both in terms of tracking performance and reduced number of transmissions.

A dynamic output feedback based ETC scheme was introduced for stabilization of Input Feedforward-Output Feedback Passive (IF-OFP) NCSs, by [47]. The triggering condition derived based on the passivity theorem, not only allowed to characterize a large class of output feedback controllers but also showed the control system to be finite gain  $\mathcal{L}_2$  stable in the presence of bounded external disturbances. The interactions between the triggering condition, the achievable  $\mathcal{L}_2$  gain of the control system, and the inter-event time were studied in terms of the passivity indices of the plant and the controller. The same results were obtained with additional imperfections such as quantization of the transmitted signal and presence of the external disturbance.

When the triggering events in both sensor and controller only use local information to decide when to transmit the data, and the transmission in one link does not necessarily trigger the transmission in the other link, then the resulting ET scheme is referred to as *weakly coupled*. These type of triggering events



in ET output feedback system with the control loop closed over a wireless network were presented in [48]. This represented an extension of the previous work, where the transmission from the controller subsystem was tightly coupled to the receipt of ET sensor data. An upper bound on the overall cost attained by the closed-loop system was given. Simulation results demonstrated that transmissions between sensors and controller subsystems are not tightly synchronized and were also consistent with derived upper bounds on the overall system cost.

The problem of dynamic output feedback controller (DOFC) design for CT LTI systems was addressed in [49]. In order to implement an output-based discrete ET condition, the methodology samples the output signal periodically instead monitoring it continuously. The closed-loop was modeled as a linear system with variable delays, and LMI based sufficient asymptotic-stability conditions were given which were used to co-design DOFC and the ET parameters. The authors assumed that the network does not have packet dropouts and disorders, however, their analysis accounted for bounded time-delays.

### **Event-based estimation**

Event-based estimation in which the receiver uses plant output, transmitted by the sensor over the communication channel to estimate the state, was considered in [50]. The objective was to achieve a trade-off between the estimation error and the communication rate using a cost function with a weighted sum of these two quantities. Previous results showed that an optimal scheduling policy exists for such problems at the cost of high computational requirements when the system's

size increases. To mitigate this issue, approximate optimal policies were considered and it was shown that a cost within a factor of six of the optimal cost is guaranteed.

To decouple triggering and control, [51] introduced an event-based state estimator (EBSE) between the sensor and the controller. This EBSE provides the controller with periodic state estimates while it receives the plant data only at the event times, which translates into the state estimate update both at the event times and at periodic update instants. Until the EBSE receives the plant's output, the estimation is done based on the knowledge that the output remains in a bounded set that characterizes the event. These characteristics of the EBSE allow its estimation error covariance matrix to be bounded. These bounds are then translated into a polytope to be fed into a robust MPC algorithm which optimizes the closed-loop trajectory dependent ISS gain. Hence, the more accurate the received information by estimator, the better the trade-off between event generation and closed-loop performance.

*Remark 12 As highlighted by the authors, the formal proof of closed-loop properties of the EBSE-MPC-plant interconnection or its variations is not yet available.*

A distributed estimation problem was addressed by [52], whereby the sensor decides when to transmit the locally estimated state to a remote observer. The trigger condition was chosen to minimize the mean square estimation error at the observer. The authors extended the earlier results for scalar linear systems to vector linear systems with nonzero mean initial conditions, and measurement noise through a computationally efficient way of computing sub-optimal ET thresholds.

Distributed ET estimation over WSN was reported in [53], with the objectives to minimize sensor's energy consumption and network congestion while guaranteeing estimator's performance. Several sensor nodes transmit the parts of the state to a central estimator based on the ET policy which depends only on the local sensory information. The proposed scheme does not require sensors to *broadcast* their measurements, which drops the need for sensor nodes to continually listen to the wireless channel, thus saving a considerable amount of energy. Furthermore, congestion is avoided by allowing the sensors to receive information from the central estimator, which informs a sensor not to transmit its state in case it already has sufficient state information. The scheme was implemented to estimate water level in a six-tank system using two wireless sensor nodes to demonstrate the decrease in sensor transmissions and network congestion.

*Remark 13 For future extensions of this work, it has been proposed to:*

1. *Evaluate the proposed mechanism in a real WSN to see the effect of delaying or avoiding transmissions in high-traffic conditions, and*
2. *Study the inclusions of a priori scheduling for estimator-sensor communication to guarantee state broadcast such that the probability of transmitting immediately after listening is reduced.*

Communication rate analysis for the estimation quality was presented in [54] and [55]. Specifically in the former, a sensor data scheduler with an accurate minimum mean squared error (MMSE) state estimator was proposed for linear

systems. The estimator was based on an approximation technique for nonlinear filtering, which gave a relationship between sensor-estimator communication rate and estimation quality. It was shown that a slightly increased tolerance of the estimation error gave a significant reduction in the communication rate.

In [55], a remote estimator sends the predicted state to the scheduler (over a wireless channel), which implements a level-based ET condition depending upon the difference between the predicted state and the actual output. For the expected value of communication rate, an exact measure was provided for scalar valued sensor measurements, and upper and lower-bounds for vector valued measurements.

*Remark 14* As an extension, one can consider other ET schemes such as time-dependent conditions that are designed to guarantee the estimation performance, and send-on-delta triggering conditions which do not require feedback communications.

Two stochastic ET sensor schedules for remote estimation namely, open-loop and closed-loop were presented in [56]. The communication channel had finite bandwidth, but no packet delays and dropouts. The presented methodology resulted in an exact MMSE estimator for both cases, which is in a simple recursive form and easy to analyze. It was shown that for the closed-loop case, upper and lower bounds of the average communication rate existed, and there was no critical value on the communication rate beyond which the estimator is unstable. For the open-loop case, a closed-form expression of the average communication rate was given. In addition to this, a parameter satisfying the desired trade-off between

the communication rate and the estimation quality was obtained by formulating an optimization problem, and a bounded expectation of the prediction estimation error covariance was given.

## Discussion

Most of the works cited here ([41, 46] and [48], and [50, 56]) consider a delay free communication channel.

In the context of ET-based output feedback control, the shortcomings of the previous works which were impractical computational complexities of optimal triggering sets for multidimensional systems, and non-convex nature of the value functions for infinite horizon problems, were addressed in [44].

From an information-theoretic perspective, the methodology in [45] puts burden on the communication channel by transmitting the whole state information instead of the plant output only. In addition, the observer computations on the sensor side are not practically favorable due to energy constraint of the sensor nodes.

For decoupling of communication and control, which is one of the major issues in NCSs design besides energy and bandwidth economy, [51] provides one way by introducing an ET-based state estimator. [53] discusses the issue of the energy economy over WSN.

In the context of ET-based state estimation, the main advantage of stochastic scheduling [56] comes from the Gaussian property of the innovation process which gives a simple linear filtering problem, compared to the works involving compli-

cated nonlinear and approximate estimation. The simulation study indicated a reduction in the estimation error covariance compared with the offline scheduling under the same communication rate.

### 2.2.6 Periodic Event-Triggered Control (PETC)

In conventional ETC (termed as continuous ETC (CETC) in [14]), the ET condition is *continuously* monitored, which requires a dedicated analog circuitry, and infinitely fast sampling may occur. To tackle these problems, [14] proposed a scheme whereby the transmissions and controller computations are event-based while the ET condition is checked *periodically*, hence retaining the low resource utilization property of conventional ETC while guaranteeing a minimum inter-event time of at least one sampling period of the ET condition. The authors named this scheme as periodic ETC (PETC). Initial analysis given in [13], was extended in [14] by providing a general framework that can be used to perform stability and performance analysis.

To analyze the stability and  $\mathcal{L}_2$ -gain properties of the resulting PETC systems, two different approaches were presented based on (i) discrete-time PWL systems, and (ii) impulsive systems, in [14]. Besides, techniques to compute (tight) lower bounds on the minimum inter-event times were also given. Numerical example showed that PETC is able to reduce communication and computation resource utilization significantly.

The authors extended their work to output-based dynamic controllers, and

decentralized ET conditions in [57]. Moreover, a third approach (other than PWL and impulsive systems) namely, DT perturbed linear (PL) systems was presented, and compared with the aforementioned approaches. The PWL system approach provides least conservative LMI-based results in case of stability analysis only, the PL system approach has the lowest computational complexity and provides useful insights for emulation-based controller synthesis, while the impulsive system approach provides a direct  $\mathcal{L}_2$ -gain analysis of the system.

In what follows, we give the stability results for PETC systems using PWL systems approach. Let  $\xi(t) = [x^T \quad \hat{x}^T]^T \in \mathbb{R}^{n_\xi}$ , where  $\hat{x}$  is the latest transmitted state. When PETC is implemented on system (2.1), then control law takes the form,

$$u(t) = K\hat{x}(t), \quad \text{for } t \in \mathbb{R}_+, \quad (2.24)$$

where,  $K \in \mathbb{R}^{m \times n}$ . Let  $\tau$  be the factor that keeps track of the time elapsed since last sampling time and  $h > 0$  be a properly chosen sampling interval, and define,

$$\bar{A} := \begin{bmatrix} A_c & B_c K \\ 0 & 0 \end{bmatrix}, \bar{B} := \begin{bmatrix} E_c \\ 0 \end{bmatrix}, J_1 := \begin{bmatrix} I & 0 \\ I & 0 \end{bmatrix}, J_2 := \begin{bmatrix} I & 0 \\ 0 & I \end{bmatrix},$$

to give an impulsive system,

$$\begin{aligned}
\begin{bmatrix} \dot{\xi} \\ \dot{\tau} \end{bmatrix} &= \begin{bmatrix} \overline{A}\xi + \overline{B}w \\ 1 \end{bmatrix}, \quad \text{when } \tau \in [0, h], \\
\begin{bmatrix} \xi^+ \\ \tau^+ \end{bmatrix} &= \begin{bmatrix} J_1\xi \\ 0 \end{bmatrix}, \quad \text{when } \xi^T Q \xi > 0, \tau = h, \\
&= \begin{bmatrix} J_2\xi \\ 0 \end{bmatrix}, \quad \text{when } \xi^T Q \xi \leq 0, \tau = h, \\
z &= \overline{C}\xi + \overline{D}w,
\end{aligned} \tag{2.25}$$

where,  $Q \in \mathbb{R}^{n_\xi \times n_\xi}$  is some symmetric matrix and  $z$  is the performance output with appropriately chosen  $\overline{C}$  and  $\overline{D}$ .

Let  $t_k = kh$ ,  $k \in \mathbb{N}$  be the periodic sampling times then whether or not the new state measurements are transmitted to the controller is based on the ET condition  $\mathcal{C}$  given by,

$$\mathcal{C}(\xi(t_k)) = \xi^T(t_k)Q\xi(t_k) > 0, \tag{2.26}$$

rendering  $\hat{x}(t)$  as,

$$\begin{aligned}
\hat{x}(t) &= x(t_k), \quad \text{when } \mathcal{C}(x(t_k), \hat{x}(t_k)) > 0, \\
&= \hat{x}(t_k), \quad \text{when } \mathcal{C}(x(t_k), \hat{x}(t_k)) \leq 0.
\end{aligned} \tag{2.27}$$

To obtain a complete PETC system (2.1), (2.24), (2.26) and (2.27) are combined.



We first define PWL system formulation for PETC system (2.25) and then present the stability result, as given in [57]. By discretizing (2.25), a bimodal PWL system is obtained as,

$$\begin{aligned}\xi_{k+1} &= A_1 \xi_k, & \text{when } \xi_k^T Q \xi_k > 0, \\ &= A_2 \xi_k, & \text{when } \xi_k^T Q \xi_k \leq 0,\end{aligned}\tag{2.28}$$

where

$$A_1 := e^{\bar{A}h} J_1 = \begin{bmatrix} A + BK & 0 \\ I & 0 \end{bmatrix}, A_2 := e^{\bar{A}h} J_2 = \begin{bmatrix} A & 0 \\ I & 0 \end{bmatrix},$$

with

$$A := e^{A_c h}, \quad B := \int_0^h e^{A_c s} B_c ds.\tag{2.29}$$

Using PWL system (2.28) and a piecewise quadratic (PWQ) Lyapunov function of the form,

$$\begin{aligned}V(\xi) &= \xi^T P_1 \xi, & \text{when } \xi_k^T Q \xi_k > 0, \\ &= \xi^T P_2 \xi, & \text{when } \xi_k^T Q \xi_k \leq 0,\end{aligned}\tag{2.30}$$

and taking  $w = 0$ , following stability theorem is defined:

**Theorem 2.4** *PETC system (2.25) is globally exponentially stable (GES) with a decay rate  $\rho$ , if there exist matrices  $P_1, P_2$ , and scalars  $\alpha_{ij} \geq 0, \beta_{ij} \geq 0$  and*

$\kappa_i \geq 0$ ,  $i, j \in \{1, 2\}$ , satisfying

$$e^{-2\rho h} P_i - A_i^T P_j A_i + (-1)^i \alpha_{ij} Q + (-1)^j \beta_{ij} A_i^T Q A_i \geq 0, \quad (2.31)$$

for all  $i, j \in \{1, 2\}$ , and

$$P_i + (-1)^i \kappa_i Q > 0, \quad (2.32)$$

for all  $i \in \{1, 2\}$ .

A dynamic programming formulation of the co-design problem for PETC approach was given by [58] for linear systems. ET controllers thus presented, guarantee quadratic discounted cost performance better than or equal to that of periodic control strategies using the same average transmission rate. Moreover, when compared with the existing Lyapunov based strategies, it was shown that with a slight compromise on the control performance, the number of transmissions was reduced.

*Remark 15 Possible future directions for research are:*

1. *To consider an average cost instead of the discounted cost, and*
2. *To consider non-Gaussian stochastic models for the disturbances acting on the plant.*

### 2.2.7 Quantized Systems

Besides using aperiodic triggering techniques to reduce the amount of traffic over the network, another way is to use *quantized* state (for sensor-controller (SC) network) and/or input (for controller-actuator (CA) network) variables. However, quantization has an adverse effect due to the inaccuracy in state representation because of the decreased number of bits used to represent the state/input information. [59]–[60] deal with these effects.

The problems of state feedback as well as output feedback control of NCSs in the presence of network imperfections such as delays, dropouts, and quantization were addressed in [59]. The methodology compensates for the effect of random packet dropouts. Sufficient conditions were also given for the asymptotic stability of the overall system. A similar work was presented by the authors in [61] which considered periodic SC, and an event-based CA network. The focus was on delays in the communication channel in both the feedback (SC), and the forward (CA) loops. The methodology introduced a predictive-control methodology to deal with packet delays, dropouts and disorders, whereby the control sequence is predicted with a prediction horizon which depends on the bounds of the delays, and sent to the actuation side.

Optimization-based approach to compute globally-stabilizing controllers for nonlinear systems with quantized and ET state information subject to random transmission delays and losses, was considered in [62]. The method was based on existing set oriented discretization of the optimality principle, and was extended

to the case where an additional external stochastic parameter is present in the system.

The problem of ET co-design of CT linear networked systems with delays, and both state and control input quantization were studied in [30]. A new delay model was used to represent the overall system to take into account ET mechanism, delays, and quantization in a unified framework. Sufficient conditions for asymptotic stability were given in terms of LMIs using Lyapunov-Krasovskii functional approach. Moreover, in order to achieve a better trade-off between control performance and network conditions, an explicit expression for the feedback gain was given with integration of signal quantization levels, delays and trigger parameters.

*Remark 16* The authors considered infinite number of quantization levels, hence to merge finite number of quantization levels and ET scheme in a unified framework can be considered as possible extension.

According to [63], a more realistic measure of channel usage for ET scheme, as compared with the inter-transmission interval, is the *stabilizing bit-rate*, which is defined as the number of bits per sampled state divided by the acceptable delay in message delivery. The bit-rates required to asymptotically stabilize nonlinear ET systems were examined, with quantization effects, and maximum acceptable delays. These imperfections might render the bit rates required by the ET scheme to be greater than those required by periodic scheme. Scaling relationships between maximum delay, inter-sampling interval, and quantization error were used

to bound the stabilizing bit-rates. Conditions were presented under which the stabilizing bit-rate asymptotically goes to a constant value, and in some cases to zero as the system approaches equilibrium.

*Remark 17* Considering the available literature, to study the scheduling problem when there are several controllers sharing the same communication network can be deemed as possible area for future research.

A bound on an ET system’s stabilizing “instantaneous” bit-rate was driven by [60], when the sampled signal was dynamically quantized in wireless NCS. This instantaneous bit-rate is a time-varying function whose average value can be made small by requiring that the instantaneous bit-rate gets smaller as the system state approaches the origin, which is the *efficient attentiveness* property exhibited by ET systems. Sufficient conditions guaranteeing the instantaneous bit-rate’s efficient attentiveness were provided. The numerical example indicated that there is a tradeoff between inter-sampling interval and instantaneous bit-rate.

## Discussion

The main limitation of [59] was the authors did not consider aperiodic communication. Moreover, in [61],

- an explicit analysis or expression, which indicates event-driven CA channel, was not given.
- the bounds on forward and feedback delays, which are directly related to the prediction horizon of control sequence, were not determined.

- the control performance depends on the control sequence prediction accuracy.

The shortcoming pointed out in [30] was the use of infinite quantization levels, which is to say that the digital system can represent an analog value with infinite accuracy.

### 2.2.8 ETC of Decentralized and Distributed systems

Ever increasing consumer demands have pushed today's industry to implement *cyber-physical* systems, whereby large scale dynamical systems consisting of a number of coupled subsystems use a communication network for control and monitoring purpose. Examples are process industry and electric power supply companies, to name a few. Control of these systems in a centralized fashion imposes stringent demands on the communication medium and modeling of subsystem coupling, necessitating the use of decentralized ([64]–[65] and [36]) or distributed ([66]–[67]) networked control strategies using aperiodic communication schemes. Former methodology is applicable when the subsystems have weak or no coupling, and later is implemented otherwise. In what follows, we present a survey on both implementing ET scheme.

#### Decentralized systems

Decentralized ET implementation of centralized nonlinear controllers over Wireless Sensor Actuator Networks (WSAN) was presented in [64], without assuming

weak-coupling between the systems. The main motivation for decentralized implementation comes from the fact that the sensor nodes are physically distributed in WSNs which implies that all measured quantities are not accessible, translating into the usage of observer-based techniques; this is impractical due to low computational capabilities of sensor nodes. Moreover, the consensus-based techniques demand a large amount of communication. The proposed computationally-efficient methodology relied only on the local information and offered large controller inter-computation times while guaranteeing performance. As mentioned by the authors, the techniques can be implemented over WirelessHART standard.

Dynamic output-based ET controllers were proposed by [43] in a decentralized setting, following the work in [42]. Due to the physical distribution of sensors and actuators (grouped into nodes), and controllers, the continuous transmission of state and control variables for ET conditions is not possible. This problem is solved by a decentralized ET mechanism whereby the events are based only on the local information. In order to guarantee a positive minimum inter-event time, the event occurs when the difference between the current value of a node and its previously transmitted value becomes larger than the current value plus an additional threshold. Moreover, the ET system was modeled as an impulsive system. Closed-loop stability and  $\mathcal{L}_\infty$  performance were guaranteed along with larger inter-event times than the previously existing results.

Besides reducing the amount of transmissions from the sensor nodes, another problem is to reduce the time in which these nodes have to *listen* to the broad-

cast of other sensor nodes, thereby saving a great amount of power. The work presented in [68] was motivated by this requirement and asynchronous decentralized ET control was presented with a central controller node, and a set of non co-located sensor nodes which do not need to coordinate with each other. It does not require synchronization of sensor measurements in time, hence they can transmit aperiodically, with the triggering condition depending only on the local conditions. Additionally, the proposed scheme reduces the payload of (most of) the packets to one bit, which translates into reduction in SC communication.

*Remark 18 As indicated in the discussion, the following directions can be pursued in future research:*

1. *To design computational methods to relax the conservative bounds,*
2. *To optimize controller design and implementation for data-rate transmissions,*
3. *To study and design protocols for wireless communications exploiting the benefits of the proposed techniques,*
4. *To study theoretically in more detail, the practical effects such as delays and disturbances. In particular, performance guarantees including the response to disturbances, and*
5. *To study controller designs for useful classes of non-linear systems.*

The same idea of asynchronous decentralized ET transmission was adopted by [69]. The proposed methodology allows asynchronous transmission of the state



information from geographically distributed sensor nodes, thus relaxing the consistency requirement at the controller. Correspondingly, the controller output is also computed and actuated in an asynchronous manner. Asymptotic stability of the overall NCS is guaranteed if the weighted sum of all minimal transmission periods and all types of delays is bounded, which translates into a tradeoff between the system performance, and overall communication and computational resources. Additionally, strictly positive minimal transmission periods were provided.

Decentralized version of model-based ET (MB-ET, see Section 2.2.10) scheme was presented in [65], whereby the events and controllers are designed based only on the local information in a decentralized manner. Network traffic is significantly reduced by using models of other subsystems at each controller node, and by requiring that every subsystem transmits its state information to others on the basis of difference between real and estimated variables. Instead, if a subsystem requests updates from all other nodes, it may result in congestion, as all other subsystems will send their information at the same time. Moreover, traditional ZOH implementation of ET schemes was generalized, and stability thresholds that are robust to model uncertainties were provided. Interestingly, a considerable reduction in communication was reported as the number of subsystems is increased.

Multiple heterogeneous control systems sharing a common communication medium to close the feedback loop were considered in [36]. Using an approximate formulation for the communication medium enables to divide the overall optimization problem into two levels: 1) a local average-cost problem for every

subsystem solved using dynamic programming, and 2) a global resource allocation problem for optimal transmission rates, which is a convex optimization problem. It was shown that the overall system is stochastically stable and that the system is asymptotically optimal as the number of subsystems is increased. The numerical examples showed an increased level of flexibility, robustness, and a significant improvement in the control performance.

*Remark 19* Considering available literature, following are the open problems for further research:

1. *To investigate online adjustment of the event-trigger according to the network traffic that also leads to a decentralization of the global resource allocation problem, and*
2. *To study complicated models for the communication network.*

The stochastic stability results due to [36] are presented as follows. Consider a networked control system with  $N$  control loops closed over a common communication medium. The process  $\mathcal{P}^i$ , where  $i \in \{1, \dots, N\}$  is described by,

$$x_{k+1}^i = A^i x_k^i + B^i u_k^i + w_k^i, \quad (2.33)$$

with state  $x_k^i \in \mathbb{R}^{n_i}$ , input  $u_k^i \in \mathbb{R}^{d_i}$  and i.i.d noise process  $w_k^i \in \mathbb{R}^{n_i}$ . The initial state  $x_0^i$  is a random variable with symmetric distribution around its mean and finite second order moment. The statistics of the random variables and the system parameters within a subsystem are known to the controller and sensor

station. The number of transmission slots are limited to  $N_{slot}$  because of the limited bandwidth, translating into the design of priority based ET mechanism on sensor nodes, whereby the node decides on the importance of sending the data.

The optimal control law is given as,

$$\begin{aligned}
u_k^i &= \gamma_k^{i,*}(Z_k^i) = -L^i E[x_k^i | Z_k^i], \\
L^i &= (B^{i,T} P^i B^i + Q_u^i)^{-1} B^{i,T} P^i A^i, \\
P^i &= A^{i,T} (P^i - P^i B^i (B^{i,T} P^i B^i + Q_u^i)^{-1} B^{i,T} P^i) A^i + Q_x^i,
\end{aligned} \tag{2.34}$$

with  $Z_k^i$  representing the observations at the controller side.

The conditions that guarantee stochastic stability of the aggregate system are given in the following theorem:

**Theorem 2.5** *Let the control law be given by (2.34) and let the scheduling policy be  $\pi_k^i(\delta_k^i = 1 | e_k^i) = 1$  for  $\|e_k^i\|_2 > M^i$  for some arbitrary  $M^i$ . If*

$$\frac{N_{slot}}{N} > 1 - \frac{1}{\|A^i\|_2^2}, \tag{2.35}$$

*is satisfied for all subsystems, then the Markov chain representing the aggregate system is stochastically stable.*

## Distributed Systems

Preliminary results on ET broadcasting of state information in distributed control systems over wireless networks were presented in [66]. The network was assumed to consist of only LTI systems with full state information. Asymptotic stability

is assured for entire system using an ET rule based on Lyapunov analysis, which uses only subsystem's local state error. Additionally, the ET level is tuned using the information from neighboring subsystems, which provides robustness against the subsystem's external disturbance environment. The time to next broadcast was also shown to be bounded.

The work in [66] was extended by [70] for nonlinear CT systems, while considering delays and packet dropouts. The main contribution was to completely decentralize the ET scheme implying that,

- subsystem broadcasts its information using only local data,
- only individual subsystem's and its immediate neighbors' information is required to determine the triggering threshold,
- the deadline for subsystem's broadcast can be anticipated based only on local information, and
- subsystem can locally identify the maximum allowable number of data dropouts.

The overall system under the proposed scheme is guaranteed to be GUUB if the transmission delays are lower bounded by a strictly positive constant, for a limited number of successive data dropouts assumption for each subsystem.

The work in [66] and [70] served as preliminary for [71], which gave an analysis that is applicable for both nonlinear and linear subsystems. In former, the event design was transformed into a local ISS design problem, while for later, the design

reduced to a local LMI feasibility problem. NCS was shown to be finite-gain  $\mathcal{L}_p$  stable for zero-delay, and bounded successive data dropouts assumptions. For non-zero transmission delay (less than the corresponding deadline), and if the external disturbance vanishes, the NCS is asymptotically stable. Simulations revealed that the average broadcast period and the computational time required to select thresholds have a good scalability with respect to the system size.

As compared with [70] and [71], results for ET distributed setting applicable to a very large class of systems were presented in [72]. The ET scheme, which depends only on the local information, introduces some disturbances in the system. This translates into a modification of general small-gain theorem because the ISS small-gain results are not applicable. It was assumed that the interconnection terms satisfy a generalized small-gain condition, and the graph modeling of the system is strongly connected. Furthermore, the infinite sampling phenomenon was mitigated using either input-to-state practical stability (ISpS), or Lyapunov function approach. This novel methodology was termed as *parsimonious triggering*, as it reduces the number of necessary events.

*Remark 20 To avoid collision, whereby events occur simultaneously at multiple subsystems, and to derive explicit bounds of inter-event times can be considered as future extensions of this work.*

The authors in [73] followed the work of [66] with the main contribution of using a model-based approach in which each subsystem contains a model of its neighboring nodes, thus reducing the amount of broadcasted events. Additionally,

an analysis was presented for the effect of interaction over the region of convergence around the equilibrium, and the state independent strictly positive lower bound of the broadcasting period. This work was further extended by [74] to consider the effects of network induced delays and packet losses. In particular, two different communication protocols were proposed which guarantee stable behavior in the presence of network imperfections. The analysis thus presented provides with bounds on the delays, and the number of successive dropouts which ensure stability and performance, while giving lower bounds on the inter-event times.

The results reported in [73] were improved by [67] to consider imperfect decoupling. A novel ET mechanism was proposed which considers time-dependent trigger functions to guarantee asymptotic stability, and existence of a strictly positive lower bound for the inter-event time. Moreover, the model uncertainties were taken into account in the inter-event time analysis.

*Remark 21* The authors highlighted to consider the following as future extensions of their work:

1. *Application of the proposed methodology to DT systems, and*
2. *Consideration of exogenous disturbances.*

A widely used distributed algorithm that solves network utility maximization (NUM) called *dual decomposition algorithm*, was compared with ET distributed algorithms by [75, 76, 77]. State-dependent ET thresholds under which the distributed NUM algorithm, based on barrier methods, converges to the optimal solution of the NUM problem, were established by [75]. Simulation results suggested

that the proposed algorithm reduces the number of message exchanges by up to two orders of magnitude when compared with dual decomposition algorithms, and is independent of the maximum path length or maximum neighborhood size (measures of network size). Exactly the same results were reported in [76] using distributed NUM algorithm based on the augmented Lagrangian methods. A general class of optimization problems was given in [77], where an ET distributed algorithm was used for sensor networks. As an example, the authors used data gathering problem and showed that the proposed algorithm reduced the number of message exchanges by an order of two as compared with dual decomposition algorithm. Additionally, the methodology was independent of the network size.

The problem of designing an appropriate distributed ET rule to achieve asymptotic synchronization of a dynamical network with linear subsystems while avoiding Zeno-behavior (infinitely-fast sampling of the plant state) was addressed by [78]. The complexity of the problem lies in the limited information constraint, whereby a subsystem has access only to its neighbor's information available at discrete instants. To overcome this problem, estimators were introduced in each subsystem which provided an estimate of the neighboring nodes' information using the limited information. The network was shown to achieve asymptotic synchronization without Zeno-behavior for all time.

*Remark 22* The methodology did not consider network imperfections such as quantization, delay, and dropouts, providing an interesting avenue to explore.

## Discussion

The methodology of [68] is opposed to [64], as it uses asynchronous decentralized ET control with a central controller node, and a set of non co-located sensor nodes which do not need to coordinate with each other, thus eliminating the need to share the information. Moreover, the weak-coupling assumptions and restrictive-dynamics conditions are not imposed unlike in [43], which considers linear systems. The work presented in [36] is also discussed in Section 2.2.3.

In the context of distributed systems, the main shortcoming of [71] is the occurrence of infinitely fast data transmission when the system reaches the origin because a lower bound for inter-broadcast times is not guaranteed.

The methodology presented in [75, 76, 77] does not consider network artifacts.

### 2.2.9 Adaptive Control

$\mathcal{L}_1$  adaptive control technique guarantees closed-loop system's stability with a very high degree of robustness. An implementation of such a controller over real-time networks using event-based scheme was studied by [79] where  $\mathcal{L}_1$  controller was used in the feedback loop. Lower-bound on the transmission periods was provided. It was shown that states and input of the system can be made arbitrarily close to that of a stable reference system by using high adaptation and transmission rates. The framework and results can also be used to get the performance measure of the system with transmission delays and quantization effects. Real-time implementation of output-feedback  $\mathcal{L}_1$  adaptive controller was reported in [80].



Stability conditions in terms of event threshold and allowable transmission delays were also provided.

Adaptive state feedback ETC of SISO affine nonlinear DT systems was presented in [81]. The knowledge of nonlinear system dynamics was partially relaxed by using a NN-based adaptive estimator which estimated the parameters as well as the states. The weights of NN were adjusted at aperiodic instants using ET scheme. Similar work was reported in [82] for uncertain DT linear systems identified as autoregressive Markov (ARMarkov) representation, for which an update law was derived to estimate the parameters at ET instants. After the convergence of parameter estimation error and output to zero, no more triggering is required.

### **2.2.10 Model-based ETC**

Model-based NCS (MB-NCS) and ETC were combined by [83], model-based event-triggered (MB-ET) control, which gave increased inter-update times as compared with the individual control strategies. In the proposed framework, a nominal model of the plant is stored in the controller node which generates state estimates of the system during update intervals, hence giving better results as compared with the traditional ZOH version of state, and providing stability thresholds that are robust to model uncertainties. This work also considers quantization and time-varying network delays. The error events, designed based on the quantized measured variables, ensure asymptotic stability as opposed to the similar results which considered non-quantized measurements.

*Remark 23 Future direction pointed out by the authors is to consider output feedback using the proposed framework.*

PETC (see section 2.2.6) was combined with MB strategy for linear systems by [84] to give MB-PETC. Advanced ET mechanisms (ETMs) were introduced which reduce the communication load in both SC and CA channels, and outperform the existing ETMs. Closed-loop performance arbitrarily close to that of MB periodic time-triggered control (PTTC) setting was achieved. Also, a decentralized MB-PETC was provided suitable for large-scale systems. This work was extended by [85] by adding an approximate disturbance model which can further enhance communication savings in the presence of disturbances.

### **2.2.11 Event-based Model Predictive Control (MPC)**

In order to save energy in a wireless network node, [86] applied ET control scheme by introducing the “predictive event”, defined as the crossing of the future predicted system response from the stable region. This event is used to determine the sleep time of the wireless nodes before a future event occurs.

Event-based nonlinear MPC (NMPC) approach for nonlinear CT systems under state and input constraints was presented by [87], with an application level solution to tackle bounded delays and information losses in ET SC and CA channels.

*Remark 24 As an extension to this work, one can consider active scheduling of the measurements to minimize the transmissions, and detailed study of asymptotic*

*stability and robustness.*

ET strategy for DT systems was proposed and analyzed in [88], where the plant was assumed ISS with respect to measurement errors, and the triggering condition was based on the norm of this error; the framework was used in MPC. The authors considered ET strategies for uncertain CT and DT nonlinear systems with additive disturbances under robust Nonlinear MPC (NMPC) in [89]. The updates of control law depended on the error between the actual and predicted trajectory of the system.

To deal with the systems with faster dynamics, the problem of robust networked static output feedback MPC design that stabilizes a class of linear uncertain systems was addressed in [90]. The methodology guaranteed cost, and gave a parameter-dependent quadratic stability (PDQS) which is based on Lyapunov-Krasovskii functional. The upper-bound on the delay was assumed to be bigger than the sampling time. Control design was based on sufficient robust stability condition formulated as a solution of bilinear matrix inequality BMI, which can be solved off-line.

A computationally efficient ET MPC scheme for CT nonlinear systems subject to bounded disturbances was given in [91]. First, an ET condition that depends on the error between the system state and its optimal prediction was designed, followed by the design of ET MPC algorithm that was built upon the triggering mechanism and the dual-mode approach. Feasibility and stability analysis were carried out in detail and sufficient conditions were thus presented. Specifically,

it was shown that the proper selection of prediction horizon, and boundedness of the disturbance can guarantee feasibility of the ET MPC algorithm. Regarding stability, which is related to the prediction horizon, the disturbance bound, and the triggering level, it was shown that the state trajectory converges to a robust invariant set.

## **Discussion**

The event-based MPC offers energy economy [86] which is vital in WSNs, where the sensor nodes are battery powered. Another result based on ET MPC was presented in [51] and is discussed in Section 2.2.5.

### **2.2.12 Event-based PID controller and actuator saturation**

The effects of actuator saturation on the behavior of the ETC loop in terms of stability and communication were investigated by [92] using simulations. A static anti-windup mechanism was introduced to remedy the adverse effects on event-based control. Moreover, by means of LMIs, stability regions were given, and a lower bound on the inter-event time was shown to exist. These results were also extended by considering a case where full-state information might not be available to the controller. The results were illustrated by simulations and experiments.

*Remark 25 It was pointed out by the authors that alternate methods for deriving the stability regions can be pursued.*

The design of an event-based PI control scheme for stable first-order processes was considered in [93] which aimed to diminish the oscillations around the set-point, and sticking effect. The conventional PI controller was replaced with PIDPLUS, a version of PI controller for NCSs which also deals with packet losses and time delays. Additionally, stability and performance analysis of the closed-loop system were provided. Simulations showed that the scheme ensures set-point tracking, disturbance rejection, and robustness against process delay while significantly reducing the number of transmissions.

*Remark 26 Some potential future directions pointed out by the authors are:*

- 1. Consideration of multi dimensional systems,*
- 2. Investigation of the derivative part of PIDPLUS, and*
- 3. To further improve the trade-off between performance and event frequency.*

## **Discussion**

Although the proposed scheme in [93] is robust against the process delays, the stability analysis was not applicable to this case; this translates into an extension of the stability analysis to consider such delays.

### **2.2.13 Miscellaneous Results**

Event-based control in multiple-loop contention-based shared medium was discussed by [94]. Specifically, they studied performance degradation of event-based

scheme in the presence of packet loss, and presented an explicit expression relating control criterion with triggering levels and packet loss probability. In multiple loops, the result can be used as a guideline for assigning level thresholds that ensure optimal usage of the communication resources.

*Efficient attentiveness* property is exhibited by an event-based system when the length of inter-sampling interval increases monotonically as the sampled state approaches equilibrium. The authors in [95] established conditions on ET under which this property can be guaranteed, in a computationally efficient manner, that the system possesses this property.

The suitability of resilient control for ET scheme was investigated in [96], and the authors suggested that such a control is achievable for at least transient faults. Resilient control system is the one which maintains state awareness while ensuring acceptable performance in response to disturbances. Required bit-rates were examined, and sufficient resilient bit-rates for nonlinear scalar systems with affine controls and disturbances were given. It was observed that the rates are independent of the initial states.

[97] presented the methodology to deal with bounded time delays in the NCSs. In order to gain apriori knowledge of the delays from a dynamic real-time behavior, dynamic priority exchange scheduling for bounding time-delays was used. The scheme also deals with faults which introduce a structural change in the dynamic model, and dynamic response due to real-time scheduling. The main contribution was to model the faults and delays, as perturbations considering nonlinear

behavior through a fuzzy TKS approach in a co-design strategy.

The work of [98] deals with the problem of the ET fuzzy  $H_\infty$  control of a nonlinear NCS by using the deviation bounds of asynchronous normalized membership functions.

## 2.3 Self-Triggered Network Control

In ST mechanism the feedback law computation is followed by determination of the next time instant to sample the state. This time instant is calculated on the basis of latest sampled state and plant dynamics; during these time instants, the system operates as open loop. This scheme mitigates the problems faced in the ET mechanism by eliminating the need to continually check plant's state against an event condition, and it can be regarded as a software based emulation of ET technique. In what follows, we present a survey of the results reported for ST scheme.

### 2.3.1 Stability

As mentioned above, the system operates in open-loop until the next update time, making stability and robustness primary issues. We present the literature which discusses the stability of ST schemes in terms of Input-to-State Stability (ISS) ([99, 100]) and  $\mathcal{L}_2$  stability ([101, 102]).

## ISS

For ISS of a general NCS [99] stated that for a class of Lyapunov U-GAS protocol if the closed-loop controller, designed without considering the network, guarantees ISS of the system with respect to disturbances then the same controller would guarantee semi-global practical ISS for the NCS implemented using Lyapunov U-GAS protocol.

The ISS for ST implementation was studied by [100] and it was shown to be exponentially uniformly ISS (U-ISS) with respect to the additive disturbances. Their main results are given in what follows. Consider an LTI system,

$$\dot{\xi}(t) = A\xi(t) + BK\xi(t_k) + \delta(t), \forall t \in [t_k, t_k + \Omega(\xi(t_k))), \quad (2.36)$$

where  $\xi \in \mathbb{R}^m$ ,  $K$  is the controller gain rendering the closed-loop system exponentially stable, and  $\delta(t)$  is the additive disturbance, with ST implementation  $\Omega : \mathbb{R}^m \rightarrow \mathbb{R}^+$ ,  $\Omega(\xi(t_k)) = \tau_k$ , determined by the policy,

$$\begin{aligned} \Omega(\xi(t_k)) &:= \max\{t_k + t_{min}, t_k + \tilde{n}_k\Delta\}, \\ \tilde{n}_k &:= \max\{s \leq N_{max} | \tilde{h}(n, \xi(t_k)) \leq 0, \forall n \in [0, s]\}, \\ \tilde{h}(n, x_k) &:= |\sqrt{P}R(n)x_k| - V(x_k)e^{-\lambda(n\Delta)}, \end{aligned} \quad (2.37)$$

where  $t_{min}$  is the minimum time between updates,  $\Delta$  is the time interval to check triggering condition,  $N_{max}$  is the ratio of maximum inter-update time  $t_{max}$ , and  $\lambda$  is the decay rate of the Lyapunov function  $V(x)$  with a positive definite symmetric



matrix  $P$  and  $R(n)$  is given as,

$$R(n) := A_d^n + \sum_{i=0}^{n-1} A_d^i B_d K; \quad A_d := e^{A\Delta}, \quad B_d := \int_0^\Delta e^{A(\Delta-\tau)} B d\tau.$$

The parameters  $\lambda$ ,  $\Delta$  and  $N_{max}$  depend on the choice of designer, and  $t_{min}$  depends on the value of  $\lambda$ .

**Theorem 2.6** *The system given by (2.36) with ST policy (2.37) is exponentially ISS.*

*Remark 27*

*The authors indicated to apply similar ideas to non-linear systems (via approximate models) as future research.*

### **$\mathcal{L}_2$ stability**

Early co-design methodologies viewed the selection of inter-event time as an optimization problem. However, the cost functions (penalizing control performance) are rarely monotonic with respect to the inter-event time, which makes hard to find the optimal sampling time. Another approach based on Lyapunov techniques was used by [101], whereby the sampling periods were selected to ensure stability and performance in the presence of disturbance by adjusting the induced  $\mathcal{L}_2$  gain. A ST real-time system implementing full information  $\mathcal{H}_\infty$  controller along with a task scheduler was presented. Sampling times were utilized by scheduler to determine the actual release times.

We now present the performance results of a ST feedback control system due to [101]. Consider a real-time system with  $N$  plants controlled by a single processor with  $N$  tasks, where a task refers to three functions combined, namely: state sampling, control law computation, and control application using ZOH. The  $i$ -th plant is given as,

$$\dot{x}_i(t) = A_i x_i(t) + B_{1i} u_i(t) + B_{2i} w_i(t), \quad x_i(0) = x_{i0}, \quad (2.38)$$

where  $i \in \{1, \dots, N\}$ ,  $w_i(t)$  is a bounded disturbance, and  $u_i(t)$  is the control input computed by  $i$ -th task. Each task is associated with release times,  $\{r_i[j]\}_{j=1}^{\infty}$ , with  $r_i[j]$  being the time when  $j$ -th job of  $i$ -th task is ready to be executed. The period for  $j$ -th job is given by,

$$T_i[j] = r_i[j + 1] - r_i[j].$$

The control law  $u_i(t)$  is of the form,

$$u_i(t) = -k^T x(r_i[j]). \quad (2.39)$$

Following theorem gives the main result.

**Theorem 2.7** *Let  $G$  denote the sampled-data control system given by (2.38) and (2.39) with the control gain  $k^T = -B_1^T P$ , where  $P$  is a positive symmetric matrix*

that satisfies following ARE for some  $\gamma > 0$ ,

$$A^T P + PA + I - P \left( B_1 B_1^T - \frac{1}{\gamma^2} B_2 B_2^T \right) P = 0. \quad (2.40)$$

Let  $x_r$  denote system's state at release time  $r[j]$ . If the state  $x(t)$  satisfies

$$\begin{bmatrix} x(t) \\ x_r \end{bmatrix}^T \begin{bmatrix} -I + PB_1 B_1^T P & -PB_1 B_1^T P \\ -PB_1 B_1^T P & 0 \end{bmatrix} \begin{bmatrix} x(t) \\ x_r \end{bmatrix} \leq -\|x(t)\|^2, \quad (2.41)$$

for all  $t \in [r[j], r[j+1])$  and  $j = 1, \dots, \infty$ , then the induced  $\mathcal{L}_2$  gain of  $G$  is less than  $\gamma$ .

Authors in [101] extended their work in [103] by deriving the bounds on a task's sampling period and deadline, to quantify how robust control system's performance will be to the variations in these parameters. They developed inequality constraints on control task's period and deadline, whose satisfaction ensured that the system's induced  $\mathcal{L}_2$  gain lies below a specified performance threshold. The results apply to LTI systems driven by bounded external disturbances.

*Remark 28* The authors pointed out that the implementation of STC over WSAAN can be pursued as an interesting future direction because of the inability of such networks to provide deterministic guarantees on message delivery.

The assumption on bounds of external disturbances in [103] was relaxed by [102], and it was shown that the sampling periods are always greater than a positive constant and larger than those generated in [103]. Moreover, the scheme

is robust against external disturbances.

## Discussion

The ISS results given here ([99, 100]) do not consider real-time network issues such as packet loss and delay, which makes the stability results conservative for real-time applications.

Preliminary results for  $\mathcal{L}_2$  stability in [101] show great robustness to scheduling delays induced by the real-time schedulers.

### 2.3.2 Self-triggered control of linear systems

ST implementation of linear state-feedback controllers was developed by [104] for LTI systems. In order to find the next update time, the scheme integrates system's dynamics using a discretization method. It was shown that the proposed scheme guarantees exponential stability while reducing the number of controller executions. Additionally, a trade-off between complexity and the resulting performance was analyzed.

A new method to calculate the lower bounds on ST update times with low computational requirements for diagonalizable LTI systems was presented in [105]. The authors used semi-definite programming-based technique to give less conservative triggering conditions as compared with the existing ones, and larger update times.

Another approach to design STC for linear systems was presented in [106] by exploiting the properties of universal formula for event-based control of nonlinear

systems. The proposed methodology was shown to give better results than the existing ST approaches.

*Remark 29 The authors indicated to extend the work to nonlinear systems and to test it on a real-time application.*

Previous results on the state feedback stabilization were extended by [107] to the case of dynamic output feedback using DT observer. Global asymptotic stability is guaranteed for some observability condition. This work was extended to the case of bounded exogenous disturbances by [108]. A cascade structure of ISS observer (with respect to disturbances), and ISS ST controller was used to render the closed-loop system robust against disturbances. Another extension was reported in [109] by proving that the LTI systems, where several plants are connected in an acyclic manner, are also robust against disturbances when using the same cascade structure of ISS observer and ST controller.

*Remark 30 The authors highlighted following future extensions of their work:*

1. *Consideration of other scheduling methods in the observer based approach,*  
*and*
2. *Consideration of more general plant interconnections.*

We now present stability results due to [107]. The LTI system is given as,

$$\begin{aligned} \dot{x}(t) &= Ax(t) + Bu(t), \\ y(t) &= Cx(t), \end{aligned} \tag{2.42}$$

where,  $x \in \mathbb{R}^n$  with initial state  $x_0$ , the input  $u \in \mathbb{R}^m$  and plant output  $y \in \mathbb{R}^p$ . The plant is assumed to be controllable and observable. The event-scheduler simulates a copy of plant dynamics (2.42) with control input  $u(t) = Kx_k$ , given as,

$$\dot{\xi}_x(t) = A\xi_x(t) + BKx, \quad \xi_x(0) = x, \quad (2.43)$$

where,  $\xi \in \mathbb{R}^n$ . The ST scheme uses Lyapunov function approach to compute the triggering time. Let  $V(x) = \sqrt{x^T P x}$  with positive definite symmetric  $P$ , be the Lyapunov function for (2.42), then its decay rate  $\lambda$  is selected by the designer such that,

$$V(x) \leq V(x_0)e^{-\lambda\tau}. \quad (2.44)$$

Let the function  $h(\tau, x)$  be defined as,

$$h(\tau, x) = V(\xi_x(\tau)) - V(x)e^{-\lambda\tau}. \quad (2.45)$$

This function is used to get sampling times as,

$$\tau_{gridded}(x) = \Delta \max\{1 \leq d_2 \leq M : h(d_1\Delta, x) \leq 0, \forall 1 \leq d_1 \leq d_2 \leq M\}, \quad (2.46)$$

where  $0 \leq \Delta \leq \tau_{min}$ , with  $\tau_{min}$  being the lower bound on triggering time, and  $M \in \mathbb{N}$  are design parameters. In order to estimate full state, observer is used.

The control is computed as,

$$\begin{aligned} u(t) &= K\hat{x}_k, \quad t \in [t_k, t_{k+1}), \\ t_{k+1} &= t_k + \tau_{gridded}(\hat{x}_k). \end{aligned} \tag{2.47}$$

Let  $\tilde{x}_k = x_k - \hat{x}_k$  for  $k \geq 0$  be the observation error then the following theorem gives the stability results.

**Theorem 2.8** *ST controller (2.47) renders plant (2.42) exponentially ISS with respect to observation errors, i.e., there exist positive constants  $\sigma$  and  $\gamma$  such that,*

$$\|x(t)\| \leq \sigma e^{-\lambda(t-t_0)} \|x_0\| + \gamma \max_{j \in \{0,1,\dots,k\}} \|\tilde{x}_j\|, \tag{2.48}$$

for all  $t \geq t_0$ , where  $k = \max\{p \geq 0 : t_p \leq t\}$ .

## Discussion

The methodology of [104] can be extended to the case of dynamic controllers, and to handle non-zero delay between sensor and actuator update. However, the drawback of this scheme comes from the choice of discretization step which has an impact on the complexity.

### 2.3.3 Self-triggered control of nonlinear systems

The first result for STC of nonlinear systems was presented by [110] for two classes of nonlinear systems, namely: state-dependent homogeneous, and polynomial systems. Conditions defining next task execution times were shown to depend upon

the dynamics of plant, desired performance, and the current state. Additionally, the authors provided an analysis to quantify the trade-off between performance requirement and communication resource usage. The proposed scheme was applied to the models of jet engine compressor and rigid body; the simulations showed that the inter-execution times due to ST scheme are an order of a magnitude larger than the periodic implementation, while giving the same performance. Also, the scheme is robust against disturbance and sensor noise.

This approach exploited the geometry of systems to scale the execution times along the surface in state-space, termed as *manifold*. As a result, a two-step approach was used to get the execution times, whereby the first step gives a rough estimate of the lower bound of inter-execution time, which is valid on a ball around the origin, and second step exactly scales this time to whole operating region to describe its evolution. In order to mitigate the conservatism introduced due to in-exact lower bound, the authors gave a detailed discussion in [111] on using *isochronous manifolds* (which are surfaces in state-space with states for which the execution times remain constant) that replace the ball used in the first step, to give an exact lower bound. This amalgam of both ST techniques was shown to outperform the existing ST methodologies. Moreover, the main results can be applied to any smooth control system by homogenizing it using the presented technique.

A limitation of [110] and [111] came from the approximation of isochronous manifolds, since it is impossible to obtain them in closed-form, in general. Also,



the method to compute the manifold is not always applicable. In addition to this, the authors did not consider the effects of external disturbances and time delays. In order to tackle these issues, [112] proposed a simple ST sampler for perturbed nonlinear systems, subject to bounded external disturbance and small time delays, which ensured UUB of the trajectories. Moreover, in order to reduce the conservativeness, techniques based on disturbance observers were proposed. The methodology was validated through simulations.

The stability results for ST sampler due to [112] are briefly presented here. Consider a perturbed system given by,

$$\dot{x} = f(x, u, d), \tag{2.49}$$

where  $x \in \mathcal{D}_x \subseteq R^n$  is the state, input is given as  $u \in \mathcal{D}_u \subseteq R^p$ , and disturbance  $d \in \mathcal{D}_d \subseteq R^d$  is bounded as  $\|d\| \leq \bar{d}$ . Assume that there exists a differentiable state feedback law  $u(t) = \kappa(x)$  with  $\kappa : \mathcal{D}_x \rightarrow \mathcal{D}_u$ , such that origin of the unperturbed system,  $\dot{x} = f(x, \kappa(x), 0)$  is a unique locally asymptotically stable equilibrium point in  $\mathcal{D}_x$ . Furthermore, assume that the function  $f(x, \kappa(x), d)$  is continuous over  $\mathcal{D}_x \times \mathcal{D}_u \times \mathcal{D}_d$  with Lipschitz continuous derivatives. Let the Lipschitz constants for  $f$  and  $\kappa$  with respect to  $u$  and  $x$  be  $L_{f,u}$  and  $L_{\kappa,x}$ , respectively.

Consider now the sampled data version of system (2.49),

$$\dot{x} = f(x, \kappa(x_k), d), \tag{2.50}$$

where,  $u(t) = \kappa(x_k)$  for  $t \in [t_k, t_{k+1})$ . Let  $g(t)$  be defined as,

$$g(t) := f(x, \kappa(x_k), d) - f(x, \kappa(x), d), \quad (2.51)$$

and this function is bounded by some  $\delta > 0$  such that,  $g(t) \leq \delta$ . A ST sampler to ensure GUUB of the system (2.50) is given by the following theorem:

**Theorem 2.9** *For sampled data system (2.50) along with the assumptions stated above, ST sampler,*

$$t_{k+1} = t_k + \frac{1}{2L} \ln \left( 1 + \frac{2\delta}{\|f(x^*, \kappa(x_k), d^*)\|} \right), \quad (2.52)$$

*ensures GUUB of the closed-loop system, with  $L = L_{f,u}L_{\kappa,x}$  and  $(x^*, d^*) := \operatorname{argmax}_{(y_1, y_2) \in \mathbb{R}^n \times \mathcal{D}_d} \|f(y_1, \kappa(x_k), y_2)\|$ .*

Small-gain approach was used in [113] to develop STC, whereby the violation of small-gain condition marks a sampling event and computation of fresh control law, yielding a stable nonlinear system. Additionally, the approach does not require construction of a Lyapunov function. The proposed scheme was successfully applied to a trajectory tracking problem.

*Remark 31 As an extension of their work, the authors highlighted the use of MB estimation of control and output signals instead of the conventional ZOH approximation to further increase the inter-sample time.*

## Discussion

The results presented in [110] take the time quantization aspect of real-time implementation into account and can be extended to time-delay case.

### 2.3.4 Minimum attention and anytime attention control

Two attention-aware control schemes in the domain of NCSs are Minimum Attention, and Anytime Attention control. The former refers to the scenario whereby the control loop is closed only when necessary while satisfying certain performance requirements, for the later, the system is allowed to run in open-loop for a *pre-scheduled* amount of time until the next control input is computed while fulfilling some performance requirements. Previous works on these control schemes had their limitations, e.g., minimum attention control introduced by [114] is computationally intensive even for linear systems. The problem addressed in [115], similar to anytime attention problem, considers the availability of smart actuators which are rarely available.

These limitations were tackled by [116], and preliminary results were presented for nonlinear systems under ST implementation. A variety of minimum attention control laws were given which are computationally efficient at the expense of performance (offered suboptimal solutions). However, the strategy has a drawback as the input might drive the system into a state where more executions are needed to stabilize the system making the method computationally intensive [95]. For anytime attention control problem, a set of inputs was computed that let the

system run in open loop for a given time duration.

This problem was addressed by [117] using the  $\infty$ -norm-based extended control Lyapunov function (CLF), which allowed the minimum attention control problem to be formulated as a linear program solved efficiently online. Additionally, they considered only a finite number of possible inter-execution times.

## Discussion

A comparison was presented between minimum attention control problem and STC by [117]. The difference lies in the fact that, the ST strategy is *emulation-based* which requires a two-step approach to design the controller i.e., firstly a feedback controller is designed assuming ideal communication and then the triggering mechanism is designed. This approach seldom gives an optimal solution. As compared with this, minimum attention control considers the control and triggering mechanism design simultaneously, and is more likely to yield a close-to optimal design. It was shown that minimum attention control outperformed the ST control scheme.

### 2.3.5 Miscellaneous results

The results for ETNC for DT systems were also extended to ST scheme by [88]. A simulation study was done in [118] on first order processes under STC framework. The proposed methodology uses a PI controller and disturbance observer, and considers process time-delays larger than the inter-sampling times.

For the first time, ST scheme for nonlinear stochastic systems with additive

noise was considered by [119]. Strictly positive inter-execution times were observed that guarantee  $p$ -moment stability of the process.

*Remark 32* As possible future extensions of this work, the authors pointed out to:

1. *Obtain a less conservative sampling rule by following the analysis for deterministic systems to further increase the inter-execution times,*
2. *Study the robustness against task delay, and*
3. *To apply the methodology to situations with limited control updates or state sampling.*

Design of ST controller with the switched system approach was presented in [120] to further improve the  $\mathcal{H}_2$  and  $\mathcal{H}_\infty$  performance. The problem was solved by first considering a linear quadratic problem for periodic sampling case, then using it for the development of  $\mathcal{H}_2$  and  $\mathcal{H}_\infty$  performance indices. The proposed methodology was validated on numerical examples.

## 2.4 Conclusion

During the last decade, the literature on ET and ST control strategies has expanded to develop systems theory on the subject due to a significant cost saving that these schemes offer as compared to the conventional periodic triggering control methodology. In this survey, we tried to cover most of the relevant theoretical aspects to give a big picture of the progress, in an effort to help organize the scattered results and also ease the search of potential research avenues.

Most of the works cited here, particularly in the context of ET-based output feedback control ([41]–[46] and [48]), and estimation ([50]–[56]) consider a delay free communication channel, translating into the consideration of real-time network conditions as a possible area for future research. In addition, the area in which the subject needs further efforts is the development of comprehensive co-design methodologies while considering practical aspects of actual implementation scenarios. In the same spirit, the work presented in this thesis addresses the issue of implementation of aperiodic triggering techniques over IEEE 802.15.4 protocol.

| <b>Ref.</b>                 | <b>Issues Considered</b>   |
|-----------------------------|--|
| [17]                        | Bounded time-varying delays in CA channel. Incorporates the delay in system definition and co-design framework.                |
| [19]                        | Time-delay in SC and CA channels. Maximizes the inter-transmission times which reduces the effect of the delays.               |
| [21]                        | Uses a congestion avoidance module, which schedules the signals, to lessen the effect of network induced delay.                |
| SCHEDULING AND EVENT DESIGN |  |
| [18]                        | Delays in embedded systems, i.e., the time it takes to read the state, compute the control law, and apply it on the actuators. |
| [23]                        | Delays in embedded systems.  |
| CO-DESIGN OF ET SYSTEMS     |  |
| [26]                        | Transmission delays. Uses a delay system model which models delays and the event-driven system.                                |

|  |  |
|--|--|
| [27]   | Co-design algorithm gives the maximum allowable communication delay bound (MADB) and the maximum allowable number of successive packet losses (MANSPL).  |
| [28]   | Robust against time delays.  |
| [31]   | The model considers retransmission of unsuccessful trials, and it interprets them as a delay associated with these retransmissions.  |
| [35]   | Result is valid in the presence of delays and dropouts if instantaneous error-free acknowledgment channel exists.  |
| [29]   | A TCP-like communication system is assumed, i.e. the communication system is equipped with an acknowledgement channel that informs the event-trigger, whether a transmission has been successful. The acknowledgement channel is error-free. |
| STATE FEEDBACK BASED ETC                             |  |
| [39]   | Bounded delays. Considers appropriate pre-processing of the delayed information.   |
| OUTPUT FEEDBACK BASED ETC AND EVENT BASED ESTIMATION |  |
| [47]   | Time-delay in SC and CA channels. Achieves finite-gain $\mathcal{L}_2$ stability in the presence of arbitrary constant or time-varying delays, with bounded jitters.   |
| [49]   | The analysis accounts for bounded time-delays.   |

|  |   |
|--|---|
| [55]   | The analysis can be extended to include packet delays, dropouts and disorder.   |
| ET QUANTIZED SYSTEMS                         |   |
| [61]   | ET-based CA network. Uses predictive-control methodology to deal with packet delays, dropouts and disorders                             |
| [62]   | Random transmission delays.   |
| [30]   | Considers delay model to take into account ET mechanism, delays, and quantization in a unified framework.                               |
| [63]   | Analyzes asymptotically stabilizing bit-rates for maximum acceptable delays.  |
| [60]   | Provides the acceptable delay, preserving ISS.  |
| ETC OF DECENTRALIZED AND DISTRIBUTED SYSTEMS |   |
| [64]   | Briefly considers bounded delays.   |
| [68]   | Reduces the transmission payload which indirectly reduces delays.   |
| [69]   | Povides global tradeoff condition between all transmission periods and all kinds of allowable delays that ensures asymptotic stability. |
| [65]   | Reduces network traffic which decreases the size of time delays, and packet loss probability.   |
| [70]   | Predicts maximal allowable transmission delay of a subsystems broadcast based on the local information.                                 |



|  |  |
|--|--|
| [71]   | Proves that for non-zero transmission delays less than the corresponding deadline, the NCS is asymptotically stable. |
| [74]   | Proposes two communication protocols which guarantee stable behavior in the presence of network imperfections.       |
| [83]   | Considers time-varying network delays.   |
| EVENT-BASED MODEL PREDICTIVE CONTROL (MPC)         |  |
| [87]   | Bounded delays in SC and CA channels. Gives an application level solution.   |
| [90]   | Assumes that the upper-bound on the delay is bigger than the sampling time.  |
| EVENT-BASED PID CONTROLLER AND ACTUATOR SATURATION |  |
| [93]   | Uses PIDPLUS, a NCS version of PI controller that deals with packet losses and time delays.                          |
| MISCELLANEOUS RESULTS FOR ET SYSTEMS               |  |
| [97]   | Bounded-time delays. Gains apriori knowledge of the delays by using dynamic priority exchange scheduling.            |
| STABILITY OF ST SYSTEMS                            |  |
| [101]  | Robust against scheduling delays induced by the real-time schedulers.  |
| STC OF NONLINEAR SYSTEMS                           |  |

|                                      |  |
|--------------------------------------|--|
| [112]                                | Small time-delays. Proposes a simple ST sampler for perturbed nonlinear systems. |
| MISCELLANEOUS RESULTS FOR ST SYSTEMS |  |
| [118]                                | Considers process time-delays larger than the inter-sampling times.              |

Table 2.1: List of papers which consider time-delays in aperiodically triggered NCSs.

# CHAPTER 3

## EVENT-BASED CONTROL OVER IEEE 802.15.4 NETWORK

### 3.1 Introduction

The availability of low-cost wireless networked platforms with sensing and actuation capabilities has escalated the use of networked feedback loops and plant monitoring for industrial applications since the last decade. The reason for this high demand can be attributed to the advantages of wireless networks over the traditional point-to-point communication, such as the ease of maintenance and the provision of distributed control. In a WNCS, some of the challenges which require special design considerations are network imperfections, low bandwidth, and the optimization of control cost, communication capabilities and computa-

tional resources. In order to mitigate these problems, several strategies can be followed, such as designing controllers which are robust to network imperfections, installing high-bandwidth network, using intelligent techniques for balancing the communication load especially when the network is shared [3], or implementing aperiodic transmission schemes such as event-triggered (ET) control, whereby an event implies the crossing by the plant state, of a predefined threshold. The standard implementations of feedback control over a network or embedded platform use periodic scheme for which a mature systems theory exists, however, it causes an enormous waste of communication bandwidth, especially when there is no need for a corrective feedback signal. In contrast, the ET transmission of state information to the controller saves considerable amount of communication resources [4, 5, 6]. In the context of aperiodic state transmission, the terminology *co-design* is used for simultaneous design and/or optimization of control and event condition, however, in the forthcoming chapters the simultaneous optimization of both these designs will be referred to as *co-optimization*.

The economic and environmental constraints on WNCSS necessitate efficient use of the available resources. This requires simultaneous optimization from control, computational, and information-theoretic perspectives, while incorporating the constraints of network artifacts, and low power consumption. Satisfying all these requirements at the same time is very difficult, if not impossible. For instance, co-optimization of control and communication costs results in opposing requirements because allowing minimal bandwidth usage results in degraded control

performance and vice versa. Hence, the designer should set appropriate priorities and trade-offs according to the performance requirement of the WNCS.

The objective in this chapter is to co-optimize control cost, communication bandwidth, and computational resources, with the main emphasis on control performance. The WNCS considered, comprises of multiple plants with feedback loops closed over a shared wireless communication network based on IEEE 802.15.4 protocol which introduces bounded-but-random delays in state transmissions. Co-optimization is achieved by using linear-quadratic (LQ) controller with ET state transmissions; the event condition is based on a comparison between the cost of the ET system against the cost of a nominal/reference periodic system. Delays are tackled by introducing modifications to the LQ controller using asynchronous sampled-data system (ASDS) approach [121]. Additionally, the scheme is shown to be fairly robust against packet drops. A brief account of some highlighted works in the related field is given as follows.

The co-optimization of electric power network performance and information flow over the communication network was considered in [122]. While considering network imperfections, [123] presented a framework for the joint optimization of control, device energies, and communication bandwidth. For the scenario of multiple control loops sharing single communication network to transmit the state information, the problem of distributing network bandwidth while optimizing the total control performance was tackled in [124]. The authors also considered packet delays and dropouts, and demonstrated that an improved LQ performance can be

obtained if the network quality of service is predicted.

To decouple communication from control, [125] limited the use of communication channel in terms of maximum allowable transmission rate which depended upon the maximum number of transmission slots offered by the channel. The authors used ET scheme and the solution of stochastic optimal control problem in order to determine optimal transmission rate for each system while optimizing the control cost.

In the context of network artifacts, [126] presented two communication protocols for a distributed ET scheme to cope with delays and packet dropouts; both protocols showed good performance against network imperfections. Asymptotic stability, and lower-bound for the inter-event times were achieved for the system using time-dependent triggering functions. Another work demonstrating the observer-based stabilization of NCSs having random delays in sensor-controller and controller-actuator channels, was presented in [127]. A model-based predictive methodology was introduced in [128] to compensate for the time delays and dropouts. The main characteristics of the scheme were that the NCS can work under random delay and packet loss with realistic structural assumptions, and a mechanism to reduce the effects of these network imperfections on the deviation of plant state estimates from actual plant states.

IEEE 802.15.4 wireless protocol, which forms the basis for industrial standards like WirelessHART and ISA100, has been the center of attention since its availability as the low data-rate and energy-efficient protocol [9]–[10]. Some of

the prominent studies that fall in the domain of network modeling, optimization, and stability analysis of the network for control of multiple loops sharing common wireless network to close the feedback loops can be found in [129]–[130]. To reduce the transmission energy in wireless network-based control systems, [131] presented the optimization problem as a trade-off between the control performance and wireless nodes’ power consumption. However, the authors did not consider aperiodic state information transmission. [132] focused on ET, ST, and hybrid techniques to minimize energy consumption in sensor/actuator networks. [8] altered IEEE 802.15.4 protocol for flexible implementation of ET, ST, and hybrid communication mechanisms. Specifically, the authors introduced the provision of increasing the number of guaranteed time-slots beyond seven, which is the limit defined in the regular IEEE protocol. The experimental results showed significant reduction in energy consumption as compared with the periodic implementation.

The chapter is organized as follows. Section 3.2 defines the problem with an overview. Section 3.3 presents the asynchronous LQG controller and the event condition design is given in Section 3.4. Network-related discussion is given in Section 3.5. Simulation results are reported in Section 3.6 and Section 6.7 concludes the chapter. For better readability, proof of forthcoming theorem is given in the appendix.

*Notations:* Set of real numbers is denoted as  $\mathbb{R}$ . Strictly positive real numbers and integers are represented by  $\mathbb{R}_+$  and  $\mathbb{N}$ , respectively, while the set of positive integers including zero is denoted as  $\mathbb{Z}_{\{0,+\}}$ . The expected values are represented

as  $E[ \cdot ]$ .

## 3.2 Problem definition and overview

In the scenario discussed here,  $N$  *independent* continuous-time (CT) LTI systems, represented as

$$\begin{aligned} \dot{x}^s(t) &= A^s x^s(t) + B_1^s u^s(t) + B_2^s w^s(t), \quad x^s(0) = x_0^s, \\ y^s(t) &= C^s x^s(t) + v^s(t), \end{aligned} \tag{3.1}$$

are considered, where  $s \in \{1, \dots, N\}$ ,  $x^s(t) \in \mathbb{R}^n$  is system's state vector,  $u^s(t) \in \mathbb{R}^m$  is the control input,  $y^s \in \mathbb{R}^q$  is the vector of system outputs,  $w^s(t) \in \mathbb{R}^l$  and  $v^s(t) \in \mathbb{R}^q$  are zero-mean white Gaussian process and measurement noise with covariance  $W^s$  and  $V^s$ , respectively, and the quadruple  $(A^s, B_1^s, B_2^s, C^s)$ , where  $A^s \in \mathbb{R}^{(n \times n)}$ ,  $B_1^s \in \mathbb{R}^{(n \times m)}$ ,  $B_2^s \in \mathbb{R}^{(n \times l)}$  and  $C^s \in \mathbb{R}^{(q \times n)}$ , represent the system model. The superscript  $s$  will be dropped in the subsequent discussion for ease.

The feedback loops of these systems are closed over a shared wireless communication medium as shown in Fig. 3.1. The ET-LQG controllers are wired with the network manager (NM), and sensor nodes acquire all the states and transmit to respective controllers wirelessly using ET sampling. In particular, the state of (3.1) is periodically monitored after every  $\alpha \in \mathbb{R}_+$  units of time to compare its cost against that of a periodically-triggered system, i.e., *reference*. The reference system is the implementation of (3.1) over a dedicated and perfect communication channel with  $\alpha$ -periodic triggering; the cost evolution of this system is simulated



offline and stored in the ET setup.

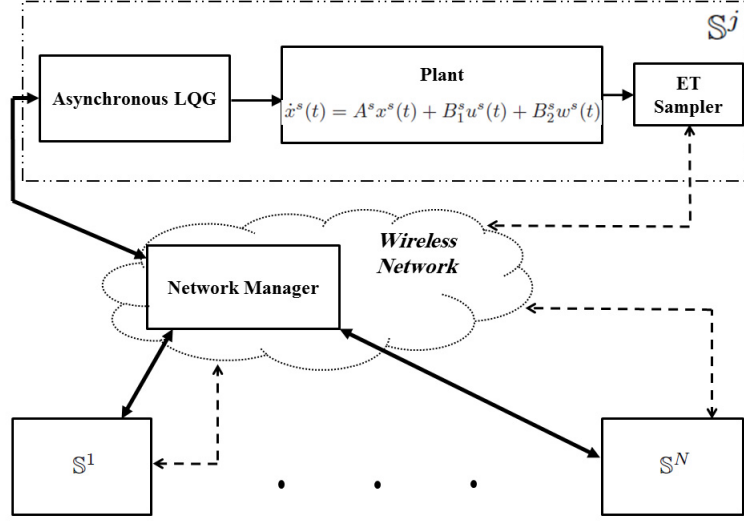


Figure 3.1: Wireless networked control system with  $N$  control loops. Solid line: wired connection; dashed line: wireless link.

An event occurs and the state is transmitted to the controller at  $\delta_i$ , where  $i \in \mathbb{Z}_{\{0,+\}}$ , when the aperiodic system's cost exceeds a threshold which depends on the reference cost. This transmission reaches the controller at  $\rho_j$ , where  $j \in \mathbb{Z}_{\{0,+\}}$ , after encountering a bounded random time-delay induced by the network,  $\sigma_{n,i} \leq \bar{\sigma}_n \in \mathbb{R}_+ \forall i$ . The controller takes  $\sigma_c \in \mathbb{R}_+$  units of time to estimate the state and compute the controller output  $u$  which will be applied at  $\eta_k$ , where  $k \in \mathbb{Z}_{\{0,+\}}$  and  $\eta_k = \rho_j + \sigma_c$ . The difference between consecutive events is denoted as  $\Delta_i \triangleq \delta_i - \delta_{i-1}$  and that between corresponding consecutive controller updates is represented by  $\Theta_k \triangleq \eta_k - \eta_{k-1}$ . Note that  $i = j = k$  translates into  $i$ -th event, and the corresponding  $j$ -th reception and  $k$ -th control update. The timing diagram in Fig. 3.2 illustrates these ideas.

The event intervals are both upper and lower-bounded, i.e.,  $\alpha \leq \Delta_i \leq \Gamma\alpha$ ,

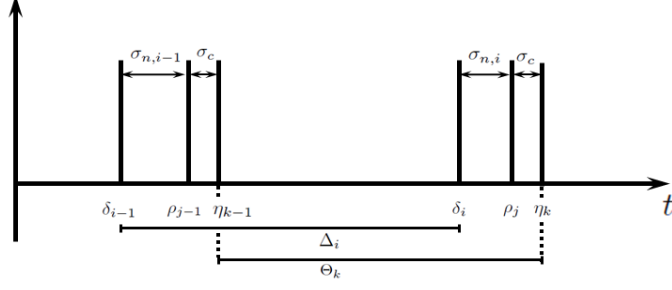


Figure 3.2: Timing diagram illustrating sampling times for ET systems with random transmission delays.

where  $1 < \Gamma \in \mathbb{Z}_+$ . The upper-bound is introduced to ensure bounded latency, and the choice of  $\alpha$  depends on the wireless protocol's parameters and systems' dynamics, as will be detailed in the forthcoming discussion. For the worst-case sampling period  $\Gamma\alpha$ ,  $\overline{\Delta} \triangleq \Gamma\alpha$  and  $\overline{\Theta} \approx \Gamma\alpha$  due to random delay.

**Assumption 1** *It is assumed that,*

1.  $\delta_0, \rho_0, \eta_0 = 0$ ,
2. *all the states of the plant are available for measurement,*
3. *the computational delay  $\sigma_c$  is constant,*
4. *the received states are time-stamped, i.e.,  $\delta_i$  is received along with  $i$ -th transmission of the state,*
5. *the delay  $\sigma_{n,i} + \sigma_c$  is less than  $\Delta_i$ , which implies that  $\delta_i < \eta_k, \forall i = k$ , and*
6.  $\Theta_k/\Delta_i$  *is irrational for all  $i, k$ .*

*Remark 33* *The last assumption is realistic due to the random nature of network-*

induced delay; this implies that there is a high probability that the ratio

$$\frac{\Theta_k}{\Delta_i} = 1 + \frac{\sigma_{n,i} - \sigma_{n,i-1}}{\Delta_i},$$

as irrational.

The wireless network uses a slotted communication mechanism which is based on the beacon-enabled mode of IEEE 802.15.4 protocol. The beacon interval (BI) is fixed at  $\alpha$ , and each sensor node is assigned a fixed time-slot in the contention-free period (CFP) of the superframe (SF). The contention access period (CAP) is left unused and an optional inactive period is allowed; the structure of BI is shown in Fig. 3.3. Due to  $BI = \alpha$  and fixed slots, the time to check the ET condition for each system will fall in its respective time-slot. Consequently,  $\delta_i$  for a system will correspond to its assigned slot in case of the occurrence of an event.

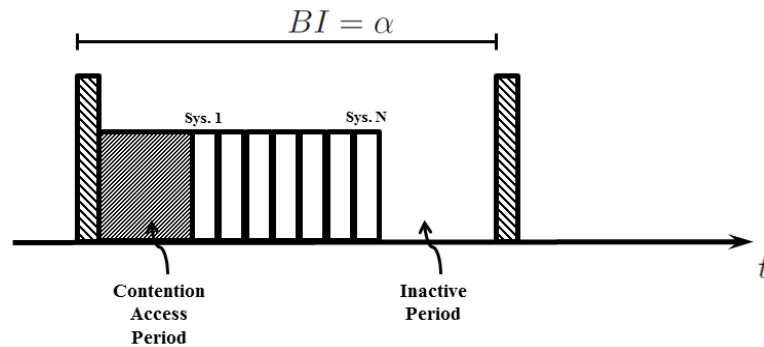


Figure 3.3: Superframe structure of IEEE 802.15.4 protocol.

**The problem** is to optimally control the participating systems, represented by (3.1) in the presence of network and computational delays,  $\sigma_{n,i}$  and  $\sigma_c$ , while saving the communication bandwidth of IEEE 802.15.4 network using ET scheme.

### 3.3 ET LQG controller

Due to the sampling scheme described above, (3.1) can be viewed as a *dual-rate* ASDS because the sampling interval at the sensor node is different from that of the control update, i.e.,  $\Delta_i \neq \Theta_k \forall i = k$ , hence with Assumption 1(2)

$$\begin{aligned} \dot{x}(t) &= Ax(t) + B_1u(t) + B_2w(t), \quad x(0) = x_0, \\ y(\delta_i) &= x(\delta_i) + v(\delta_i), \\ u(t) &= u_{\eta_k} = f(\hat{x}(\delta_i)), \quad \forall t \in [\eta_k, \eta_{k+1}), \end{aligned} \tag{3.2}$$

where  $f(\cdot) : \mathbb{R}^n \rightarrow \mathbb{R}^m$  is a causal mapping which optimizes a certain cost function.

The solution to the optimal control problem of ASDS was given in [121], where the sampling (at the sensors) and hold (at the controllers) times were disproportionate, i.e.,  $\delta_i \neq \eta_k$ . It was shown that the control that minimizes certain cost function depends on the state estimated for  $\eta_k$  using the state information at  $\delta_i$ . It was assumed that the sampling, and consequently the hold rates are fixed, however, in the case under consideration, the sampling time is aperiodic which renders the time of control application aperiodic. The sampling and hold times are translated into event and control update instants, respectively.

**Assumption 2** *It is assumed for all  $i, k$  that,*

1. *the discrete-time (DT) systems  $(C, A_{\Delta_i})$  are detectable,*
2. *the DT systems  $(A_{\Theta_k}, B_{\Theta_k})$  are stabilizable,*
3. *system (3.2) is stabilizable and detectable,*

where  $A_a = e^{A(a)}$  and  $B_a = \int_0^a A_s B_1 ds$  are the discretized system matrices for any time-interval  $a$ . In the context of ET, these assumptions imply that non-pathological sampling will not occur when the sampling interval varies between the enforced upper- and lower-bounds.

Let  $\hat{x}_\tau$ ,  $x_\tau$ , and  $u_\tau$  represent the estimated state, sampled-state, and control input at time  $\tau$ , respectively, and  $Q_\tau \in \mathbb{R}^{n \times n} > 0$  and  $R_\tau \in \mathbb{R}^{m \times m} > 0$  denote the state and input weighting matrices at  $\tau$ , then the controller which minimizes following discrete cost function

$$J_\Theta = \sum_{k=0}^{K-1} \frac{1}{K\eta_k} \mathbb{E} \left[ x_{\eta_k}^T Q_{\eta_k} x_{\eta_k} + u_{\eta_k}^T R_{\eta_k} u_{\eta_k} \right], \quad (3.3)$$

is given as

$$\begin{aligned} u_{\eta_k} &= -(R_{\eta_k} + B_{\Theta_k}^T P_k B_{\Theta_k})^{-1} (B_{\Theta_k}^T P_k A_{\Theta_k}) \hat{x}_{\eta_k}, \\ &= -K_{\eta_k} \hat{x}_{\eta_k}, \end{aligned} \quad (3.4)$$

where, the state estimate  $\hat{x}_{\eta_k}$  is given as

$$\begin{aligned} \hat{x}_{\eta_k} &= A_{\eta_k - \delta_i} \hat{x}_{\delta_i} + B_{\eta_k - \delta_i} u_{\eta_{k-1}}, \quad \forall k = i, \\ \hat{x}_{\eta_0} &= x_0. \end{aligned} \quad (3.5)$$

$Q_{\eta_k}$  and  $R_{\eta_k}$  are given as

$$Q_{\eta_k} = \int_{\eta_{k-1}}^{\eta_k} [A_{s-\eta_{k-1}}^T A_{s-\eta_{k-1}}] ds; \quad R_{\eta_k} = \int_{\eta_{k-1}}^{\eta_k} [B_{s-\eta_{k-1}}^T B_{s-\eta_{k-1}}] ds, \quad (3.6)$$

and  $\{P_k\}$  is given by the unique positive semi-definite solution of DT Riccati

equation

$$P_k = A_{\Theta_k}^T [P_{k+1} - P_{k+1} B_{\Theta_k} (R_{\eta_k} + B_{\Theta_k}^T P_{k+1} B_{\Theta_k})^{-1} B_{\Theta_k}^T P_{k+1}] A_{\Theta_k} + Q_{\eta_k}, \quad (3.7)$$

$$P_K = 0.$$

According to (3.5), the estimated state for time instant  $\eta_k$  depends upon the state estimate for  $\delta_i$ , which is given as

$$\hat{x}_{\delta_i} = \hat{x}_{\delta_i^-} + S_i [I + S_i]^{-1} (y_{\delta_i} - \hat{x}_{\delta_i^-}), \quad (3.8)$$

where

$$\hat{x}_{\delta_i^-} = A_{\delta_i - \eta_{k-1}} \hat{x}_{\eta_{k-1}} + B_{\delta_i - \eta_{k-1}} u_{\eta_{k-1}}, \quad (3.9)$$

$$\hat{x}_{\delta_0^-} = x_0,$$

and  $\{S_i\}$  is the solution of following Riccati equation

$$S_i = A_{\Delta_i} S_{i-1} A_{\Delta_i}^T - A_{\Delta_i} S_{i-1} [I + S_{i-1}]^{-1} S_{i-1} A_{\Delta_i}^T + W_{\delta_i}, \quad (3.10)$$

$$S_0 = 0,$$

with  $W_{\delta_i} = \int_{\delta_{i-1}}^{\delta_i} A_{\delta_i-t} B_2 B_2^T A_{\delta_i-t}^T dt$ .

However, the time-varying controller (3.4) is computationally intensive which translates into larger  $\sigma_c$ , and the solution of (3.7) requires the knowledge of  $P_{k+1}$  which can not be determined offline due to aperiodic triggering. To deal with these problems, worst-case system is defined (from control perspective) as the one with control update interval  $\bar{\Theta} \forall k$ , and optimization done over infinite horizon

which render (3.3) as

$$J_{\Theta} = \lim_{K \rightarrow \infty} \sum_{k=0}^{K-1} \frac{1}{K \eta_k} \mathbb{E} \left[ x_{\eta_k}^T Q_{\Theta} x_{\eta_k} + u_{\eta_k}^T R_{\Theta} u_{\eta_k} \right]. \quad (3.11)$$

This assumption allows the designer to compute a constant control gain

$$K_{\Theta} = (R_{\Theta} + B_{\Theta}^T P B_{\Theta})^{-1} (B_{\Theta}^T P A_{\Theta}), \quad (3.12)$$

offline, such that

$$u(t) = -K_{\Theta} \hat{x}(\eta_k), \quad \forall t \in [\eta_k, \eta_{k+1}), \quad (3.13)$$

with the ARE being:

$$P = A_{\Theta}^T [P - P B_{\Theta} (R_{\Theta} + B_{\Theta}^T P B_{\Theta})^{-1} B_{\Theta}^T P] A_{\Theta} + Q_{\Theta}. \quad (3.14)$$

In order to maintain the estimation accuracy, the estimation is done using (3.5), (3.8), (3.9), and (3.10). To further reduce the computational time, the integral in (3.10) is computed offline for the interval  $\alpha$ , i.e.,  $W_{\alpha}$ . Then during the real-time estimation, it is multiplied with the number of  $\alpha$ -spaced intervals in  $\Delta_i$  to get  $W_{\delta_i}$ ; this is true because the integrand of (3.10) is constant. In what follows, it is shown that the actual cost of the aperiodic system is lower than (or at most equal to) the cost paid for the worst-case system.

**Theorem 3.1** *If the system (3.2) implements controller (3.13) with the Assump-*

tions 1 and 2, then the value of the cost

$$J_{\Theta} = \sum_{k=0}^{K-1} \frac{1}{K\eta_k} \mathbb{E} \left[ x_{\eta_k}^T Q_{\Theta} x_{\eta_k} + u_{\eta_k}^T R_{\Theta} u_{\eta_k} \right], \quad (3.15)$$

for the ET system is less than (or at most equal to) the cost paid for the system with worst-case sampling period  $\bar{\Theta}$ , i.e.,

$$J_{\Theta} \leq \bar{J} \triangleq \frac{1}{K\bar{\Theta}} \mathbb{E} \sum_{k=0}^{K-1} \left[ x_{\eta_k}^T Q_{\bar{\Theta}} x_{\eta_k} + u_{\eta_k}^T R_{\bar{\Theta}} u_{\eta_k} \right]. \quad (3.16)$$

**Proof of Theorem 3.1:** For any interval  $\Delta_i$  and corresponding  $\Theta_k$ ,

$$\begin{aligned} J_{\Theta_k} &= \frac{1}{\Theta_k} \mathbb{E} \left[ \int_{\eta_{k-1}}^{\eta_k} \left( x^T(t) Q_{\Theta} x(t) + u_{\eta_{k-1}}^T R_{\Theta} u_{\eta_{k-1}} \right) dt \right], \\ &= \frac{1}{\Theta_k} \mathbb{E} \left[ \int_{\eta_{k-1}}^{\eta_k} \left( x^T(t) Q_{\Theta} x(t) + \hat{x}_{\eta_{k-1}}^T K_{\Theta}^T R_{\Theta} K_{\Theta} \hat{x}_{\eta_{k-1}} \right) dt \right], \end{aligned} \quad (3.17)$$

where  $u_{\eta_{k-1}} = -K_{\Theta} \hat{x}_{\eta_{k-1}}$  for all  $t \in [\eta_{k-1}, \eta_k)$ . The constant control input renders the second term of the integral as constant, which results in,

$$J_{\Theta_k} = \frac{1}{\Theta_k} \mathbb{E} \left[ \underbrace{\int_{\eta_{k-1}}^{\eta_k} x^T(t) Q_{\Theta} x(t) dt}_{\triangleq \mathcal{J}_{1,k}} \right] + \hat{x}_{\eta_{k-1}}^T K_{\Theta}^T R_{\Theta} K_{\Theta} \hat{x}_{\eta_{k-1}}. \quad (3.18)$$

Similarly, for the system with worst-case sampling time, the cost paid for any interval  $\bar{\Theta}$  will be,

$$J_{\bar{\Theta}} = \frac{1}{\bar{\Theta}} \mathbb{E} \left[ \underbrace{\int_{\eta_{k-1}}^{\eta_{k-1} + \bar{\Theta}} x^T(t) Q_{\bar{\Theta}} x(t) dt}_{\triangleq \mathcal{J}_{2,k}} \right] + \hat{x}_{\eta_{k-1}}^T K_{\bar{\Theta}}^T R_{\bar{\Theta}} K_{\bar{\Theta}} \hat{x}_{\eta_{k-1}}. \quad (3.19)$$



It can be seen that  $\mathfrak{J}_{1,k} \leq \mathfrak{J}_{2,k}$  due to the fact that  $\Theta_k \leq \bar{\Theta}$ . Now comparing (3.18) and (3.19) and taking sum over complete time horizon, we get

$$\sum_{k=0}^{K-1} \mathfrak{J}_{1,k} \leq \sum_{k=0}^{K-1} \mathfrak{J}_{2,k}, \quad (3.20)$$

and due to the fact that  $\mathfrak{J}_{1,k} \leq \mathfrak{J}_{2,k}$ , the LHS of (3.20) will be at most equal to the RHS. This completes the proof.

### 3.4 Event condition

As mentioned earlier, the plant's state is periodically monitored. At every periodic instant, the cost  $J_{\Theta}(p\alpha)$ , where  $p \in \{0, 1, 2, \dots\}$ , of ET system is compared against the optimal cost of reference system

$$\begin{aligned} x((p+1)\alpha) &= Ax(p\alpha) + B_1u(p\alpha), \\ y(p\alpha) &= x(p\alpha) + v(p\alpha), \\ u(p\alpha) &= -(R_{\alpha} + B_{\alpha}^T P B_{\alpha})^{-1} (B_{\alpha}^T P A_{\alpha}) \hat{x}(p\alpha), \\ &= -K_{\alpha} \hat{x}(p\alpha), \end{aligned} \quad (3.21)$$

which is given as

$$J_d^*(p\alpha) = \mathbb{E}[x_{p\alpha}^T P_{\alpha} x_{p\alpha}], \quad (3.22)$$

where  $P_\alpha$  is the solution of the following DT ARE

$$P_\alpha = A_\alpha^T [P_\alpha - P_\alpha B_\alpha (R_\alpha + B_\alpha^T P_\alpha B_\alpha)^{-1} B_\alpha^T P_\alpha] A_\alpha + Q_\alpha, \quad (3.23)$$

and the measurement noise  $v(p\alpha)$  is zero-mean white Gaussian noise sequence with the variance  $V \forall p$ . The cost evolution  $J_d^*(p\alpha)$  is simulated offline and stored in the ET setup. When  $J_\Theta(p\alpha)$  crosses  $J_d^*(p\alpha)$ -dependent threshold, then the state is transmitted to the controller at  $\delta_i$ , i.e.,

$$\delta_i = \{t | \delta_i - \delta_{i-1} \leq \bar{\Delta} \wedge J_\Theta(p\alpha) \geq \gamma J_d^*(p\alpha) + \epsilon\}, \quad (3.24)$$

where  $\delta_{-1} = \delta_0 = 0$ , and  $\gamma \geq 1$  determines the amount of control cost that the designer is ready to trade for the reduction in the communication cost, and  $\epsilon \in \mathbb{R}_+$ . The simulation studies for various models show that the value of  $\epsilon$  should be chosen 10 – 20% less than the variance of process disturbance  $W$ . It should be noted that large values of  $\epsilon$  have adverse effect on the average cost and bandwidth usage due to the fact that when the cost approaches below  $\epsilon$  the system starts transmitting at  $\bar{\Delta}$ , which translates itself into an increase in cost. This in turn requires more transmissions to reduce the cost.

### 3.5 IEEE 802.15.4 Network

The superframe structure of IEEE 802.15.4 protocol allows a maximum of seven guaranteed time slots (GTSs) in CFP for time critical applications. Hence, in the

proposed ET setup of multiple control loops, a maximum of seven systems are allowed to participate. The BI is fixed to  $\alpha$  and each system is assigned a fixed GTS in the CFP. Hence, the time to check the ET condition and transmission (in case of the occurrence of an event) for each system will fall in its assigned GTS. The contention access period (CAP) is left unused and it can be reserved for other applications over the network.

The choice of  $\alpha$  depends on two factors, i) minimum BI allowed by the protocol, i.e., *minBeaconInterval* or *minBI* for short, and ii) the dominant pole of the fastest control loop in the system  $\lambda_{min}$ . Specifically

$$minBI \leq \alpha \leq \frac{1}{\lambda_{min}}, \quad (3.25)$$

The protocol parameter *minBI* is given as

$$minBI = aBaseSFDuration \times 2^{min\ macBO}, \quad (3.26)$$

where  $aBaseSFDuration \triangleq SFD \equiv$  No. of symbols/Symbol rate and  $min\ macBO = 0$  (SF: Superframe; BO: Beacon Order). The symbol rate and number of symbols can be obtained from [9] for the PHY layer used for a particular application.

### 3.6 Simulation results and discussion

Matlab-based network simulation tool TrueTime [133] is used. Three ( $N = 3$ ) identical inverted pendulum over a moving cart systems represented by (3.2) are considered, with state vector  $x = [y \quad \dot{y} \quad \theta \quad \dot{\theta}]^T$ , where  $y$  and  $\theta$  denote the cart's position and bob's angle, respectively. The system matrices are given as

$$A = \begin{bmatrix} 0 & 1 & 0 & 0 \\ 0 & 0 & -\frac{m_b g}{M_c} & 0 \\ 0 & 0 & 0 & 1 \\ 0 & 0 & \frac{g}{l} & 0 \end{bmatrix}; B_1 = \begin{bmatrix} 0 \\ \frac{1}{M_c} \\ 0 \\ -\frac{1}{M_c l} \end{bmatrix}; B_2 = \begin{bmatrix} 1 \\ 1 \\ 1 \\ 1 \end{bmatrix}. \quad (3.27)$$

The description and values of all the parameters are given in Table 3.1.

Table 3.1: System parameters.

| Parameter        | Description                          | Value                    |
|------------------|--------------------------------------|--------------------------|
| $m_b$            | Bob's mass                           | 1                        |
| $M_c$            | Cart's mass                          | 10                       |
| $l$              | Length of the pendulum               | 3                        |
| $g$              | Gravitational acceleration           | 9.8                      |
| $x_o^1$          | Initial condition of Sys. 1          | $[0.98 \ 0 \ 0.2 \ 0]^T$ |
| $x_o^2$          | Initial condition of Sys. 2          | $[0.4 \ 0 \ 0.1 \ 0]^T$  |
| $x_o^3$          | Initial condition of Sys. 3          | $[1 \ 0 \ 0.6 \ 0]^T$    |
| $V$              | Measurement noise variance           | $0.1 \times 10^{-3}$     |
| $W$              | Process noise variance               | $1 \times 10^{-3}$       |
| $\gamma$         | See eq. (3.24)                       | 15                       |
| $\epsilon$       | See eq. (3.24)                       | $0.8 \times 10^{-3}$     |
| $\Gamma$         | Upper-bound for bounded latency      | 8                        |
| $\sigma_c$       | Computational delay                  | $0.3 \times 10^{-3}$ sec |
| $\bar{\sigma}_n$ | Upper-bound on network induced delay | $10 \times 10^{-3}$ sec  |

**Choice of  $\alpha$ :** From (3.25), the value of  $\alpha$  is upper-bounded by  $1/\lambda_{min}$ . For the

systems defined above,  $\lambda_{min} = 1.8257$  which gives the upper-bound  $\approx 0.55sec$ .

Currently, TrueTime offers ZigBee platform for IEEE 802.15.4 protocol-based simulations and assumes BPSK modulation. Following this information, the protocol-specific parameters taken from [9] are presented in Table 3.2, as the lower-bound  $minBI$  (3.26) depends on them. According to these parameters,  $SFD = 24msec$  which gives  $minBI = \alpha = 24msec$ .

Table 3.2: Parameters of ZigBee protocol.

| Parameter                 | Value                   |
|---------------------------|-------------------------|
| Modulation                | BPSK                    |
| Frequency band            | 915 MHz                 |
| Bit-rate                  | 40 kbits/sec            |
| No. of symbols in a frame | 960                     |
| Symbol rate               | 40 ksymbols/sec         |
| Output power of radios    | 0 - 20 dBm (1 - 100 mW) |

The state trajectories of ET systems are compared with that of  $\alpha$ -periodic systems implemented over ZigBee network with the same delay characteristics. The results are shown in Fig. 3.4, which reveal satisfactory performance of all the systems.

The occurrence of events and network schedule for aperiodic and periodic implementations are shown in figs. 3.5 and 3.6, respectively. The event-rate, i.e., the number of events per second for systems 1, 2, and 3 is 27.77, 28.17, and 27.72, respectively, which translates into %-age decrease in event-rate of 33.5%, 32.4%, and 33.5%, against 41.67 *events/sec* for  $\alpha$ -periodic systems. Furthermore, low usage of the network bandwidth can be seen from Fig. 3.6 for ET implementation, as the GTSs in which events do not occur remain unused. The average costs of

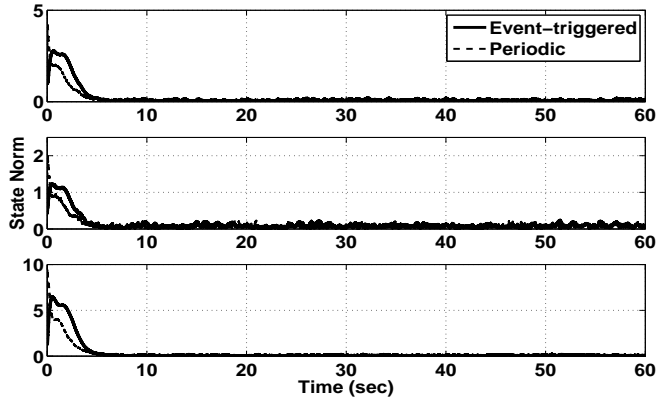


Figure 3.4: State norms of System 1 (Top), System 2 (Middle), and System 3 (Bottom).

ET systems 1, 2, and 3 are 0.1643, 0.0369, and 0.7618, respectively; for periodic implementation the average costs are 0.1352, 0.0295, and 0.636 which reveal %age increase of 21.5%, 25.1%, and 19.8% with ET implementations over  $\alpha$ -periodic triggering.

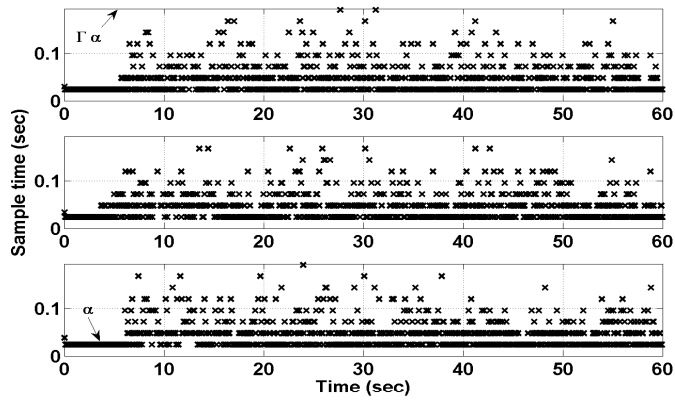


Figure 3.5: Sampling times of System 1 (Top), 2 (Middle), and 3 (Bottom).

Fig. 3.7 shows the estimation error for three systems; the MSEs are  $0.692 \times 10^{-3}$ ,  $0.182 \times 10^{-3}$ , and  $0.426 \times 10^{-3}$  for systems 1,2, and 3, respectively.

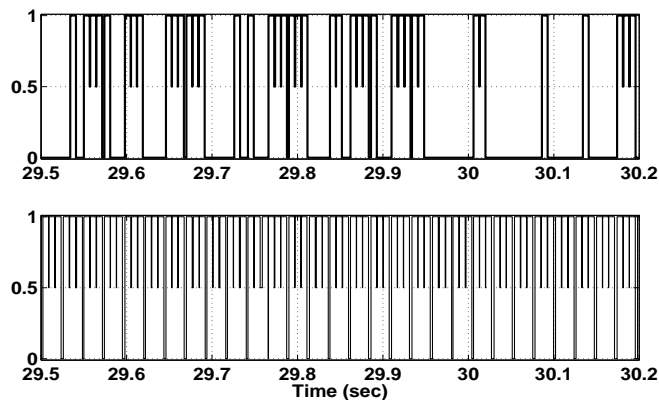


Figure 3.6: Network usage of aperiodic (Top) and periodic (Bottom) implementation. Used slot: 1, free slot: 0.

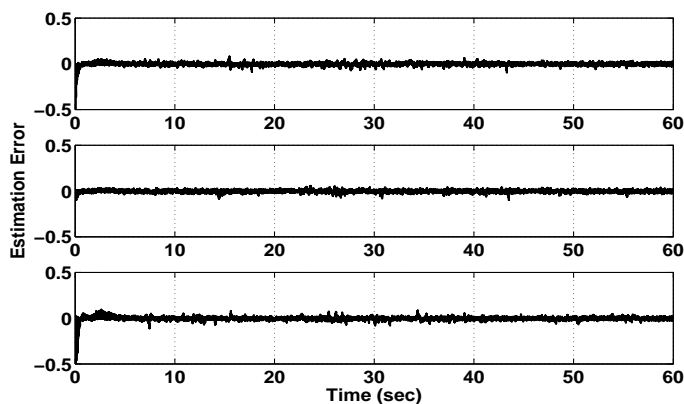


Figure 3.7: Estimation error  $|x(t)| - |\hat{x}(t)|$  of System 1 (Top), 2 (Middle), and 3 (Bottom).

### 3.6.1 Robustness against packet-dropouts:

Although the methodology is not designed to be robust against dropouts, as a test case the implementation is investigated by running the simulation with 5% dropout probability. The resulting performance errors are given in Fig. 3.8 with MSEs for systems 1, 2, and 3 as  $2.5 \times 10^{-3}$ ,  $2.4 \times 10^{-3}$ , and  $3.6 \times 10^{-3}$ . Similarly, the estimation errors are presented in Fig. 3.9 and the MSEs for three systems are  $2.3 \times 10^{-3}$ ,  $2.2 \times 10^{-3}$ , and  $3.6 \times 10^{-3}$ . Furthermore, the resulting average

costs are 0.1661, 0.037, and 0.7620 for systems 1, 2, and 3, which reveal negligible increase in cost against the case when the dropout probability is zero. Also, similar results are observed for the event-rates of three systems. However, higher values of dropout probabilities result in system instability.

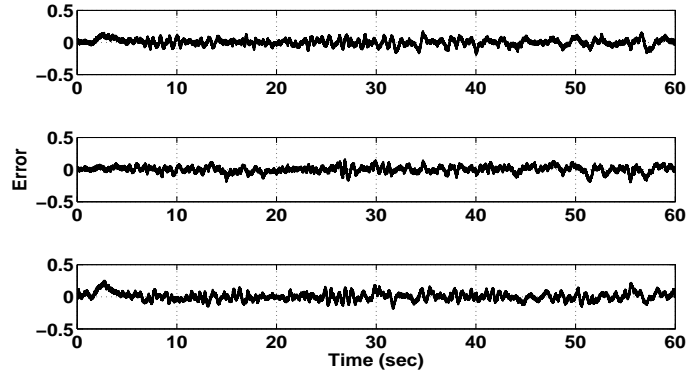


Figure 3.8: Error between state trajectories with and without packet-drop,  $|x_{drop}(t)| - |x(t)|$  of System 1 (Top), 2 (Middle), and 3 (Bottom).

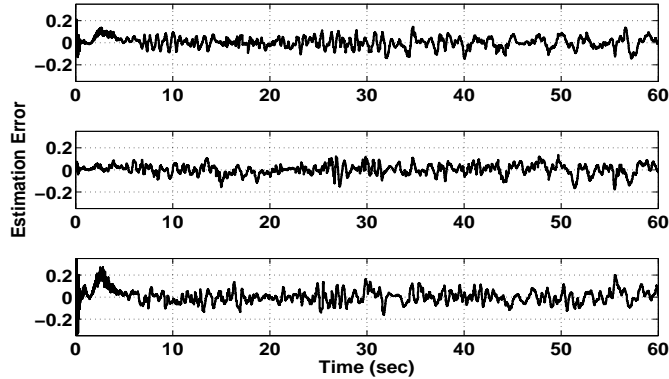


Figure 3.9: Estimation error between state trajectories with and without packet-drop,  $|\hat{x}_{drop}(t)| - |\hat{x}(t)|$  of System 1 (Top), 2 (Middle), and 3 (Bottom).

The reason for this slight robustness can be understood from Fig. 3.10. When the packet arrives at  $\rho_j$  due to  $i + 1$ -th transmission, the controller considers it as  $j$ -th reception, as if there was no transmission at  $\delta_i$ . Moreover, the controller



estimates the state using the information at  $\eta_{k-1}$ .

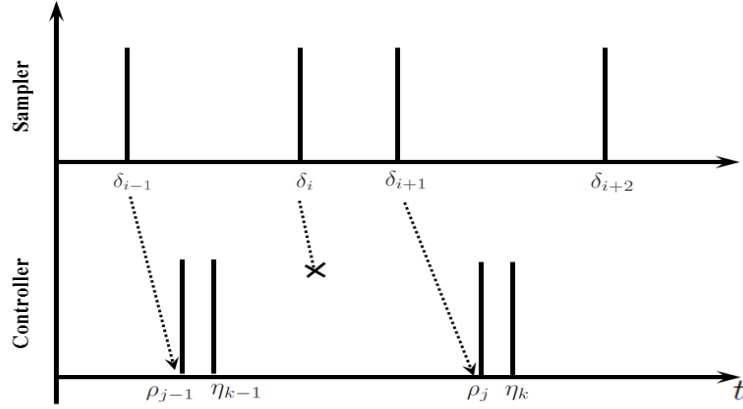


Figure 3.10: Timing diagram illustrating packet-dropouts.

### 3.7 Conclusion

Multiple ET feedback loops were considered which share ZigBee network for sensor-controller communication. In order to take care of the asynchronous nature of transmissions, and network-induced and computational delays, asynchronous LQG controller was used. The proposed event-condition allows transmissions only when the cost of the ET system is above or equal to the threshold dependent upon the cost of reference periodic system. The scheme was simulated in TrueTime and the results showed a significant decrease in the number of events with acceptable control cost. Although the scheme was not designed to handle packet-dropouts, a test case with 5% dropout probability revealed its slight robustness.

The ET scheme is not suitable for applications employing wireless sensor networks due to the limited battery power of the nodes. Furthermore, it may require a separate hardware circuitry appended with the sensor node. Also, in the specific

case discussed in this chapter, the ET methodology does not give a low sampling frequency when the systems are regulated. All these facts motivated us to use ST strategy as described in forthcoming chapters.

## CHAPTER 4

# SELF-TRIGGERED (ST) CONTROL OVER IEEE 802.15.4 NETWORK

### 4.1 Introduction

Previous chapter reported the results of application of ET mechanism over a shared communication channel based on IEEE 802.15.4 protocol. However, for event-triggered sampling, energy consumption at the sensing node is high due to continuous (or periodic) monitoring of the plant state, which is not well-suited for battery powered sensor nodes in a wireless sensor network (WSN). Furthermore, the practical implementation requires a dedicated hardware to check the event condition. ST mechanism introduced in [7], provides a remedy to these problems by *predicting* the next update time on the basis of previously sampled state and

plant dynamics. As an attractive aperiodic scheme, ST methodology has been the focus of many works with prominent studies being [1] for the development of ST LQR controller, [134] and [135] which presented the solution of ST  $\mathcal{H}_2$  and  $\mathcal{H}_\infty$  optimal control problems, [103] and [102] which showed finite-gain  $\mathcal{L}_2$  stability of linear systems affected by bounded disturbances, and [136] for ST model predictive control.

In the same spirit and due to the studies mentioned in Chapter 1, this chapter presents the application of ST methodology for multiple systems sharing a common IEEE 802.15.4 network with following main contributions:

1. Two-level design method for WNCS, which comprises of multiple plants with feedback loops closed over a shared wireless communication network based on IEEE 802.15.4 protocol which introduces random-but-bounded delays in state transmissions,
2. Asynchronous LQG controller to optimize the control cost while dealing with the aperiodic nature of transmissions, and network and computational delays,
3. Novel ST scheme, and
4. Modifications in IEEE 802.15.4 protocol for ST control.

*Organization:* In Section 4.2 the reader will find problem definition and a concise description of the two-level design. Section 4.3 presents the modified LQG controller and proposed novel ST scheme. Section 4.4 details the modified wireless

protocol. Section 4.5 gives the simulation results and discussion, and Section 4.6 concludes the chapter.

*Notations:* In this chapter, sets of real numbers and integers are denoted by  $\mathbb{R}$  and  $\mathbb{Z}$ , respectively. Set of strictly positive real numbers are represented by  $\mathbb{R}_+$  and those including zero are denoted as  $\mathbb{R}_{\{0,+ \}}$ . The set of positive definite and semi-definite integers are represented as  $\mathbb{Z}_+$  and  $\mathbb{Z}_{\{0,+ \}}$ , respectively. The expected values are represented as  $\mathbf{E}[ \cdot ]$ .

## 4.2 Problem Definition and Overview

A class of  $N$  *independent* LQ ST control systems is considered, each associated with a continuous-time (CT) LTI plant given by

$$\begin{aligned} \dot{x}^s(t) &= A^s x^s(t) + B_1^s u^s(t) + B_2^s w^s(t), \quad x^s(0) = x_0^s, \\ y^s(t) &= C^s x^s(t) + v^s(t), \quad s \in \{1, 2, \dots, N\}, \end{aligned} \tag{4.1}$$

where  $x^s(t) \in \mathbb{R}^n$  is system's state vector,  $u^s(t) \in \mathbb{R}^m$  is the control input,  $y^s \in \mathbb{R}^q$  is the vector of system outputs,  $w^s(t) \in \mathbb{R}^l$  and  $v^s(t) \in \mathbb{R}^q$  are zero-mean white Gaussian process and measurement noise with covariance  $W^s$  and  $V^s$ , respectively, and the matrices  $A^s \in \mathbb{R}^{(n \times n)}$ ,  $B_1^s \in \mathbb{R}^{(n \times m)}$ ,  $B_2^s \in \mathbb{R}^{(n \times l)}$  and  $C^s \in \mathbb{R}^{(q \times n)}$  represent the system model. The superscript  $s$  will be dropped in the subsequent discussion for ease.

The feedback loops of these systems are closed over the same wireless communication medium as shown in Fig. 4.1. The controllers are wired with the

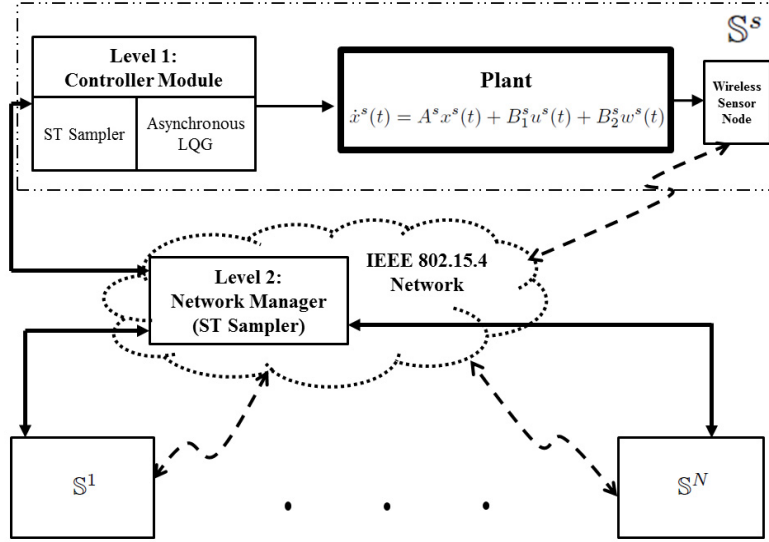


Figure 4.1: Wireless networked control system with  $N$  control loops. Solid line: wired connection; dashed line: wireless link.

network manager (NM), and sensor nodes acquire all the states and transmit to the NM wirelessly. This type of setting, which follows star topology for sensor-controller network and wired connections for controller-actuator link, is common in industrial applications such as process control [10]. Each system  $\mathbb{S}$  implements an asynchronous version of LQG controller based on the results of [121], to ensure control cost optimization in the presence of computational and communication delays, and aperiodic nature of the transmissions. The ST sampler is based on a novel design which uses the cost versus sampling frequency relationship given by [137]. To take the benefit of the proactive nature of ST scheme, IEEE 802.15.4 protocol is modified such that the controllers requesting state information are assigned time slots according to their predicted triggering times instead of fixed slots assigned in the original protocol. The NM gets state information from sensor nodes in their assigned time slots and passes this information to respective con-

trollers. Due to limited bandwidth of the communication network, the number of time slots is restricted to  $N_{max}$  in each beacon interval [9].

To decouple the controller design from ST mechanism synthesis, the sampling time is bounded between  $\alpha \in \mathbb{R}_+$  and  $\Gamma\alpha$ , where  $1 \leq \Gamma \in \mathbb{Z}$  ensures bounded latency. With the introduction of these bounds the overall design is split into two levels, the controller module and NM, and their design is decoupled. This allows independent design of asynchronous LQG controller, ST sampler, and the algorithm for NM because each of these *modules* will have prior knowledge of the sampling interval bounds. The value of  $\alpha$  depends on the communication network's physical layer and the dynamics of the participating plants; the details of the procedure to choose  $\alpha$  will be given in Section 4.4.

*The problem is to implement LQG on the participating systems to optimize the control cost, represented by (4.1), in the presence of network and computational delays, while saving the battery power of the sensor nodes and communication bandwidth in IEEE 802.15.4 network using ST scheme.*

### 4.3 First Level: Controller Module

As mentioned earlier, due to the bounds imposed on the triggering interval the overall design is split into two levels. The level-1 controller module (as shown in Fig. 4.1) is responsible for supplying the control input to the plant, and next sampling time to the level-2 controller, i.e., NM. Every participating system has its own level-1 module. This module is composed of two routines, the first has the

asynchronous LQG controller, and the second consists of the ST sampler. It depends on the designer to implement the level-1 controller on single microprocessor or on two independent computing platforms (one for each routine), in which case the computation time will decrease but at an increased implementation cost (i.e., parallel processing). In this work, it is assumed that both these routines are implemented by single machine to save the implementation cost. Furthermore, some steps are taken to save the computational cost (and time) of control computation, as will be seen in the forthcoming subsection.

### 4.3.1 Asynchronous LQG controller

Refer to Fig. 4.2 for the sampling scheme described as follows. For any control loop  $s \in \{1, 2, \dots, N\}$ , let the sampling time provided to the sensor node by the ST sampler be  $\delta_i \in \mathbb{R}_+$ , where  $i \in \mathbb{Z}_{\{0,+\}}$ . The state is transmitted at  $\delta_i$  which reaches the controller at  $\rho_j \in \mathbb{R}_+$ , where  $j \in \mathbb{Z}_{\{0,+\}}$ , after encountering a random-but-bounded time-delay induced by the network,  $\sigma_{n,i} \leq \bar{\sigma}_n \in \mathbb{R}_+ \forall i$ .

*Remark 34* The simple network topology and time-slots allotted to the control loops according to their predicted triggering times, justify the assumption of a bounded network-induced time-delay. Also, see [10] which uses similar assumption.

*Remark 35* This work only considers star topology for simplicity.

The controller takes  $\sigma_c \in \mathbb{R}_+$  units of time to estimate the state and compute the controller output  $u$  which will be applied at  $\eta_k \in \mathbb{R}_+$ , where  $k \in \mathbb{Z}_{\{0,+\}}$ , and  $\eta_k = \rho_j + \sigma_c$ . The difference between consecutive events is denoted as  $\Delta_i \triangleq \delta_i - \delta_{i-1}$  and



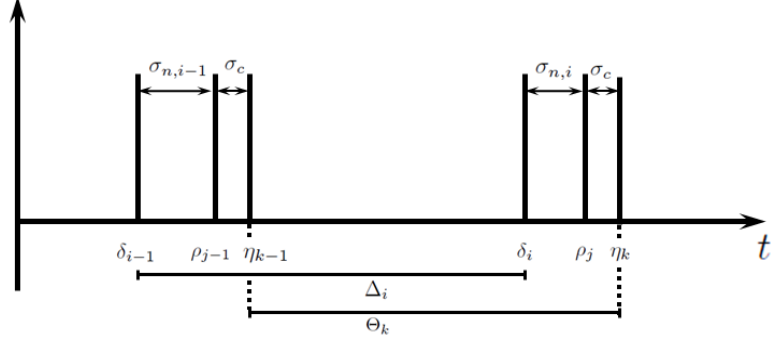


Figure 4.2: Timing diagram illustrating sampling ( $\delta$ ), reception ( $\rho$ ), and control application ( $\eta$ ) times with transmission and computation delays.

that between corresponding consecutive controller updates is represented by  $\Theta_k \triangleq \eta_k - \eta_{k-1}$ . Note that  $i = j = k$  translates into  $i$ -th event, and the corresponding  $j$ -th reception and  $k$ -th control update. Following these notations,  $\underline{\Delta}, \underline{\Theta} \triangleq \alpha$  and  $\overline{\Delta}, \overline{\Theta} \triangleq \Gamma\alpha$ .

**Assumption 3** *It is assumed that,*

1.  $\delta_0, \rho_0, \eta_0 = 0$ , i.e., the initial time for state-sampling and reception, and control-update are all equal to zero,
2. all the states of the plant are available for measurement,
3. the computational delay  $\sigma_c$  is constant,
4. the received states are time-stamped, i.e.,  $\delta_i$  is received along with  $i$ -th transmission of the state,
5. the delay  $\sigma_{n,i} + \sigma_c$  is less than  $\Delta_i$ , which implies that  $\delta_i < \eta_k, \forall i = k$ , and
6.  $\Theta_k/\Delta_i$  is irrational for all  $i, k$ .

*Remark 36* In author's opinion,  $\sigma_{n,i} + \sigma_c < \Delta_i$  is realistic because firstly, the low data-rate wireless network is suitable for low-speed control applications which do not require very fast sampling; secondly, the controller module and NM have high speed computational power. Both these facts imply  $\delta_i < \eta_k, \forall i = k$ .

Similar to the case of ET scheme described in the previous chapter, (4.1) can be viewed as a *dual-rate* asynchronous sampled-data system (ASDS) because the sampling interval at the sensor node is different from that of the control update, i.e.,  $\Delta_i \neq \Theta_k \forall i = k$ . Hence with Assumption 3(2),

$$\begin{aligned} \dot{x}(t) &= Ax(t) + B_1u(t) + B_2w(t), \quad x(0) = x_0, \\ y(\delta_i) &= x(\delta_i) + v(\delta_i), \\ u(t) &= u_{\eta_k} = f(\hat{x}(\delta_i)), \quad \forall t \in [\eta_k, \eta_{k+1}), \end{aligned} \tag{4.2}$$

where  $f(\cdot) : \mathbb{R}^n \rightarrow \mathbb{R}^m$  is a causal mapping which optimizes certain cost function.

The solution to the optimal control problem of ASDSs was given in [121], where the sampling (at the sensors) and hold (at the controllers) times were disproportionate, i.e.,  $\delta_i \neq \eta_k$ . It was shown that the control that minimizes certain cost function depends on the state estimated for  $\eta_k$  using the state information at  $\delta_i$ . It was assumed that the sampling, and consequently the hold rates are fixed, however, in the case under consideration, the sampling time is aperiodic which renders the time of control application aperiodic. The sampling and hold times are translated into event and control update instants, respectively.

**Assumption 4** *It is assumed  $\forall i, k$  that,*

1. for the discrete-time (DT) systems, the pairs  $(C, A_{\Delta_i})$  are detectable,
2. for the DT systems, the pairs  $(A_{\Theta_k}, B_{\Theta_k})$  are stabilizable,
3. system (4.2) is stabilizable and detectable,

where  $A_a = e^{A(a)}$  and  $B_a = \int_0^a A_s B_1 ds$  are the discretized system matrices for any time-interval  $a$ .

Let  $\hat{x}_\tau$ ,  $x_\tau$ , and  $u_\tau$  represent the estimated state, sampled-state, and control input at time  $\tau$ , respectively, and  $Q_\tau \in \mathbb{R}^{n \times n} > 0$  and  $R_\tau \in \mathbb{R}^{m \times m} > 0$  denote the state and input weighting matrices at  $\tau$ , then the controller which minimizes following discrete cost function

$$J_\Theta = \sum_{k=0}^{K-1} \frac{1}{K\eta_k} \mathbb{E} \left[ x_{\eta_k}^T Q_{\eta_k} x_{\eta_k} + u_{\eta_k}^T R_{\eta_k} u_{\eta_k} \right], \quad (4.3)$$

is given as

$$\begin{aligned} u_{\eta_k} &= -(R_{\eta_k} + B_{1,\Theta_k}^T P_k B_{1,\Theta_k})^{-1} (B_{1,\Theta_k}^T P_k A_{\Theta_k}) \hat{x}_{\eta_k}, \\ &= -K_{\eta_k} \hat{x}_{\eta_k}, \end{aligned} \quad (4.4)$$

where, the state estimate  $\hat{x}_{\eta_k}$  is given as

$$\hat{x}_{\eta_k} = A_{\eta_k - \delta_i} \hat{x}_{\delta_i} + B_{1,\eta_k - \delta_i} u_{\eta_{k-1}}, \quad \forall k = i; \quad \hat{x}_{\eta_0} = x_0. \quad (4.5)$$

$Q_{\eta_k}$  and  $R_{\eta_k}$  are given as

$$\begin{aligned} Q_{\eta_k} &= \int_{\eta_{k-1}}^{\eta_k} [A_{s-\eta_{k-1}}^T A_{s-\eta_{k-1}}] ds, \\ R_{\eta_k} &= \int_{\eta_{k-1}}^{\eta_k} [B_{1,s-\eta_{k-1}}^T B_{1,s-\eta_{k-1}}] ds, \end{aligned} \quad (4.6)$$

and  $\{P_k\}$  is given by the unique positive semi-definite solution of DT Riccati equation

$$\begin{aligned} P_k &= A_{\Theta_k}^T [P_{k+1} - P_{k+1} B_{1,\Theta_k} (R_{\eta_k} + B_{1,\Theta_k}^T P_{k+1} B_{1,\Theta_k})^{-1} B_{1,\Theta_k}^T P_{k+1}] A_{\Theta_k} + Q_{\eta_k}, \\ P_K &= 0. \end{aligned} \quad (4.7)$$

According to (4.5), the estimated state for time instant  $\eta_k$  depends upon the state estimate for  $\delta_i$ , which is given as

$$\hat{x}_{\delta_i} = \hat{x}_{\delta_i^-} + S_i [I + S_i]^{-1} (y_{\delta_i} - \hat{x}_{\delta_i^-}), \quad (4.8)$$

where

$$\hat{x}_{\delta_i^-} = A_{\delta_i-\eta_{k-1}} \hat{x}_{\eta_{k-1}} + B_{1,\delta_i-\eta_{k-1}} u_{\eta_{k-1}}; \quad \hat{x}_{\delta_0^-} = x_0, \quad (4.9)$$

and  $\{S_i\}$  is the solution of following Riccati equation

$$\begin{aligned} S_i &= A_{\Delta_i} S_{i-1} A_{\Delta_i}^T - A_{\Delta_i} S_{i-1} [I + S_{i-1}]^{-1} S_{i-1} A_{\Delta_i}^T + W_{\delta_i}, \\ S_0 &= 0, \end{aligned} \quad (4.10)$$

with  $W_{\delta_i} = \int_{\delta_{i-1}}^{\delta_i} A_{\delta_i-t} B_2 B_2^T A_{\delta_i-t}^T dt$ .

However, the time-varying controller (4.4) is computationally intensive which translates into larger  $\sigma_c$ , and the solution of (4.7) requires the knowledge of  $P_{k+1}$  which can not be determined offline due to aperiodic triggering. These problems require a time-invariant controller, and the best choice for a constant control gain is to design it using the *worst-case* sampling time defined from control perspective, i.e.,  $\bar{\Theta} \forall k$ , and optimization done over infinite horizon which render (4.3) as

$$J_{\Theta} = \lim_{K \rightarrow \infty} \sum_{k=0}^{K-1} \frac{1}{K \eta_k} \mathbb{E} \left[ x_{\eta_k}^T Q_{\bar{\Theta}} x_{\eta_k} + u_{\eta_k}^T R_{\bar{\Theta}} u_{\eta_k} \right]. \quad (4.11)$$

This assumption allows the designer to compute a constant control gain

$$K_{\bar{\Theta}} = (R_{\bar{\Theta}} + B_{1,\bar{\Theta}}^T P B_{1,\bar{\Theta}})^{-1} (B_{1,\bar{\Theta}}^T P A_{\bar{\Theta}}), \quad (4.12)$$

offline, such that

$$u(t) = -K_{\bar{\Theta}} \hat{x}(\eta_k), \quad \forall t \in [\eta_k, \eta_{k+1}), \quad (4.13)$$

with the ARE

$$P = A_{\bar{\Theta}}^T [P - P B_{1,\bar{\Theta}} (R_{\bar{\Theta}} + B_{1,\bar{\Theta}}^T P B_{1,\bar{\Theta}})^{-1} B_{1,\bar{\Theta}}^T P] A_{\bar{\Theta}} + Q_{\bar{\Theta}}. \quad (4.14)$$

*Remark 37* This choice of controller will ensure cost optimization for all the sampling periods that fall in  $[\alpha, \Gamma\alpha]$ .

In order to maintain the estimation accuracy, the estimation is done using (4.5), (4.8), (4.9), and (4.10). To further reduce the computational time, the integral

in (4.10) is computed offline for interval  $\alpha$ , i.e.,  $W_\alpha$ . Then, during the real-time estimation, it is multiplied with the number of  $\alpha$ -spaced intervals in  $\Delta_i$  to get  $W_{\delta_i}$ .

### 4.3.2 ST Sampler

The novel ST sampling method presented here is based on the fact that an exponential relationship exists between the difference of costs of DT and CT systems, and the sampling frequency  $f$  [137]. Let the difference be denoted as  $\Delta J^*(f) \triangleq J_{DT}^*(f) - J^*$ , where  $J_{DT}^*(f)$  represents the optimal cost of the DT system sampled periodically at  $f$ , and  $J^*$  gives the optimal cost of the CT system. The relationship is thus given by

$$\Delta J^*(f) = ae^{-bf}, \quad (4.15)$$

where  $a, b \in \mathbb{R}_+$  are system-dependent constants which can be determined by simulating the plant at several sampling frequencies in the desired range. Recently, this relationship is used in [138] to optimize the control costs and transmission frequencies of multiple systems sharing the same wireless network. However, their methodology determines the optimal rates offline, which remain constant through the operating time of the systems, i.e., periodic triggering.

The objective of this work is to design an ST sampler which can predict the *cost-dependent sampling frequency* online. The idea is to keep the control cost of the ST system as close to the reference ( $\alpha$ -periodic) system as possible, while

ensuring communication-bandwidth economy, especially when the ST system is regulated. The reference system is the sampled-data implementation of the plant sampled periodically at every  $\alpha$  units of time, with a perfect feedback communication channel. In particular, the reference system is given as

$$\begin{aligned} \dot{x}(t) &= Ax(t) + B_1u(t) + B_2w(t), \quad x(0) = x_0, \\ y(t) &= Cx(t) + v(t), \\ u(t) &= -K_\alpha x(p\alpha) \quad \forall t \in [p\alpha, (p+1)\alpha), \end{aligned} \tag{4.16}$$

where  $p \in \mathbb{Z}_{\{0,+\}}$ , and it is assumed that the variance of the noise terms  $W$  and  $V$  are known.

*Remark 38 Note that instead of taking the CT feedback implementation of the plant as a reference,  $\alpha$ -periodic sampled-data system is considered. This is due to the over stringent demand on the control cost if the ST system's cost is compared with the CT implementation, which will translate into very high sampling frequency.*

*Remark 39 When the cost difference is taken against the reference system, it follows the same relation as (4.15).*

In order to design the ST sampler, the sampling frequency range is defined by the bounds introduced on the sampling time, i.e.,  $\alpha \leq \Delta_i \leq \Gamma\alpha \quad \forall i$ . The minimum sampling frequency  $f_m \triangleq \frac{1}{\Gamma\alpha}$  and maximum is given as  $f_M \triangleq \frac{1}{\alpha}$ . For several sampling frequencies in the range  $[f_m, f_M]$ , the respective controllers are

computed and control cost difference at each of these frequencies is computed as

$$\Delta J^*(f) = x_0^T (P_f - P_{f_M}) x_0, \quad (4.17)$$

where  $P_f$  is the Riccati matrix for any sampling frequency in the selected range, and  $x_0$  is the initial state of the plant which is assumed to be known. During the operation of ST system, the *cost-to-go* from  $\delta_i \forall i$  is obtained as  $J_{ST}|\delta_i \triangleq x_{\delta_i}^T P_{f_m} x_{\delta_i}$  due to the static controller which corresponds to the worst-case sampling interval  $\overline{\Delta}$ , and the cost difference is computed as

$$\Delta J_{ST}|\delta_i \triangleq J_{ST}|\delta_i - J_{f_M}^*|\delta_i = x_{\delta_i}^T P_{f_m} x_{\delta_i} - x_{\delta_i}^T|_{\alpha} P_{f_M} x_{\delta_i}|_{\alpha}, \quad (4.18)$$

where  $x_{\delta_i}$  and  $x_{\delta_i}|_{\alpha}$  represent the state of the ST and reference systems at  $\delta_i$ , respectively. The cost evolution of the reference system is simulated offline and stored in the ST setup.

Note that the variation in the cost difference (4.17) is due to the change in the sampling frequency which in turn changes the matrix  $P_f$ . However, in (4.18) the variation will only result from the change in  $x_{\delta_i}$  due to the static control gain. This problem requires to translate  $\Delta J_{ST}|\delta_i$  into (4.17). In order to achieve this, the cost difference (4.17) is normalized with respect to  $x_0^T (P_{f_m} - P_{f_M}) x_0$ . After normalization, the  $\Delta J^*(f)$  vs  $f$  graph is scaled from 0 to 1 for  $[f_m, f_M]$  and an exponential relationship is obtained using curve fitting which gives the values of the parameters  $a$  and  $b$ , as shown in Fig. 4.3 where  $\mathcal{C}_f$  represents the fitted curve.



During the course of operation, the cost difference of ST system (4.18) is also

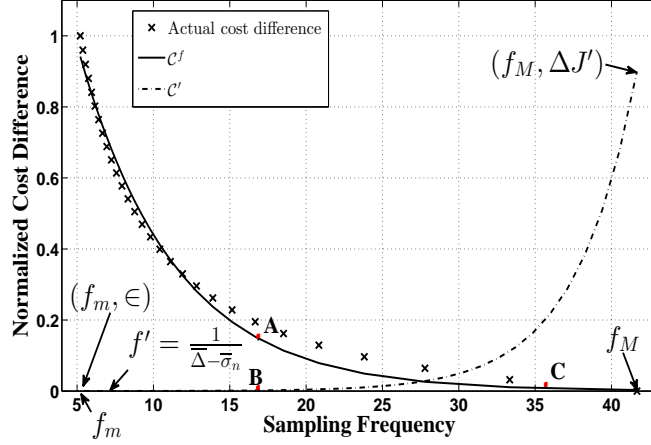


Figure 4.3: ST sampler synthesis.

normalized with  $x_0^T (P_{f_m} - P_{f_M}) x_0$  at  $\delta_i \forall i$ .

The desired behavior of the ST sampler should be to choose a high sampling frequency when the cost of the ST system is far from that of the reference system and vice versa. Solving a relationship similar to (4.15) for frequency, cannot fulfill this requirement. Therefore, there has to be a mechanism whereby the ST sampler *reacts* to the change in  $\Delta J_{ST}$  at every  $\delta_i$  such as to imitate the desired behavior.

To achieve this, following requirements are listed:

- At maximum cost difference of the ST system, the sampling frequency should be maximum,
- When the difference is close to zero, the sampling frequency should be close to minimum,
- For a sharp increase (decrease) in the cost difference, the sampling frequency should be *immediately* increased (decreased), and

- When choosing the minimum sampling frequency (corresponding to  $\bar{\Delta}$ ), the sampler should take care of the network-induced delay.

Following these requirements, another curve  $\mathcal{C}'$  is introduced on  $\Delta J$  vs.  $f$  graph, as shown in Fig. 4.3, which is an exponentially rising function of the form

$$\mathcal{C}' \triangleq he^{pf}, \quad (4.19)$$

defined over  $f \in [f_m, f_M]$  with the parameters  $h, p \in \mathbb{R}_+$  which are determined with the knowledge of two points resulting from the requirements stated above. The first point has the coordinates  $(f_m, \epsilon)$  and the second is located at  $(f_M, \Delta J')$ , where  $\epsilon \in \mathbb{R}_+ \ll 1$  to avoid numerical problems, and  $\Delta J'$  is the cost difference on  $\mathcal{C}'$  at frequency  $f' = \frac{1}{\Delta - \sigma_n}$  to tackle the network induced delay. With these two points, equation (4.19) is solved which yields  $h$  and  $p$ .

The mechanism by which the ST sampler will compute the next triggering time is composed of the following steps:

1. Given the sampled state of the plant  $x_{\delta_i}$ , the normalized cost difference is computed as

$$\Delta J_{ST|\delta_i, N} = \frac{\Delta J_{ST|\delta_i}}{x_0^T (P_{f_m} - P_{f_M}) x_0}. \quad (4.20)$$

2. Given  $\Delta J_{ST|\delta_i, N}$ , (4.15) is solved for frequency, i.e.,

$$f_1 = -\frac{1}{b} \ln \left( \frac{\Delta J_{ST|\delta_i, N}}{a} \right). \quad (4.21)$$

See point A in Fig. 4.3.

3. With  $f_1$ , (4.19) is solved for  $\Delta J'_N$ , i.e.,

$$\Delta J'_N = he^{pf_1}. \quad (4.22)$$

See point B in Fig. 4.3.

4. With  $\Delta J'_N$ , (4.15) is again solved to compute the sampling frequency as

$$f_s = -\frac{1}{b} \ln \left( \frac{\Delta J'_N}{a} \right). \quad (4.23)$$

See point C in Fig. 4.3.

5. The next triggering time  $\delta_{i+1}$  is computed as

$$\delta_{i+1} = \delta_i + \frac{1}{f_s}. \quad (4.24)$$

These steps are repeated every time the state is received.

The working of the ST sampler and satisfaction of the above requirements can be understood with an example. For instance, the cost difference is close to 1, then by following above steps, it can be observed that the sampling frequency  $f_s$  will be close to  $f_M$ . Because the slope of  $\mathcal{C}'$  is almost zero for all the values of cost differences close to 1, any sharp change in the cost difference will result in the selection of a high sampling frequency. Similarly, when the cost difference is close to zero,  $f_s$  will lie in the region close to  $f_m$ . For the extreme case of  $\Delta J_{ST} \approx 0$ ,

$f_s = \frac{1}{\Delta - \sigma_n}$ ; this sampling frequency will take care of the network-induced delays (see Fig. 4.3).

*Remark 40 Normalization of  $\Delta J$  vs.  $f$  curve with respect to  $x_0^T(P_{f_m} - P_{f_M})x_0$  allows the designer to use same relationship (values of  $a$ ,  $b$ ,  $p$ , and  $h$ ) for a system regardless of its initial state. This is also demonstrated in the simulation results.*

## 4.4 Second Level: Network Manager

The slotted mode of IEEE 802.15.4 wireless networking protocol with modified NM and superframe (SF) structures is considered. Details of the said protocol are left due to limited space and can be found in [9]. The motivation for modifications comes mainly from the use of ST strategy, which does not require the controllers to contend for transmission slot due to the predicted triggering times, hence eliminating the need for Contention Access Period (CAP). The predicted triggering times allow the scheduler to pre-schedule the transmission slots for the next SF. In addition, as it will be seen in the forthcoming text and simulation results, significant energy savings can be achieved at the battery-powered sensor nodes at the expense of slightly increased computational load at the mains powered NM.

### 4.4.1 Superframe (SF)

In the modified SF structure, as shown in Fig. 4.4, the CAP is eliminated and the active and inactive portions are distributed. This allows the systems to get their states at any time during the beacon interval (BI), unlike “fixed” time slots in

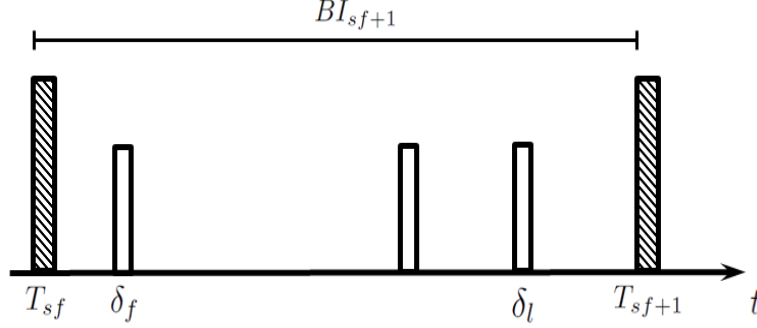


Figure 4.4: Modified SF structure. The duration is denoted as  $BI_{sf+1}$ . Active period includes a beacon packet and three slots for transmission; remaining time constitutes the inactive period. Each slot is of duration  $\Delta_s$ .

the Contention Free Period (CFP). Due to bandwidth constraint, a SF can allow at most  $N_{max}$  transmissions each of duration  $\Delta_s$  (slot-duration). The timing constraints imposed by the physical layer of the protocol and plant dynamics are

- $\min BI \leq \alpha \leq \frac{1}{5\lambda_{min}}$ ,
- $\min BI \leq BI \leq \max BI$ ,
- $\Gamma\alpha \leq \max BI$ ,

where  $\lambda_{min}$  denotes the dominant pole of the fastest plant among the participating systems, following the rule-of-thumb the upper-bound of  $\alpha$  is chosen as inverse of five times  $\lambda_{min}$ , and  $\min BI$  and  $\max BI$  represent the minimum and maximum values of BI corresponding to the constraint  $0 \leq \text{BeconOrder (macBO)} \leq 14$  imposed by the original protocol [9] as

$$BI = aBaseSFDuration \times 2^{macBO}, \quad (4.25)$$

with  $aBaseSFDuration \triangleq SFD \equiv \frac{\text{No. of symbols}}{\text{Symbol rate}}$ .

Given the predicted triggering time by the sampler of each system, the length of next SF is computed as  $BI_{sf+1} = \delta_f - T_{sf} - \Delta_s + N_{max}\Delta_s + IaP$ , where  $\delta_f$  is the first system which will transmit in the next SF, and  $IaP$  denotes the inactive period which will allow the scheduler ample time to construct the next SF and economize energy. In order to ensure schedulability of the first system of next SF in worst-case scenario, whereby that system's predicted triggering time might be  $\alpha$ , the duration  $N_{max}\Delta_s + IaP \leq \alpha - \Delta_s$ . This results in

$$BI_{sf+1} = \delta_f - T_{sf} - 2\Delta_s + \alpha. \quad (4.26)$$

#### 4.4.2 Network Manager

The NM has wired connection with the ST controllers and communicates over a wireless link with the sensor nodes. The proposed NM structure appends a scheduler module with the Personal Area Network (PAN) coordinator as shown in Fig. 4.5. The coordinator broadcasts beacon packets that contain the assigned trans-

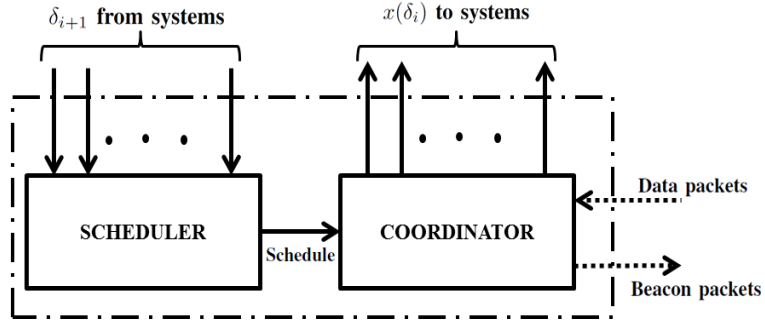


Figure 4.5: Modified structure of the Network Manager. Solid line: wired connections; dotted line: wireless link.

mission time/slot for each sensor node and the beacon interval. This enables each

sensor node to sleep until its transmission time, transmit the state information in the assigned slot, and sleep again until the next beacon broadcast. After sampling the states of their systems in the assigned slots, the sensor nodes transmit this information over the wireless network to the coordinator, which delivers this information to respective controllers. Each controller computes  $\delta_{i+1}$ , and sends this information to the scheduler over the wired connection. The scheduler keeps storing this information in a buffer until it receives it from all the controllers scheduled for that particular beacon interval, and then starts the scheduling algorithm. The NM performs following tasks:

- Ensures that no two transmissions overlap in the next SF.
- Keeps track of the slow systems and places their transmission slots in the appropriate SF; this is possible due to the algorithms defined in forthcoming text. This way, the need to sample every system in each SF is eliminated.
- Provides the coordinator with a transmission schedule.

*Remark 41* The overlap is avoided such that the assigned time for the slots remains between  $\alpha$  and  $\Gamma\alpha$ , and does not exceed the required triggering time.

After getting the scheduling information, the coordinator forms a beacon packet and broadcasts it.

**Assumption 5** *It is assumed that,*

- *all the controllers have knowledge of the initial state,  $x(0)$ , of respective systems,*

- the scheduler takes  $\varsigma \leq \bar{\varsigma} \in \mathbb{R}^+$  units of time for all computations during a SF,
- a sensor node requires only  $\Delta_s$  to transmit the state information  $(x(\delta_i))$  and time-stamp  $(\delta_i)$ ,
- the duration of beacon transmission is  $\Delta_s$ ,
- $\Delta_s$  includes inter-frame spacing (IFS) (see [9]).

Initially, all the controllers use  $x(0)$  to compute the next triggering times. This information is used by the scheduler to schedule the first SF and compute its duration following (4.26) as

$$BI_1 = \delta_f - T_0 - 2\Delta_s + \alpha, \quad (4.27)$$

where  $\delta_f$  denotes the first system which will transmit in the first SF. The coordinator generates first beacon packet at  $T_0 = 0$ , which contains triggering times for all the nodes and the beacon interval  $BI_1$ . For any SF, the scheduler computes  $BI_{sf+1}$  using (4.26) and also,

$$a \triangleq \delta_{l,sf+1} - T_{sf} + \Delta_s, \quad (4.28)$$

where  $\delta_{l,sf+1}$  denotes the last system which will transmit in the next SF. The scheduler then compares  $a$  and  $BI_{sf+1}$ ; if  $a \leq BI_{sf+1}$  then all the nodes are allowed to transmit in the next SF, otherwise only the nodes for which the next



triggering time falls in the next SF duration are allowed to transmit, and the remaining nodes' slots are placed in the appropriate future SF. This way, there is no need to sample every sensor node in each SF, thus saving energy. The algorithm is given as follows:

### Algorithm 1

Initialization

1.  $sf = 0$  and  $i = 0$ .

End Initialization

2. At  $\delta_i^s$  in  $sf$ -th SF, scheduler gets  $\delta_{i+1}^s$  for those systems which transmit in  $BI_{sf}$ ;

3. Wait until  $\delta_{l,sf}$ ;

4. Compute (4.26) and (4.28);

If  $a \leq BI_{sf+1}$  then

5. All the nodes are allowed transmission in  $BI_{sf+1}$ ;

6. Increment  $sf$  and  $i$  by one;

7. GOTO 2;

else

8. The nodes with  $\delta_{i+1} \in [T_{sf} + \Delta_s, T_{sf+1})$  are allowed transmission in  $BI_{sf+1}$ ;

Table 4.1: Parameters for simulation.

| Par.            | Description                             | Value                 |
|-----------------|---|-----------------------|
| $\lambda_{min}$ | Dominant pole                           | 1.8257                |
| $N_{max}$       | Maximum number of slots in a superframe | 4                     |
| $N$             | Number of participating systems         | 3                     |
| BW              | Frequency band of IEEE network          | 915 MHz               |
| BR              | Bit-rate                                | 40 kbits/sec          |
| SS              | No. of symbols in one slot              | 60                    |
| SR              | Symbol rate                             | 40 ksymbols/sec       |
| $a$             | Parameter of $\mathcal{C}_f$            | 2.152                 |
| $b$             | —                                       | 0.1587                |
| $p$             | Parameter of $\mathcal{C}'$             | 0.2497                |
| $h$             | —                                       | $0.27 \times 10^{-6}$ |
| $\epsilon$      | First point on $\mathcal{C}'$           | $0.1 \times 10^{-3}$  |

9. Increment  $sf$ ;
  10. Increment  $i$  for those systems which transmit in  $BI_{sf+1}$ ;
  11. GOTO 2;
- end

## 4.5 Simulation Results and Discussion

Simulation results of the application of the above defined scheme are now presented for three identical inverted-pendulum-over-cart systems; the states, system matrices and simulation parameters can be obtained from the previous chapter. The description and values of the remaining parameters are given in Table 4.1. To simulate the three systems over IEEE 802.15.4 network with modifications, MATLAB based simulation tool TrueTime [133] is used. The systems are placed

at a distance of 30m from the NM node which is assumed to be at the origin. The modifications are introduced with a separate TrueTime kernel block which runs the code for Algorithm 2, and implements the modules of scheduler and coordinator. The network related parameters are also given in Table 4.1.

*Remark 42 Although identical systems are chosen due to space constraints, the ST scheme presented in this chapter with modified protocol is valid for heterogeneous systems.*

From (4.25), the minimum and maximum BI are computed using the values listed in the table, which give  $\text{minBI} = 1.5 \times 10^{-3}\text{sec}$  and  $\text{maxBI} = 24.576\text{sec}$ . With these values and  $\lambda_{\min}$ , the value of  $\alpha$  is chosen as  $24 \times 10^{-3}\text{sec}$  because it is less than  $\frac{1}{5\lambda_{\min}}$ . With the bounds defined for the sampling interval as  $\alpha \leq \bar{\Delta} \leq \Gamma\alpha$ , the frequency range is given as  $f_m = 5.2\text{Hz}$  and  $f_M = 41.7\text{Hz}$ . Fig. 4.3 shows the results of curve fitting  $\mathcal{C}_f$  and synthesis of  $\mathcal{C}'$ ; the parameters are given in Table 4.1.

The implementation results of the proposed scheme are compared against  $\alpha$ -periodic triggering for the same three systems over a conventional IEEE 802.15.4 network with the same delay characteristics, where the value of  $\alpha$  is  $24 \times 10^{-3}\text{sec}$ . The results are given in figs. 4.6 to 4.8. All the systems are stabilized within 5 seconds and it can be observed from Fig. 4.6 that the states follow same trajectories as the periodic implementation, especially in the transient phase. This similarity can be explained on the basis of the adaptive nature of ST methodology, which results in a sampling time of  $\alpha$  seconds in the transient phase of the response, as

demonstrated in Fig. 4.7.

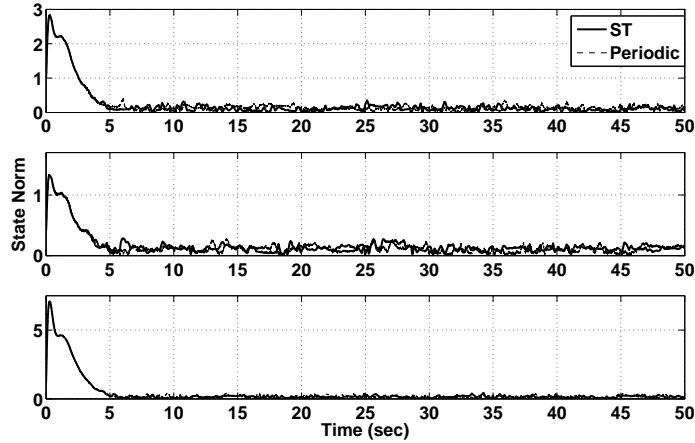


Figure 4.6: State norm, solid:  $\|x_{ST}(t)\|$ , dashed:  $\|x|_{\alpha}(t)\|$ . Top: System 1, middle: System 2, bottom: System 3.

Fig. 4.7 shows that the ST scheme adjusts the sampling frequency according to the system's cost, and as soon as the states are regulated the frequency is reduced. This validates the working of the proposed ST sampler. Moreover, the adaptive length of BIs (or SFs) can be observed in Fig. 4.7 (bottom), thus saving the communication bandwidth and battery power. The event-rates which give the number of events per second for systems 1, 2, and 3 are 9.22, 16.54, and 8.1, respectively, for the proposed scheme. This demonstrates a percentage decrease of 77.87%, 60.31%, and 80.6% in the event-rates of systems 1, 2, and 3, respectively, as compared with the periodic implementation. The reason for the difference in event-rates for three identical systems is due to the difference in their initial states and the instantaneous values of noise.

The average costs of systems 1, 2, and 3 are 0.0831, 0.0224, and 0.3809, respectively, which demonstrate a mere increase of approximately 10% against their periodic counterparts. Also, the estimation results can be observed in Fig. 4.8

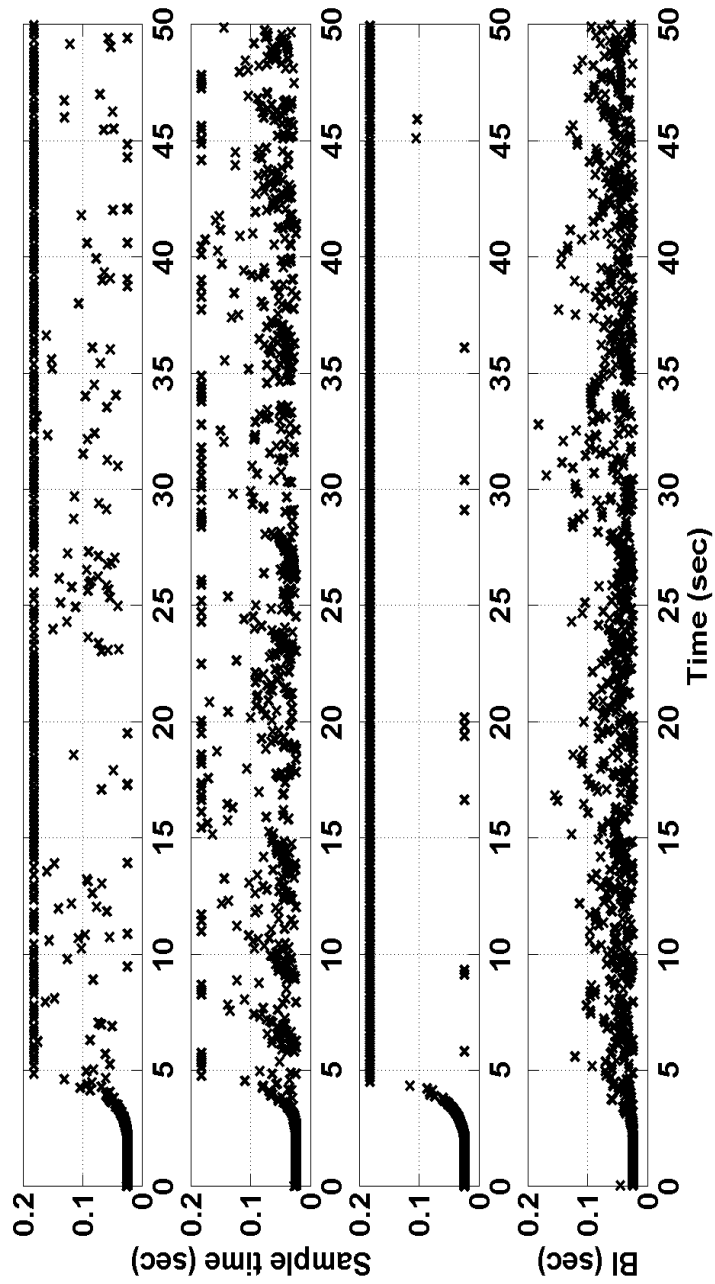


Figure 4.7: Event times of systems 1 (first), 2 (second), and 3 (third). Length of beacon intervals (BIs) (fourth).

which shows the estimation error. The MSEs for systems 1, 2, and 3 are respectively  $2.1 \times 10^{-3}$ ,  $0.4 \times 10^{-3}$ , and  $4.9 \times 10^{-3}$ .

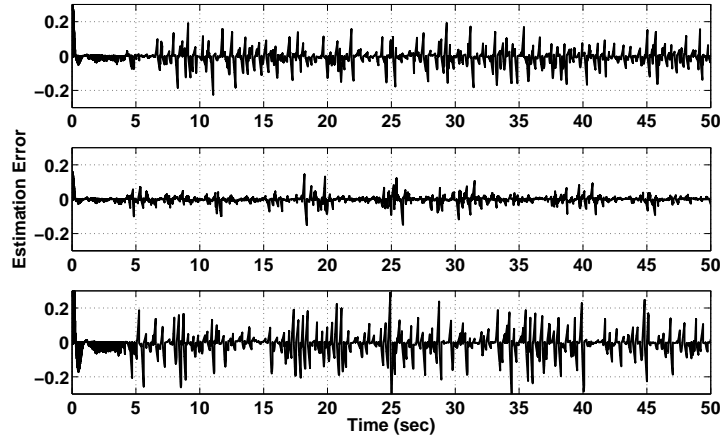


Figure 4.8: Estimation error  $\|x_{ST}(t)\| - \|\hat{x}_{ST}(t)\|$ .

## 4.6 Conclusion

A two-level design approach was presented for multiple ST-based LQ systems sharing IEEE 802.15.4 network with modified protocol. The main motivation of this work was to optimize control, communication, and computation costs while tackling the network induced and computational delays, and decoupling the design of controller from that of the ST sampler and NM. To this end, the transmission time was upper- and lower-bounded to solve the decoupling problem, asynchronous LQG controller was implemented to deal with the delays and aperiodic nature of transmissions, a novel ST scheme was designed along with the modifications in IEEE 802.15.4 protocol to ensure bandwidth economy, and enhance energy savings offered by the conventional IEEE protocol. Simulation results of the proposed scheme were compared with the periodic implementation which demonstrated

upto 80% reduction in the bandwidth usage at a slight increase in the control cost for the particular case of the system considered.

A detailed comparison of this scheme is presented against ST LQR controller reported in the literature [1]. Furthermore, in this chapter and the subsequent ones, we do not consider packet-drops.

# CHAPTER 5

## AN EVALUATION OF SELF-TRIGGERING METHODS

### 5.1 Introduction

A comparison of the recently proposed STLQR technique [1] is presented against the novel scheme reported in the previous chapter, on the basis of the amount of control cost incurred, communication bandwidth usage, and computational requirements. To present a fair comparison, the time-delays are not considered because in [1] a perfect communication channel is assumed.

*Organization:* Section 5.2 defines the problem, and the reader will find a brief description of the methodology presented by [1] in Section 5.3. A comparison of both schemes is given in 5.4. Finally, Section 5.5 concludes the chapter.



*Notations:* Sets of real numbers and integers are denoted by  $\mathbb{R}$  and  $\mathbb{Z}$ , respectively. A set of strictly-positive real numbers is represented by  $\mathbb{R}_+$  and that including zero is denoted as  $\mathbb{R}_{\{0,+}}$ . The sets of positive-definite and semi-definite integers are represented as  $\mathbb{Z}_+$  and  $\mathbb{Z}_{\{0,+}}$ , respectively. The expected value is represented as  $\mathbb{E}[\cdot]$ .

## 5.2 Problem Definition

A class of LQ ST control systems is considered, associated with a continuous-time (CT) LTI plant given as

$$\begin{aligned} \dot{x}(t) &= Ax(t) + B_1u(t) + B_2w(t), \quad x(0) = x_0, \\ y(t) &= x(t), \end{aligned} \tag{5.1}$$

where  $x(t) \in \mathbb{R}^n$  is the state,  $u(t) \in \mathbb{R}^m$  is the control input,  $y \in \mathbb{R}^q$  represents outputs, and  $w(t) \in \mathbb{R}^l$  is zero-mean white Gaussian process noise with covariance  $W$ . The feedback loop is closed over a bandwidth-limited communication channel which is assumed to be free of time-delays and packet-drops.

The objective is to control system 5.1 such that the control cost, communication bandwidth and computational load are optimized. Following this, the controller is based on LQ design and the states are transmitted using ST sampling,

due to which (6.22) becomes sampled-data system, given by

$$\begin{aligned}
\dot{x}(t) &= Ax(t) + B_1u(t) + B_2w(t), \quad x(0) = x_0, \\
y(\delta_i) &= x(\delta_i), \\
u(t) &= f(x(\delta_i)), \quad \forall t \in [\delta_i, \delta_{i+1}),
\end{aligned} \tag{5.2}$$

where  $\delta_i \in \mathbb{R}_{\{0,+\}}$  represents the sampling time with  $i \in \mathbb{Z}_{\{0,+\}}$  and  $f(\cdot) : \mathbb{R}^n \rightarrow \mathbb{R}^m$  is a causal mapping which optimizes certain cost function.

### 5.3 ST Linear Quadratic Regulator [1]

A recently proposed ST LQ regulation technique [1] is reproduced briefly. The co-design problem is solved for (6.24) with the idea of maximizing the sampling interval while guaranteeing performance based on discounted LQ cost,

$$J = \sum_{t=0}^{\infty} \mathbb{E}[\gamma^t(x_t^T Q x_t + u_t^T R u_t + 2x_t^T H u_t) | x_0], \tag{5.3}$$

where  $0 < \gamma < 1$  represents the discount factor and  $Q$ ,  $R$ , and  $H$  represent the standard weighting matrices. Particularly, the codesign problem is stated as

$$\begin{aligned}
t_{l+1} &= t_l + M(x_{t_l}), \\
u_t &= \bar{u}_l \in \mathcal{U}_M(x_{t_l}), \quad t \in \mathbb{Z}_{\{0,+\}}
\end{aligned} \tag{5.4}$$

where  $t_l \in \mathbb{R}_{\{0,+\}}$  represents the sampling time at sample number  $l \in \mathbb{Z}_{\{0,+\}}$ .  $M : \mathbb{R}^n \rightarrow \{1, \dots, \bar{M}\}$  is the sampling interval with  $\bar{M} \in \mathbb{Z}_+$  arbitrarily large for

bounded latency, and  $\mathcal{U} : \mathbb{R}^n \rightarrow \mathbb{R}^m$  is a set-valued map representing the set of possible control values.

To present  $M$  and  $\mathcal{U}$  in (5.4),  $\mathcal{U}_M(x)$  is defined, for  $x \in \mathbb{R}^n$ , as the set of control values that can be held constant for  $M$  steps while satisfying

$$\mathbb{E} \left[ \left( \sum_{t=t_l}^{t_{l+1}-1} \gamma^{t-t_l} (x_j^T Q x_j + \bar{u}_j^T R \bar{u}_j + 2x_j^T H \bar{u}_j) \right) + \gamma^{t_{l+1}-t_l} V_{\beta_1, \beta_2}(x_{t_{l+1}}) | x_{t_l} \right] \leq V_{\beta_1, \beta_2}(x_{t_l}), \quad (5.5)$$

at transmission time  $t_l$ , where  $V_{\beta_1, \beta_2}(x)$  is the reference performance function and is given as

$$V_{\beta_1, \beta_2}(x) := \beta_1 x^T P x + \beta_2 \frac{\alpha}{1 - \alpha} \text{tr}(P B_2 B_2^T), \quad (5.6)$$

with  $P$  as the solution of following discrete algebraic Riccati equation (DARE)

$$P = Q + \gamma A^T P A - (\gamma A^T P B_1 + H)(R + \gamma B_1^T P B_1)^{-1} (\gamma B_1^T P A + H^T). \quad (5.7)$$

This leads to

$$\mathcal{U}_M(x) := \left\{ \bar{u} \in \mathbb{R}^n \mid \mathbb{E} \left[ \left( \sum_{j=0}^{M-1} \gamma^j (\bar{x}_j^T Q \bar{x}_j + \bar{u}_j^T R \bar{u}_j + 2\bar{x}_j^T H \bar{u}_j) \right) + \gamma^M V_{\beta_1, \beta_2}(\bar{x}_M) \mid x \right] \leq V_{\beta_1, \beta_2}(x) \right\}, \quad (5.8)$$

where  $\bar{x}_j$ ,  $j \in \{1, 2, \dots, M\}$ , is the solution of the discretized version of  $\dot{x} = Ax(t) + B_1 u(t) + B_2 w(t)$  with  $\bar{x}_0 = x$  and  $u_t = \bar{u}$ ,  $t \in \mathbb{Z}$ , i.e.,

$$\bar{x}_j = \bar{A}_j x + \bar{B}_{1,j} \bar{u} + \bar{B}_{2,j}^M w_M, \quad (5.9)$$

where,  $\bar{A}_j := A^j$ ,  $\bar{B}_{1,j} := \sum_{i=0}^{j-1} A^i B_1$  and  $\bar{B}_{2,j}^M \in \mathbb{R}^{n \times Ml}$  is given as

$$\bar{B}_{2,j}^M := [A^{j-1}B_2 \ \cdots \ AB_2 \ B_2 \ 0 \ \cdots \ 0] \quad (5.10)$$

and  $w_M := [w_0^T, w_1^T, \dots, w_{M-1}^T]^T$ .

From above discussion it can be seen that  $\mathcal{U}_M(x) \neq \emptyset$  if and only if

$$\min_{\bar{u} \in \mathbb{R}^n} \mathbb{E} \left[ \left( \sum_{j=0}^{M-1} \gamma^j (\bar{x}_j^T Q \bar{x}_j + \bar{u}_j^T R \bar{u}_j + 2\bar{x}_j^T H \bar{u}_j) \right) + \gamma^M V_{\beta_1, \beta_2}(\bar{x}_M) | x \right] \leq V_{\beta_1, \beta_2}(x). \quad (5.11)$$

Using (5.6) and (5.9), the above equation becomes

$$\min_{\bar{u} \in \mathbb{R}^n} \mathbb{E} \left[ \bar{x}^T F_M \bar{x} + \bar{x}^T G_M \bar{u} + \frac{1}{2} \bar{u}^T U_M \bar{u} + c_M \right] \leq V_{\beta_1, \beta_2}(x), \quad (5.12)$$

where

$$\begin{aligned} F_M &= \gamma^M \beta_1 \bar{A}_M^T P \bar{A}_M + \sum_{j=0}^{M-1} \gamma^j \bar{A}_j^T Q \bar{A}_j, \\ G_M &= 2 \left[ \gamma^M \beta_1 \bar{A}_M^T P \bar{B}_M + \sum_{j=1}^{M-1} \gamma^j (\bar{A}_j^T Q \bar{B}_j + \bar{A}_j^T H) \right], \\ U_M &= 2 \left[ \gamma^M \beta_1 \bar{B}_M^T P \bar{B}_M + \sum_{j=0}^{M-1} \gamma^j (\bar{B}_j^T Q \bar{B}_j + \bar{B}_j^T H + H^T \bar{B}_j + R) \right], \\ c_M &= d_M + \beta_2 \alpha^M \frac{\alpha}{1 - \alpha} \text{tr}(P B_2 B_2^T), \\ d_M &= \gamma^M \beta_1 \text{tr}(P \bar{B}_{2,M}^M (\bar{B}_{2,M}^M)^T) + \sum_{j=1}^{M-1} \gamma^j \text{tr}(Q \bar{B}_{2,j}^M (\bar{B}_{2,j}^M)^T). \end{aligned} \quad (5.13)$$

The optimal control input

$$\bar{u}^* := \operatorname{argmin}_{\bar{u} \in \mathcal{U}_M(x)} x^T F_M x + x^T G_M \bar{u} + \frac{1}{2} \bar{u}^T U_M \bar{u} + c_M$$

is obtained by solving

$$\frac{\partial}{\partial \bar{u}} \left( x^T F_M x + x^T G_M \bar{u} + \frac{1}{2} \bar{u}^T U_M \bar{u} + c_M \right) = 0,$$

which leads to  $x^T G_M + \bar{u}^T U_M = 0$ , and thus

$$\bar{u}^* = -U_M^{-1} G_M^T x =: K_M x, \quad (5.14)$$

and

$$M(x) = \max\{M \in \{1, 2, \dots, \bar{M}\} | x^T P_M^* x + \bar{c}_M \leq \beta_1 x^T P x\}, \quad (5.15)$$

where  $P_M^* = F_M - \frac{1}{2} G_M U_M^{-1} G_M^T$  and  $\bar{c}_M = d_M - \beta_2 \sum_{j=1}^M \gamma^j \operatorname{tr}(P B_2 B_2^T)$ .

Hence the codesign problem, given by (5.4) is solved with the control input (5.14) for the sampling time computed as (5.15).

## 5.4 Comparison

In this section, the proposed methodology is compared with [1] from three perspectives: 1) Controller design, 2) ST sampling, and 3) Computational requirements,

and simulation results are presented for three case studies.

### 5.4.1 Controller design

The controller presented in [1] does not incorporate time-delays, which makes the scheme unsuitable for implementation over real-time networks. In contrast, the proposed approach can tackle computational and communication delays by estimating the state for the time when control input will be actually applied, given the state at the transmission time. Furthermore, the choice of static control simplifies the design.

Regarding the control cost, both approaches use similar idea of keeping the cost close that of the to periodic system. Particularly, in [1] the cost of ST system is compared to the *scaled* (by  $\beta_1$ ) cost of the reference system (5.15), and in the proposed scheme, the sampler increases frequency if the cost difference between ST and reference systems increases.

### 5.4.2 ST sampling

The novel sampler reacts to the change in cost of the ST system such that, the further the cost of ST system goes from that of the reference system, the higher the sampling frequency becomes, and vice versa. Consequently, the sampling intervals in the transient period are shorter than those in the regulated period. On the other hand, the sampler in [1] based on condition (5.15), results in higher average sampling interval in the transient period than that during regulation. In

general, this leads to higher communication cost than the proposed scheme.

### 5.4.3 Computational requirements

For the case without time-delays, i.e., unrealistic case, computational time for the proposed scheme is 5 times less than that for [1] due to the static gain. However, when delays are considered (realistic case), the computational time increases by four times as the asynchronous controller estimates the state for  $\eta_k$ .

When comparing the sampling methodology, computational time of proposed sampler is less than that in [1]. However, the memory requirements are higher because of the storage of cost evolution of the reference system.

### 5.4.4 Case Studies

Simulation study of the above-defined approaches is presented for mass-spring, water-level control and inverted-pendulum over cart systems, which offer both slow and fast dynamics. For a fair comparison, a perfect communication channel is assumed, and same values of weighting matrices are taken for both approaches. The clock speed and precision of the computational platform are 3300 MHz and 30 ns, respectively. The results are analyzed on the basis of control cost, communication bandwidth usage in terms of event-rate (number of events per second), and computational time.

## Mass-spring system

The system, described in [1], consists of two masses ( $m_1 = m_2 = 1$ ) connected by spring and damper. It is represented by (6.22) with  $x = [y_1 \ y_2 \ \dot{y}_1 \ \dot{y}_2]^T$  and

$$A = \begin{bmatrix} 0 & 0 & 1 & 0 \\ 0 & 0 & 0 & 1 \\ -k_s & k_s & -d & d \\ k_s & -k_s & d & -d \end{bmatrix}; B_1 = \begin{bmatrix} 0 \\ 0 \\ 1 \\ 0 \end{bmatrix}; B_2 = \begin{bmatrix} 0 \\ 0 \\ 0.02 \\ 0 \end{bmatrix}, \quad (5.16)$$

where  $k_s = 5$  and  $d = 1$  are the spring and damper coefficients. The initial state  $x_0 = [0.49 \ -0.4 \ 0.74 \ -0.25]^T$  and  $W = 1$ . The value of  $\alpha$  is chosen on the basis of the rule-of-thumb as  $\frac{1}{5\lambda_{dom}}$ , where  $\lambda_{dom}$  represents the dominant pole; for this system  $\alpha = 63.2$  ms and the upper-bound  $\Gamma = 5$ . For the proposed approach, the results of ST sampler synthesis are given in Fig. 5.1.

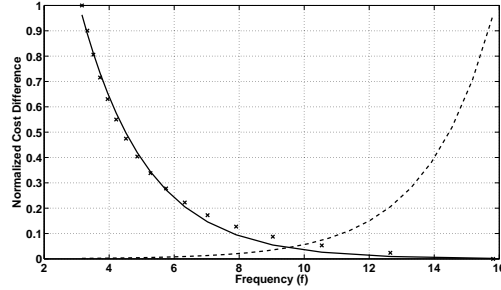


Figure 5.1: ST sampler synthesis for mass-spring system.

For [1]  $\beta_1 = 1.1$ ,  $\beta_2 = 1.5$ ,  $\gamma = 0.99$ ,  $Q = I^{(4)}$  and  $R = 1$ , which are discretized for sampled-data implementation using (4.6), with period  $\alpha$  for reference system and [1], and  $\Gamma\alpha$  for the proposed method. Fig. 5.2 shows the state response and it can be seen that the proposed methodology results in lesser settling time



than that for [1]. The control costs for [1] and proposed scheme are 5.48 and 5.29,

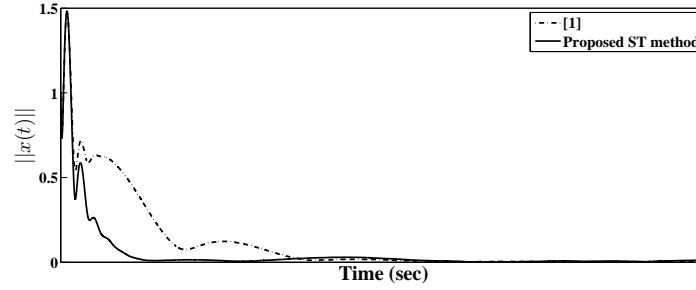


Figure 5.2: State norm.

respectively. Fig. 5.3 presents the sampling times for both methodologies, and the performance of novel approach can be clearly observed. During the period when the states are completely regulated, the sampling time increases, which results in a lesser number of events, translating into a communication bandwidth economy. Specifically, the event rate for [1] is 15.8 which is greater than 8.58 for the proposed scheme.

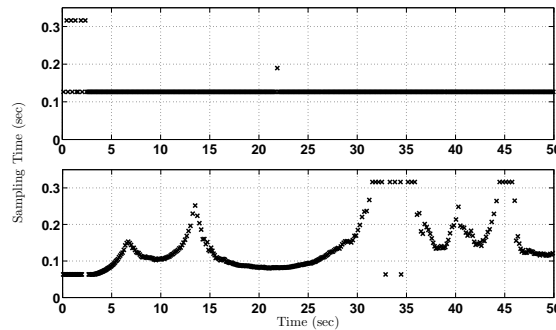


Figure 5.3: Sampling times for mass-spring system. Top: [1]; bottom: novel ST scheme.

With regards to the computational time, the new approach requires 0.016 ms whereas [1] takes 0.02 ms. Conclusively, the proposed methodology results in a better performance than the one in [1] with 3.5%, 44%, and 20% reduction in

control cost, event-rate, and computational time, respectively.

### Four-tank system

The process, given in [139], contains four tanks and two pumps, and the objective is to control the water level in tanks 1 and 2. The pump flows are divided by valves and their position determines the location of system's zeros, making the system the minimum or non-minimum phase. In this analysis, only minimum phase case is considered, and that all the states are measurable. Table 6.1 gives the parameters and description.

Table 5.1: Parameters of the four-tank system.

| Par.     | Description                      | Value                   |
|----------|----------------------------------|-------------------------|
| $h_{ss}$ | Steady state water level         | 15 cm                   |
| $a$      | Cross-section area of the tanks  | 15.52 cm                |
| $o$      | Cross-section area of the outlet | 0.178 cm                |
| $g$      | Acceleration due to gravity      | 981 cm/s <sup>2</sup>   |
| $k_p$    | Pump flow constant               | 3.3 cm <sup>3</sup> /sV |
| $\theta$ | Valve flow ratio                 | 0.75                    |

The states of the linearized system (6.22) are  $x_i := h_i - h_{ss}$  for  $i \in \{1, 2, 3, 4\}$ , inputs  $u := v_j - v_{j,ss}$  where  $v_j$  represents the voltage input of  $j$ -th pump with  $v_{j,ss}$  as its steady state value and  $j \in \{1, 2\}$ , and

$$A = \begin{bmatrix} a_1 & 0 & a_2 & 0 \\ 0 & a_1 & 0 & a_2 \\ 0 & 0 & a_1 & 0 \\ 0 & 0 & 0 & a_1 \end{bmatrix}; B_1 = \begin{bmatrix} b_1 & 0 \\ 0 & b_1 \\ 0 & b_2 \\ b_2 & 0 \end{bmatrix}; B_2 = \begin{bmatrix} 2 \\ 2 \\ 0.4 \\ 0.6 \end{bmatrix}, \quad (5.17)$$

where  $a_1 = -\frac{1}{T}$  and  $a_2 = \frac{1}{T}$  with  $T = \frac{\alpha\sqrt{2g}}{a} \frac{1}{2\sqrt{h_{ss}}}$ , and  $b_1 = \frac{\theta k_p}{a}$  and  $b_2 = \frac{1-\theta k_p}{a}$ . The initial state  $x_0 = [10 \ 5 \ -7 \ -10]^T$  and  $W = 1$ . The sampling period  $\alpha$  is chosen as 13.1 ms and  $\Gamma = 5$ , which give the ST sampler similar to Fig. 5.1 with  $f_m = 15.27$  Hz and  $f_M = 76.34$  Hz.

The values of  $\beta_1 = 1.5$ ,  $\beta_2 = 1.1$ ,  $Q = I^{(4)}$  and  $R = 25I^{(2)}$ . The norm of state trajectories is shown in Fig. 5.4 (a), and both methodologies result in similar performance. The control cost for [1] is 167.48 and that for the new approach is

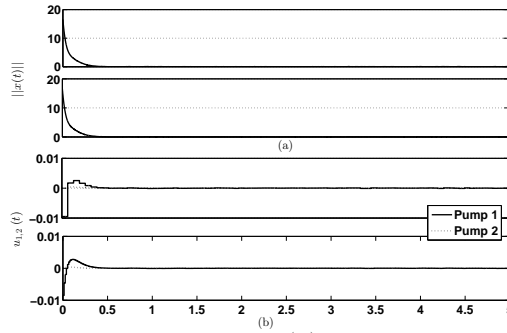


Figure 5.4: (a) State norm. Top: [1]; bottom: novel ST scheme. (b) Inputs. Top: [1]; bottom: novel ST scheme.

111.15; the reason for this difference is slightly greater amount of control effort exerted by the controller of [1] in the transient period as demonstrated by Fig. 5.4 (b). Fig. 5.5 demonstrates the behavior of samplers, and rates for [1] and the proposed scheme are 65 and 52.8, respectively.

Conclusively, the proposed method gives 33.6% and 18.76 % decrease in control and communication costs as compared with [1], respectively. The computational times are similar to that of the mass-spring system.

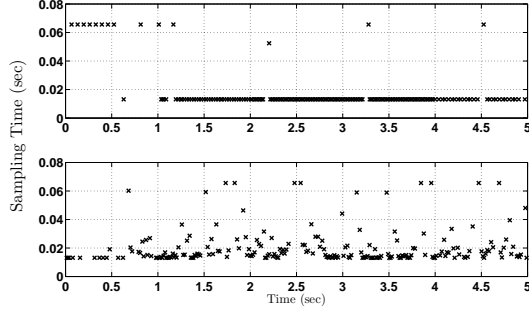


Figure 5.5: Sampling times for the four-tank system. Top: [1]; bottom: novel ST scheme.

### Pendulum-cart system

The system is described in [103] with states  $x = [y \dot{y} \phi \dot{\phi}]^T$ , where  $y$  and  $\phi$  denote cart's position and bob's angle. Bobs mass  $m_b = 1$ , the carts mass  $M_c = 10$ , length of the pendulum  $l = 3$ , gravitational acceleration  $g = 10$ , and  $W = 1$ ; system represented by (6.22) is given as

$$A = \begin{bmatrix} 0 & 1 & 0 & 0 \\ 0 & 0 & -\frac{m_b g}{M_c} & 0 \\ 0 & 0 & 0 & 1 \\ 0 & 0 & \frac{g}{l} & 0 \end{bmatrix}; B_1 = \begin{bmatrix} 0 \\ \frac{1}{M_c} \\ 0 \\ -\frac{1}{M_c l} \end{bmatrix}; B_2 = \begin{bmatrix} 0.02 \\ 0.02 \\ 0.02 \\ 0.02 \end{bmatrix}. \quad (5.18)$$

The values of  $x_0 = [0.9 \ 0 \ 0.4 \ 0]^T$ ,  $\alpha = 109.5$  ms,  $\Gamma = 8$ ,  $\beta_1 = \beta_2 = 1.1$ ,  $Q = 100I^{(4)}$ ,  $R = 1$ , and  $\gamma = 0.99$ . The results of ST sampler synthesis are similar to Fig. 5.1 with  $f_m = 1.14$  Hz and  $f_M = 9.13$  Hz.

For [1], the controller was unable to stabilize the system even for different values of  $\beta_{1,2}$  and weighting matrices. In contrast, the proposed scheme gave a stable system with events and state norm shown in Fig. 5.6. The reason for

stability of the system is the high sampling frequency in transient phase resulting from the proposed ST sampler; this is not true for the controller presented in [1]. The sensitivity of the proposed sampler can be observed as the sampling interval decreases even for a slight increase in the ST system's cost against the reference system. The event-rate, control cost, and computation time are 4.26,  $9.12 \times 10^4$ , and 0.012 ms, respectively.

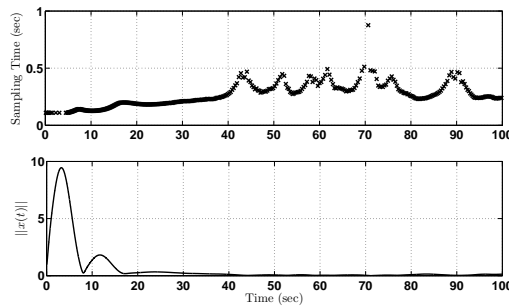


Figure 5.6: Top: sampling times; bottom: state norm.

## 5.5 Conclusion

A novel ST LQR scheme was presented which addresses the shortcomings in the existing literature, and a comparative study against [1] was presented with simulation results for three case studies. It can be concluded that the proposed approach is suitable for the case where control, communication, and computational resources are critical, and if the communication channel introduces delays then this scheme is the only choice. The simulation results showed superior control performance as compared with [1], which failed to stabilize the system in one of the cases. With regards to the sampling methodology, the proposed sampler

results in significant communication-bandwidth economy than [1]. This is due to the fact that the sampler tries to achieve the same performance as the reference periodic system at much lower sampling frequency, particularly when the system is regulated.

In terms of the computational requirements, the proposed methodology takes less time as compared with [1]. Although the memory requirements are higher due to the storage of reference system's cost evolution, this requirement is less stringent than higher computational time which may affect the real-time capability of the proposed scheme. Nevertheless, for limited memory applications, a copy of the reference system may run in real-time to compare its cost against that of the ST system.

## CHAPTER 6

# $\mathcal{H}_\infty$ -BASED SELF-TRIGGERED CONTROL OVER IEEE 802.15.4 NETWORK

### 6.1 Introduction

In view of the studies mentioned in the previous chapters and the existing results, to the best of our knowledge, the present literature lacks in:

- Taking advantage of the proactive nature of ST methodology which provides the triggering time *in advance*.
- The provision of including more control loops than the maximum number of transmission slots.
- A decoupled design of communication and control in multiple control loop

setting, which saves computational resources besides energy efficiency.

These form the main motivation for this work which has the following contributions and significance:

- Two-level design method for NCS in which control and communication designs are decoupled. The first level is based on ST  $\mathcal{H}_\infty$  controller and the second level comprises the network manager (NM),
- Modifications in the IEEE 802.15.4 protocol to benefit from ST control. Specifically, the predicted triggering time is used to schedule the next beacon interval thus saving considerable amount of energy at the sensor node, which enhances energy efficiency of the applications based on IEEE 802.15.4 protocol. Additionally, this characteristic can avoid contention and congestion in the network,
- Priority-Based Scheduling (PBS) algorithm is integrated in the modified protocol to accommodate more systems than the maximum number of available transmission slots,
- The proposed design does not require a two-step ahead triggering time predictor and a disturbance observer, as opposed to [10], thus saving computational cost.

The chapter is organized as follows: Section 6.2 defines the problem and gives an overview of the design. Section 6.3 reproduces the work presented in [103] and compares ET and ST methodologies. Sections 6.4 and 6.5 present first and



second level controllers, respectively. Simulation results are given in Section 6.6, and Section 6.7 concludes the chapter.

Sets of real numbers and integers are denoted by  $\mathbb{R}$  and  $\mathbb{Z}$ , respectively. Set of strictly positive real numbers are represented by  $\mathbb{R}^+$  and those including zero are denoted as  $\mathbb{R}^{\{0,+ \}}$ . The set of positive definite and semi-definite integers are represented as  $\mathbb{Z}^+$  and  $\mathbb{Z}^{\{0,+ \}}$ , respectively. The second norm is given as  $\|\cdot\|_2$ .

## 6.2 Problem Definition and Overview

A class of  $N$  independent  $\mathcal{H}_\infty$ -based ST control systems is considered. The feedback loops of these systems are closed over the same wireless communication medium as shown in Fig. 6.1. The controllers are wired with the network man-

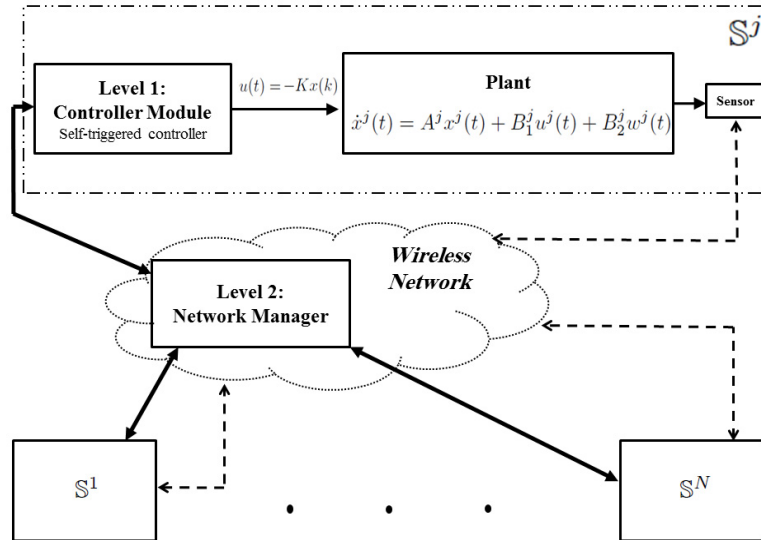


Figure 6.1: NCS with two-level control. Solid lines: wired connection; dashed lines: wireless link.

ager (NM), and the sensor nodes acquire all the states and transmit them to the

NM wirelessly. This type of setting, which follows the star topology for sensor-controller network and wired connections for controller-actuator link, is common in industrial applications such as process control [10]. Each system  $\mathbb{S}^j$ , where  $j \in \{1, \dots, N\}$ , implements a ST  $\mathcal{H}_\infty$  controller to ensure finite-gain  $\mathcal{L}_2$  stability. In particular, the results of [102] are extended to incorporate the constraints introduced on triggering time, as explained in Section 6.4. The wireless network uses a slotted communication mechanism which is based on the modifications proposed for IEEE 802.15.4 protocol. The controllers requesting state information are assigned fixed time slots according to their predicted triggering times. NM gets state information from sensor nodes in their respective time slots, and passes this information to respective controllers.

Due to the limited bandwidth of the communication network, the number of time slots is restricted to  $N_{max}$  in each beacon interval [9]. The aim is to guarantee finite-gain  $\mathcal{L}_2$  stability using  $\mathcal{H}_\infty$  controllers for all the control loops, while reducing the communication cost. However, due to correlation introduced between the states of the systems because of a bandwidth-limited communication medium, this problem is difficult to solve. In order to decouple communication from control and avoid Zeno behavior, the transmission interval of each system is lower-bounded by minimum inter-sampling period (or maximum transmission rate)  $\underline{\tau} \in \mathbb{R}^+$ . This splits the problem into two levels.

At the first level, ST controller module for each system guarantees  $\mathcal{L}_2$  stability using full-information  $\mathcal{H}_\infty$  controller, besides computing next sampling time.

These controllers send their *System's Overall State Indicator (SOSI)* and *next sampling times* to the second level controller through the wired connection, as soon as they finish the computations. At the second level the NM, which is based on the proposed modifications in IEEE 802.15.4 protocol, implements PBS algorithm which uses this information of each plant to schedule their transmissions. Moreover, unlike [10] the SOSI in proposed PBS mechanism does not require a disturbance observer and two-steps ahead triggering-time predictor, which imply less computational load.

Here two cases are considered; first, when the number of control loops is at most  $N_{max}$ , and second, when this number exceeds  $N_{max}$ . For this work,  $N \leq N_{max} + 1$  is considered as the bound on the number of systems for second case. In the first case, all the systems are allowed to transmit, i.e., no transmission request is denied while optimizing the bandwidth usage. In the second case, PBS accepts transmission requests of only those systems which encounter more performance degradation (revealed by SOSI) as compared with the other systems, for which the transmission slot is postponed. In this way, the proposed methodology can accommodate more systems than the number of available transmission slots, as opposed to [10].

### 6.3 Comparison

In this section we compare ET and ST control by re-simulating the work presented in [103], which compared their proposed ST and ET schemes. Due to space

constraint, we briefly describe the methodologies. The LTI system considered is given as,

$$\dot{x}(t) = Ax(t) + B_1u(t) + B_2w(t), \quad x(0) = x_0, \quad (6.1)$$

where  $x_0 \in \mathbb{R}^n$  is non-zero initial state,  $u : [0, \infty) \rightarrow \mathbb{R}^m$  is control input and  $w : [0, \infty) \rightarrow \mathbb{R}^l$  is exogenous disturbance in  $\mathcal{L}_2$  space. The controller used for both ET and ST schemes is full-information  $\mathcal{H}_\infty$  controller which is designed assuming a symmetric positive semi-definite matrix  $P$  satisfying the following ARE,

$$0 = PA + A^T P - Q + R, \quad (6.2)$$

where,

$$Q = PB_1B_1^T P; \quad R = I + \frac{1}{\gamma^2}PB_2B_2^T P, \quad (6.3)$$

for some real  $\gamma > 0$ . This renders the closed-loop system,

$$\begin{aligned} \dot{x}(t) &= Ax(t) + B_1u(t), \\ u(t) &= -B_1^T Px(t), \end{aligned} \quad (6.4)$$

asymptotically stable. It can be denoted as  $A_{cl} = A + B_1K$  with  $K = -B_1^T P$ . The closed-loop system is finite-gain  $\mathcal{L}_2$  stable from the disturbance  $w$  to  $(x^T, u^T)^T$  with an induced gain less than  $\gamma$ .

A sampled data implementation of the closed-loop,

$$\begin{aligned}\dot{x}(t) &= Ax(t) + B_1u(t) + B_2w(t), \\ u(t) &= -B_1^T Px(t),\end{aligned}\tag{6.5}$$

is considered, whereby the control computation is done by a computer task. Each task is characterized by release times  $r_k$  and finish times  $f_k$  with  $k = 0, \dots, \infty$ , illustrated in the timing diagram in Fig. 2.2. The control signal is kept constant by ZOH until the next finishing time and the state trajectories are continuous, giving the sampled data system as,

$$\begin{aligned}\dot{x}(t) &= Ax(t) + B_1u(t) + B_2w(t), \\ u(t) &= -B_1^T Px(r_k),\end{aligned}\tag{6.6}$$

for  $t \in [f_k, f_{k+1})$ .

Let  $e_k(t) = x(t) - x(r_k)$  be the error representing the difference between current and last release time state  $x(r_0) = x_0$ , and  $Q$  be the real matrix satisfying (6.3).

For any  $\beta \in [0, 1)$ , let

$$M = (1 - \beta^2)I + Q; \quad N = \frac{1}{2}(1 - \beta^2)I + Q.\tag{6.7}$$

Now, let

$$z_k(t) = \sqrt{(1 - \beta^2)I + Q}e_k(t) = \sqrt{M}e_k(t),\tag{6.8}$$

and

$$\rho(x) = \sqrt{x^T N x}, \quad (6.9)$$

then the ET scheme is given by the following theorem.

**Theorem 6.1** *Consider sampled data system (6.6) satisfying the assumption that, for a real constant  $W > 0$ ,  $\|w(t)\|_2 \leq W\|x(t)\|_2$  for all  $t \geq 0$ . Assume that  $M$  has full rank and for some  $\delta \in [0, 1)$  the release time sequence  $\{r_k\}_{k=0}^{\infty}$  satisfies,*

$$\|z(r_{k+1})\|_2 = \delta\rho(x(r_k)), \quad (6.10)$$

where  $f_k = r_k \forall k = 0, \dots, \infty$ . Then sampled data system is finite-gain  $\mathcal{L}_2$  stable from  $w$  to  $x$  with an induced gain less than  $\gamma/\beta$ .

Let,

$$\alpha = \|\sqrt{M}A\sqrt{M}^{-1}\| + W\|\sqrt{M}B_2\|\|\sqrt{M}^{-1}\|, \quad (6.11)$$

and  $\mu_0 : \mathbb{R}^n \rightarrow \mathbb{R}$  is a real-valued function given as,

$$\mu_0(x(r_k)) = \|\sqrt{M}A_{cl}x(r_k)\|_2 + W\|\sqrt{M}B_2\|\|x(r_k)\|_2. \quad (6.12)$$

For some  $\epsilon \in (0, 1)$ , let  $\phi : \mathbb{R}^n \times \mathbb{R}^n \times \mathbb{R} \rightarrow \mathbb{R}$  and  $\mu_1 : \mathbb{R}^n \times \mathbb{R}^n \rightarrow \mathbb{R}$  be real valued

functions defined as,

$$\begin{aligned}\mu_1(x(r_k), x(r_{k-1})) &= W\|\sqrt{M}B_2\| \|x(r_k)\|_2 + \|\sqrt{M}(Ax(r_k) - B_1B_1^T Px(r_{k-1}))\|_2, \\ \phi(x(r_k), x(r_{k-1}); t - r_k) &= \frac{\mu_1(x(r_k), x(r_{k-1}))}{\alpha} (e^{\alpha(t-r_k)} - 1).\end{aligned}\tag{6.13}$$

For  $0 \leq D_k = f_k - r_k$  and some  $\eta \in (\epsilon, 1]$ , let  $L_2 : \mathbb{R}^n \times \mathbb{R}^n \times \mathbb{R} \times (0, 1] \rightarrow \mathbb{R}$  be defined as,

$$L_2(x(r_k), x(r_{k-1}); D_k, \eta) = \frac{1}{\alpha} \ln \left( 1 + \alpha \frac{\eta \rho(x(r_k)) - \phi(x(r_k), x(r_{k-1}); D_k)}{\mu_0(x(r_k)) + \alpha \phi(x(r_k), x(r_{k-1}); D_k)} \right).\tag{6.14}$$

Furthermore, let  $\xi : \mathbb{R}^n \times (0, 1) \times (0, 1) \rightarrow \mathbb{R}$  be a real valued function defined as,

$$\xi(x(r_{k-1}); \epsilon, \delta) = \frac{1}{\alpha} \ln \left( 1 + \frac{\epsilon \delta \rho(x(r_{k-1}))}{\delta \rho(x(r_{k-1})) + \frac{\mu_0(x(r_{k-1}))}{\alpha}} \right),\tag{6.15}$$

then the proposed ST scheme is given by the following theorem.

**Theorem 6.2** *Consider sampled data system (6.6) satisfying the bounded disturbance assumption that, for a real constant  $W > 0$ ,  $\|w(t)\|_2 \leq W\|x(t)\|_2 \forall t \geq 0$ . Assume that  $M$  has full rank, for some  $\epsilon \in (0, 1)$  and  $\delta \in (\epsilon, 1)$ , we assume that*

1. *The initial release and finish times satisfy,  $r_{-1} = r_0 = f_0 = 0$ .*

2. *For any non-negative integer  $k$ , the release times are generated by,*

$$r_{k+1} = f_k + L_2(x(r_k), x(r_{k-1}); D_k, \delta),\tag{6.16}$$

where  $L_2$  is given in (6.14), and the finish times satisfy,

$$r_{k+1} \leq f_{k+1} \leq r_{k+1} + \xi(x(r_k); \epsilon, \delta), \quad (6.17)$$

with  $\xi$  defined in (6.15).

Then the sampled data system is said to be finite-gain  $\mathcal{L}_2$  stable from  $w$  to  $x$  with an induced gain less than  $\gamma/\beta$ .

### 6.3.1 Simulation

The plant considered is an inverted pendulum on top of a moving cart with states  $x = [y \ \dot{y} \ \theta \ \dot{\theta}]^T$ , where  $y$  and  $\theta$  denote cart's position and pendulum bob's angle, respectively. The system matrices are given as,

$$A = \begin{bmatrix} 0 & 1 & 0 & 0 \\ 0 & 0 & -\frac{mg}{M} & 0 \\ 0 & 0 & 0 & 1 \\ 0 & 0 & \frac{g}{l} & 0 \end{bmatrix}; B_1 = \begin{bmatrix} 0 \\ \frac{1}{M} \\ 0 \\ -\frac{1}{Ml} \end{bmatrix}; B_2 = \begin{bmatrix} 1 \\ 1 \\ 1 \\ 1 \end{bmatrix}, \quad (6.18)$$

where,  $m$  is bob's mass,  $M$  denotes cart's mass,  $l$  is the length of the pendulum, and  $g$  is gravitational acceleration. The values taken for these parameters are  $m = 1$ ,  $M = 10$ ,  $l = 3$  and  $g = 10$ . The initial state for the system is  $x_0 = [0.98 \ 0 \ 0.2 \ 0]^T$ . The  $\mathcal{H}_\infty$  controller is designed using MATLAB with  $\gamma = 200$



to obtain the vector  $K$  as,

$$K = \begin{bmatrix} -2 & -12 & -378 & -210 \end{bmatrix}. \quad (6.19)$$

### 6.3.2 Results

The ET and ST schemes, given by Theorems 6.1 and 6.2, were implemented using Simulink on the given system, with  $\epsilon = 0$  and  $\delta = 1$ , i.e., without delay. The state errors resulting from both schemes are compared using the normalized state error (NSE) given as,

$$E(t, x) = \frac{|\sqrt{V(x(t))} - \sqrt{V(x_c(t))}|}{\sqrt{V(x_c(t))}}, \quad (6.20)$$

where,  $x(t)$  denotes the state of ET or ST controlled system,  $x_c(t)$  is the CT system state and  $V(x)$  represents the Lyapunov function for the system i.e.,  $V(x) = x^T P x$ .

Fig. 6.2 shows NSE for both schemes with  $w(t) = 0$ . It can be seen that the error

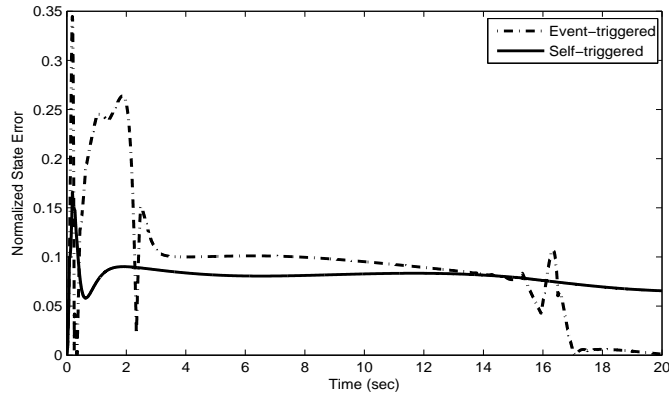


Figure 6.2: Normalized state errors for event- and self-triggered control schemes for  $w(t) = 0$ ,  $\delta = 1$  and  $\epsilon = 0$ .

for ST controlled system is slightly greater than that for ET scheme. Fig. 6.3 shows similar results for the case when the system was subject to a bounded

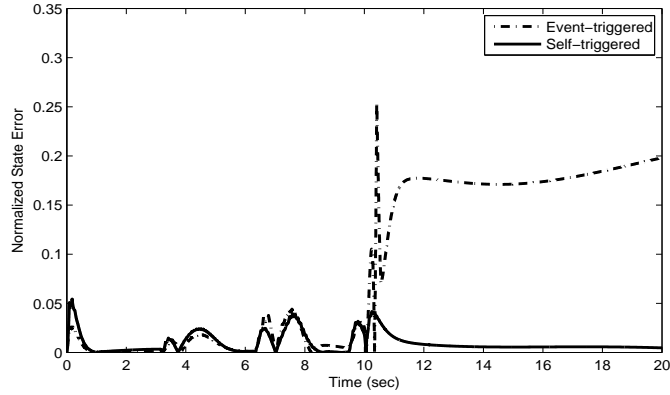


Figure 6.3: Normalized state errors for event- and self-triggered control schemes for  $w(t)$  as given in (6.21),  $\delta = 1$  and  $\epsilon = 0$ .

disturbance with  $W = 0.01$ , given as,

$$\begin{aligned}
 w(t) &= \text{sgn}(\sin t), & 0 \leq t < 10, \\
 &= 0, & \text{otherwise.}
 \end{aligned}
 \tag{6.21}$$

Figs. 6.4 and 6.5 show the periods generated by ET and ST schemes, respectively,

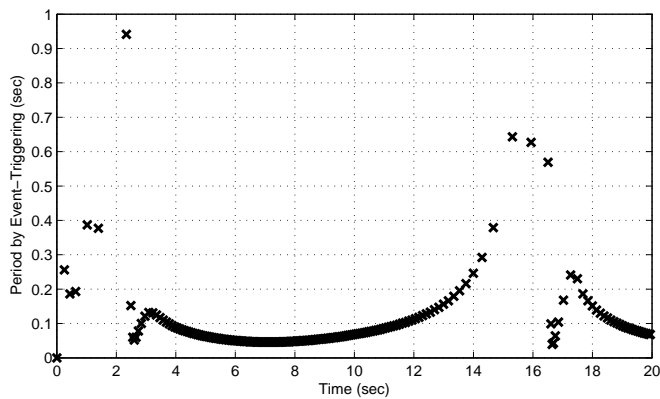


Figure 6.4: Sampling period versus time for event-triggered control scheme for  $w(t) = 0$ ,  $\delta = 1$  and  $\epsilon = 0$ .

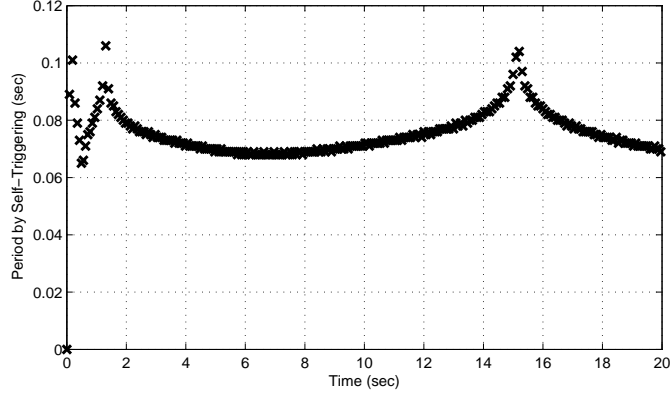


Figure 6.5: Sampling period versus time for self-triggered control scheme for  $w(t) = 0$ ,  $\delta = 1$  and  $\epsilon = 0$ .

for the case without disturbance. ET generated periods which range from 0.039 to 0.9410 seconds and ST gave periods ranging from 0.065 to 0.106 seconds. These results conform with those reported in [103], i.e., the periods generated by ET methodology are larger as compared with the ST scheme due to the conservative nature of ST update times. Also, for the case with disturbance, ET scheme (Fig. 6.6) generated periods that are larger than ST scheme (Fig. 6.7); ET periods ranged between 0.034 and 0.4910 seconds while that for ST were between 0.066 and 0.1 seconds. It can also be observed that the periods get smaller when there is a disturbance affecting the system, this ensures the required performance of the overall system showing that both the schemes are robust against changes in the disturbance.

*Remark 43* The robustness against changes in the disturbance is mainly due to the use of  $\mathcal{H}_\infty$  controller. The ET or ST schemes have been co-designed with the controller, consequently the sampling occurs to satisfy the  $\mathcal{L}_2$ -gain inequality.

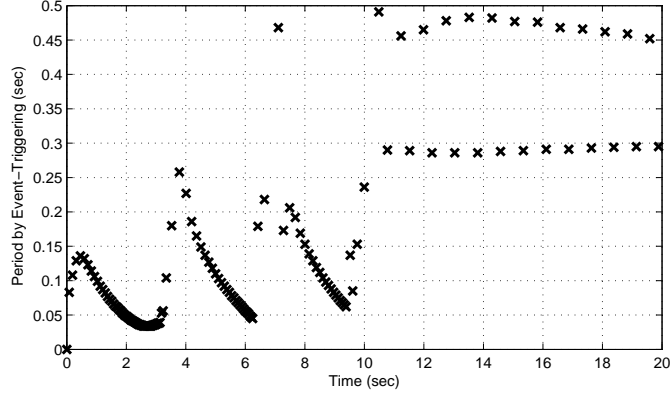


Figure 6.6: Sampling period versus time for event-triggered control scheme for  $w(t)$  as given in (6.21),  $\delta = 1$  and  $\epsilon = 0$ .

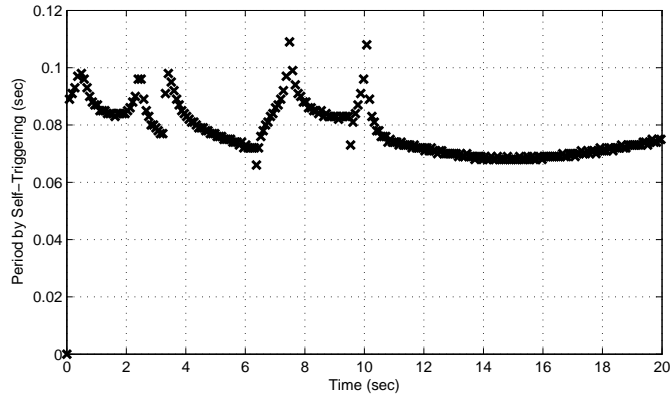


Figure 6.7: Sampling period versus time for self-triggered control scheme for  $w(t)$  as given in (6.21),  $\delta = 1$  and  $\epsilon = 0$ .

## 6.4 First Level: ST $\mathcal{H}_\infty$ controller

The  $j^{\text{th}}$  control system  $\mathbb{S}^j$ , where  $j \in \{1, \dots, N\}$ , consists of a plant  $\mathcal{P}^j$ , a controller module  $\mathcal{C}^j$ , and a sensor  $\mathcal{S}^j$ . The plants have continuous-time linear dynamics described as [102],

$$\begin{aligned} \dot{x}^j(t) &= A^j x^j(t) + B_1^j u^j(t) + B_2^j w^j(t), \\ u^j(t) &= -B_1^{j,T} P^j x^j(t) = -K^j x^j(t), \end{aligned} \tag{6.22}$$

where  $x^j(t) \in \mathbb{R}^n$  is  $j^{\text{th}}$  system's state vector,  $w^j(t) \in \mathbb{R}^m$  is the control input,  $w^j(t) \in \mathbb{R}^l$  is the exogenous disturbance in  $\mathcal{L}_2$  space, and the matrices  $A^j \in \mathbb{R}^{(n \times n)}$ ,  $B_1^j \in \mathbb{R}^{(n \times m)}$  and  $B_2^j \in \mathbb{R}^{(n \times l)}$  represent the system model.

The positive-definite symmetric matrix  $P^j$  represents the solution of the following  $\mathcal{H}_\infty$  ARE,

$$P^j A^j + A^{j,\text{T}} P^j - P^j B_1^j B_1^{j,\text{T}} P^j + I + \frac{1}{\gamma^{j,2}} P^j B_2^j B_2^{j,\text{T}} P^j = 0, \quad (6.23)$$

for some  $\gamma^j > 0$ . For the ease of notation, superscript  $j$  is dropped in the forthcoming analysis.

The controller module is a digital system which performs two sets of tasks. In the first set, it receives the sampled state and computes the control input. In the second set, it computes the next sampling time and SOSI, and sends this information to the NM. The timing diagram in Fig. 6.8 illustrates these steps. Let  $k \in \mathbb{Z}^{\{0,+ \}}$ , then at time instants  $\delta_k \in \mathbb{R}^{\{0,+ \}}$  the controller performs first set

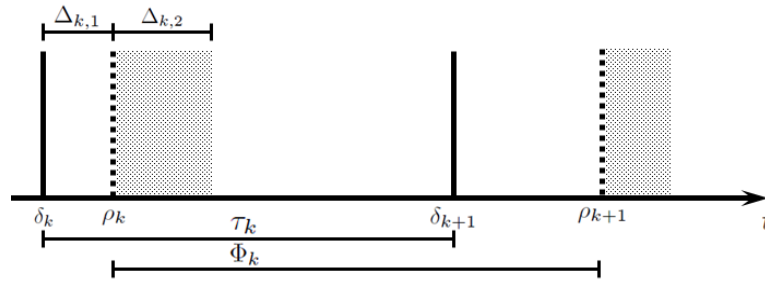


Figure 6.8: Timing diagram. Controller module performs two sets of computations; first set:  $\Delta_{k,1}$ , second set:  $\Delta_{k,2}$ .

of computations which takes  $\Delta_{k,1} \in \mathbb{R}^+$  units of time. As soon as the controller module completes these calculations, it applies the control input on the plant at

$\rho_k \in \mathbb{R}^{\{0,+ \}}$  and also starts the second set of computations; in this way, the time taken for the second set does not effect the control function. For  $\Phi_k \in \mathbb{R}^+$  units of time, this control input is held constant until the next finishing time  $\rho_{k+1}$ . This renders (6.22) as a sampled-data system,

$$\begin{aligned} \dot{x}(t) &= Ax(t) + B_1u(t) + B_2w(t), \\ u(t) &= -B_1^T Px(k) = -Kx(k), \quad \forall t \in [\rho_k, \rho_{k+1}), \end{aligned} \tag{6.24}$$

where  $x(k)$  denotes the state sampled at  $\delta_k$ .

**Definition 6.4.1** [102] *Sampled-data system (6.24) is said to be finite-gain  $\mathcal{L}_2$  stable from  $w$  to  $x$  with an induced gain less than  $\gamma > 0$ , if there exists non-negative constant  $\epsilon$  such that*

$$\left( \int_0^\infty \|x(t)\|_2^2 dt \right)^{\frac{1}{2}} \leq \gamma \left( \int_0^\infty \|w(t)\|_2^2 dt \right)^{\frac{1}{2}} + \epsilon, \tag{6.25}$$

for any  $w$  satisfying  $(\int_0^\infty \|w(t)\|_2^2 dt)^{1/2} < \infty$ .

The aperiodic inter-sampling time, denoted by  $\tau_k$ , is both upper and lower-bounded as,

$$\underline{\tau} \leq \tau_k = \delta_{k+1} - \delta_k \leq \bar{\tau}, \quad \forall k \in \mathbb{Z}^+, \tag{6.26}$$

where,  $\bar{\tau} \in \mathbb{R}^+$  represents the upper-bound to ensure bounded latency, and  $\underline{\tau}$  is the lower-bound to decouple control and communication. The choice of these bounds is made according to the dynamics of the participating systems in the NCS, while satisfying the communication constraints imposed by the protocol;

this will be detailed in forthcoming text. Before the ST  $\mathcal{H}_\infty$  scheme is presented which ensures finite-gain  $\mathcal{L}_2$  stability, the following assumption is stated.

**Assumption 6** *The computational delays  $\Delta_{k,1}$  and  $\Delta_{k,2}$  (Fig. 6.8) are negligible as compared with the inter-sampling time  $\tau_k$ . This assumption is realistic because firstly, the low data-rate wireless network is suitable for low-speed control applications which do not require very fast sampling. Secondly, the controller module and NM have high-speed computational power. Both these facts imply that  $\Delta_{k,1} + \Delta_{k,2} \ll \tau_k$ , hence  $\delta_k \approx \rho_k$  for all  $k \in \mathbb{Z}^+$ .*

**Lemma 6.1** [102] *For  $j$ -th sampled-data system given as (6.24) with Assumption 6, let  $V : \mathbb{R}^n \rightarrow \mathbb{R}^+$  be a positive semi-definite function defined by  $V(x) = x^T P x$  with  $P$  given in (6.23). For any real constant  $\beta \in (0, 1]$ , the directional derivative of  $V$  satisfies*

$$\dot{V} \leq -\beta^2 \|x(t)\|_2^2 + \gamma^2 \|w(t)\|_2^2 + (e_t^k)^T M e_t^k - x^T(k) N x(k), \quad \forall t \in [\delta_k, \delta_{k+1}), \quad (6.27)$$

for all  $k \in \mathbb{Z}^+$ , where  $e_t^k = x(t) - x(k)$  represents the measurement error. The matrices  $M$  and  $N$  are defined as

$$\begin{aligned} M &= (1 - \beta^2)I + P B_1 B_1^T P, \\ N &= \frac{1}{2}(1 - \beta^2)I + P B_1 B_1^T P. \end{aligned} \quad (6.28)$$

The proof of this lemma is given in [102] and left out of here for brevity.

From (6.27), finite-gain  $\mathcal{L}_2$  stability is guaranteed as long as the following

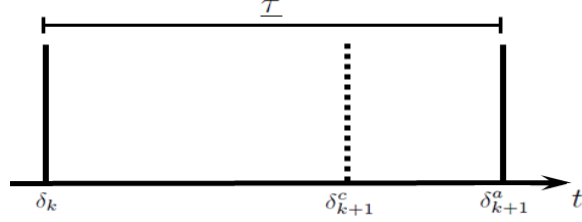


Figure 6.9: When the computed triggering time is less than the assigned one.

inequality is satisfied

$$(e_t^k)^T M e_t^k \leq x^T(k) N x(k), \quad \forall t \in [\delta_k, \delta_{k+1}]. \quad (6.29)$$

Since it is assumed that the disturbance can be any signal in  $\mathcal{L}_2$  space, it is necessary to show that the error  $\|\sqrt{M}e_t^k\|_2$  remains bounded for all  $t \in [\delta_k, \delta_{k+1}]$ .

Furthermore, there can be a case wherein the NM assigns  $\delta_{k+1}^a$  to a control loop if it demands to sample the state at  $\delta_{k+1}^c$  such that  $\delta_{k+1}^c < \delta_{k+1}^a$ , where the superscripts  $c$  and  $a$  denote the *computed* and *assigned* triggering times, respectively. This covers both the cases, i.e., (1) when the demanded time falls below  $\tau$  i.e., if  $\delta_{k+1}^c - \delta_k < \tau$ , as shown in Fig. 6.9, and (2) when the NM assigns a different time slot when implementing PBS algorithm. These facts necessitate to show that the error remains bounded during the interval  $t \in [\delta_{k+1}^c, \delta_{k+1}^a]$ .

Following lemma shows that these bounds indeed exist. For the ease of anal-



ysis, following notations are defined,

$$\begin{aligned}
\mu(x) &= \|\sqrt{N}x\|_2, \\
\mu_0(x(k)) &= \|\sqrt{M}\bar{A}x(k)\|_2, \\
\alpha &= \|\sqrt{M}A\sqrt{M}^{-1}\|_2,
\end{aligned} \tag{6.30}$$

where,  $\bar{A} = A - B_1B_1^T P$  represents the closed-loop matrix. Here it is assumed that,

**Assumption 7** For a bounded constant  $\tau' > 0$ ,

$$0 < \delta_{k+1}^a - \delta_{k+1}^c \leq \tau',$$

*i.e., the difference between computed and assigned triggering times is bounded for all initial states and for all time, i.e., uniformly-bounded.*

**Lemma 6.2 Case 1:**  $\delta_{k+1}^a = \delta_{k+1}^c$ .

For the sampled-data system (6.24) with Assumption 6, let  $\beta \in (0, 1]$  be such that the matrix  $M$  defined in (6.28) has full rank. The following inequality must hold for all  $t \in [\delta_k, \delta_{k+1})$ :

$$\|\sqrt{M}e_t^k\|_2 \leq \frac{\mu_0(x(k))}{\alpha} (e^{\alpha(t-\delta_k)} - 1) + \int_{\delta_k}^t e^{\alpha(t-s)} \|\sqrt{M}B_2\|_2 \|w(s)\|_2 ds. \tag{6.31}$$

**Case 2:**  $\delta_{k+1}^a > \delta_{k+1}^c$ .

For the sampled-data system (6.24) with Assumptions 6 and 7, let  $\beta \in (0, 1]$  be

such that the matrix  $M$  defined in (6.28) has full rank. The following inequality must hold for all  $t \in [\delta_{k+1}^c, \delta_{k+1}^a)$ :

$$\begin{aligned} \|\sqrt{M}e_t^k\|_2 &\leq \frac{\mu_0(x(k))}{\alpha} (e^{\alpha(t-\delta_k)} - 1) + \int_{\delta_k^c}^t e^{\alpha(t-s)} \|\sqrt{M}B_2\|_2 \|w(s)\|_2 ds \\ &+ e^{\alpha(t-\delta_{k+1}^c)} \int_{\delta_k}^{\delta_{k+1}^c} e^{\alpha(\delta_{k+1}^c-s)} \|\sqrt{M}B_2\|_2 \|w(s)\|_2 ds. \end{aligned} \quad (6.32)$$

**Proof. Case 1:** Let  $\Omega = \{t \in [\delta_k, \delta_{k+1}) : \|\sqrt{M}e_t^k\|_2 = 0\}$ , i.e., the time for which error is zero. The time derivative of  $\|\sqrt{M}e_t^k\|_2$  for  $t \in [\delta_k, \delta_{k+1}) \setminus \Omega$  satisfies

$$\begin{aligned} \frac{d}{dt} \|\sqrt{M}e_t^k\|_2 &\leq \|\sqrt{M}\dot{e}_t^k\|_2 = \|\sqrt{M}\dot{x}(t)\|_2 = \|\sqrt{M}(Ae_t^k + (A - B_1B_1^T P)x(k) + B_2w(t))\|_2 \\ &(\because x(t) = e_t^k + x(k)) \\ &= \|\sqrt{M}A\sqrt{M}^{-1}\sqrt{M}e_t^k + \sqrt{M}\bar{A}x(k) + \sqrt{M}B_2w(t)\|_2 \leq \alpha \|\sqrt{M}e_t^k\|_2 + \mu_0(x(k)) \\ &+ \|\sqrt{M}B_2\|_2 \|w(t)\|_2. \end{aligned} \quad (6.33)$$

Solving above differential inequality with  $\|\sqrt{M}e_k^k\|_2 = 0$  for  $t = \delta_k$ , we get

$$\|\sqrt{M}e_t^k\|_2 \leq \frac{\mu_0(x(k))}{\alpha} (e^{\alpha(t-\delta_k)} - 1) + \int_{\delta_k}^t e^{\alpha(t-s)} \|\sqrt{M}B_2\|_2 \|w(s)\|_2 ds,$$

which gives the error bound for  $t \in [\delta_k, \delta_{k+1})$ .

**Case 2:** Refer to Fig. 6.9. For duration  $t \in [\delta_k, \delta_{k+1}^a)$ , the closed-loop system is given as,

$$\dot{x}(t) = \bar{A}x(k) + B_2w(t). \quad (6.34)$$

Divide  $t \in [\delta_k, \delta_{k+1}^a)$  into two parts,  $t_1 \in [\delta_k, \delta_{k+1}^c)$  and  $t_2 \in [\delta_{k+1}^c, \delta_{k+1}^a)$ . Let

$\Omega_1 = \left\{ t_1 \in [\delta_k, \delta_{k+1}^c) : \|\sqrt{M}e_t^k\|_2 = 0 \right\}$  i.e., the time at which error goes to zero.

The error bound for  $t_1 \in [\delta_k, \delta_{k+1}^c) \setminus \Omega_1$  satisfies the same inequality as (6.31). Let

$\Omega_2 = \left\{ t_2 \in [\delta_{k+1}^c, \delta_{k+1}^a) : \|\sqrt{M}e_t^k\|_2 = 0 \right\}$ , then

$$\frac{d}{dt} \|\sqrt{M}e_t^k\|_2 \leq \alpha \|\sqrt{M}e_t^k\|_2 + \mu_0(x(k)) + \|\sqrt{M}B_2\|_2 \|w(t)\|_2.$$

Solving above differential inequality with

$$\|\sqrt{M}e_{k+1}^k\|_2 \leq \frac{\mu_0(x(k))}{\alpha} (e^{\alpha(\delta_{k+1}^c - \delta_k)} - 1) + \int_{\delta_k}^{\delta_{k+1}^c} e^{\alpha(\delta_{k+1}^c - s)} \|\sqrt{M}B_2\|_2 \|w(s)\|_2 ds, \quad (6.35)$$

obtained from (6.31) at  $t = \delta_{k+1}^c$ , we get

$$\begin{aligned} \|\sqrt{M}e_t^k\|_2 &\leq \frac{\mu_0(x(k))}{\alpha} (e^{\alpha(t - \delta_k)} - 1) + \int_{\delta_{k+1}^c}^t e^{\alpha(t-s)} \|\sqrt{M}B_2\|_2 \|w(s)\|_2 ds \\ &\quad + e^{\alpha(t - \delta_{k+1}^c)} \int_{\delta_k}^{\delta_{k+1}^c} e^{\alpha(\delta_{k+1}^c - s)} \|\sqrt{M}B_2\|_2 \|w(s)\|_2 ds, \end{aligned}$$

which gives the error bound for  $t \in [\delta_{k+1}^c, \delta_{k+1}^a)$ . ■

With the error bounds given in Lemma 6.2, (6.31) and (6.32) are substituted in (6.27) to obtain an upper-bound on  $\dot{V}$  in terms of the induced gain. It is natural to expect that the gain will be upper- and lower-bounded due to the bounds defined in (6.26) for the first case, and for the second case, an additional term will be added due to the difference between computed and assigned triggering times.

**Theorem 6.3 Case 1:**  $\delta_{k+1}^a = \delta_{k+1}^c$

*Consider the sampled-data system (6.24) with Assumption 6. Let*

- $\beta \in (0, 1]$  be such that the matrix  $M$  defined in (6.28) has full rank, and
- the bounded constants  $\bar{\tau}, \underline{\tau}, \underline{\Gamma}, \bar{\Gamma} \in \mathbb{R}^+$ .

If for any  $k \in \mathbb{Z}^+$ , the inequalities

$$\delta_k < \delta_{k+1}, \quad (6.36)$$

$$\underline{\tau} \leq \tau_k \leq \bar{\tau}, \quad (6.37)$$

$$\zeta(x(k), \delta_k, \delta_{k+1}) \leq \int_{\delta_k}^{\delta_{k+1}} x^T(k) N x(k) dt, \quad (6.38)$$

hold where

$$\zeta(x(k), \delta_k, \delta_{k+1}) = \frac{2\mu_0^2}{\alpha^3} [2\alpha(\delta_{k+1} - \delta_k) - 4e^{\alpha(\delta_{k+1} - \delta_k)} + e^{2\alpha(\delta_{k+1} - \delta_k)} + 3], \quad (6.39)$$

then the sampled-data system (6.24) is said to be finite-gain  $\mathcal{L}_2$  stable from  $w$  to  $x$  with an induced gain bounded between  $\underline{\Gamma}$  and  $\bar{\Gamma}$ , where

$$\begin{aligned} \underline{\Gamma} &= \frac{1}{\alpha} \left[ \alpha^2 \gamma^2 + 4 \|\sqrt{M} B_2\|_2^2 (e^{\alpha \underline{\tau}} - 1)^2 \right]^{\frac{1}{2}}, \\ \bar{\Gamma} &= \frac{1}{\alpha} \left[ \alpha^2 \gamma^2 + 4 \|\sqrt{M} B_2\|_2^2 (e^{\alpha \bar{\tau}} - 1)^2 \right]^{\frac{1}{2}}. \end{aligned} \quad (6.40)$$

**Case 2:**  $\delta_{k+1}^a > \delta_{k+1}^c$

Consider the sampled-data system (6.24) with Assumptions 6 and 7. Let

- $\beta \in (0, 1]$  be such that the matrix  $M$  defined in (6.28) has full rank, and
- the bounded constants  $\xi_k, \bar{\tau}, \underline{\tau}, \underline{\Gamma}, \bar{\Gamma} \in \mathbb{R}^+$ .

If for any  $k \in \mathbb{Z}^+$ , the inequalities

$$\delta_k < \delta_{k+1}, \quad (6.41)$$

$$\underline{\tau} \leq \tau_k \leq \bar{\tau}, \quad (6.42)$$

$$\eta(x(k), \delta_{k+1}^c, \delta_{k+1}^a) \leq \int_{\delta_{k+1}^c}^{\delta_{k+1}^a} x^T(k) N x(k) dt + \xi_k (\delta_{k+1}^a - \delta_{k+1}^c), \quad (6.43)$$

hold where

$$\begin{aligned} \eta(x(k), \delta_{k+1}^c, \delta_{k+1}^a) &= \frac{2\mu_0^2}{\alpha^3} [2\alpha(\delta_{k+1}^a - \delta_{k+1}^c) \\ &+ e^{-2\alpha\delta_k} (e^{\alpha\delta_{k+1}^a} - e^{\alpha\delta_{k+1}^c}) (e^{\alpha\delta_{k+1}^a} + e^{\alpha\delta_{k+1}^c} - 4e^{\alpha\delta_k})], \end{aligned} \quad (6.44)$$

then the sampled-data system (6.24) is said to be finite-gain  $\mathcal{L}_2$  stable from  $w$  to  $x$  with the  $\mathcal{L}_2$  gain inequality given by

$$\int_{\delta_{k+1}^c}^{\delta_{k+1}^a} \dot{V} dt \leq -\beta^2 \int_{\delta_{k+1}^c}^{\delta_{k+1}^a} \|x(t)\|_2^2 dt + \Psi^2 \int_{\delta_{k+1}^c}^{\delta_{k+1}^a} \|w(t)\|_2^2 dt + \psi^2 + \xi_k \tau'.$$

where the induced gain  $\Psi$  is

$$\Psi = \frac{1}{\alpha} \left[ \alpha^2 \gamma^2 + 4 \|\sqrt{M} B_2\|_2^2 (e^{\alpha \tau'} - 1)^2 + \|\sqrt{M} B_2\|_2^2 (e^{2\alpha \tau'} - 1) (e^{2\alpha(\underline{\tau} - \tau')} - 1) \right]^{\frac{1}{2}}, \quad (6.45)$$

and the additional term  $\psi$  is

$$\psi = \frac{\|\sqrt{M} B_2\|_2}{\alpha} \left[ (e^{2\alpha \tau'} - 1) (e^{2\alpha(\underline{\tau} - \tau')} - 1) \int_{\delta_k}^{\delta_{k+1}^c} \|w(s)\|_2^2 ds \right]^{\frac{1}{2}}. \quad (6.46)$$

**Proof.** A similar methodology as in [102] is followed here:

**Case 1:** Form lemma 6.2 it is known that (6.31) holds for  $t \in [\delta_k, \delta_{k+1})$ .

Squaring both sides of (6.31), we get

$$\|\sqrt{M}e_t^k\|_2^2 \leq 4 \left( \frac{\mu_0(x(k))}{\alpha} (e^{\alpha(t-\delta_k)} - 1) \right)^2 + 4 \left( \int_{\delta_k}^t e^{\alpha(t-s)} \|\sqrt{M}B_2\|_2 \|w(s)\|_2 ds \right)^2. \quad (6.47)$$

Substituting (6.47) in (6.27) (Lemma 6.1), we get

$$\begin{aligned} \dot{V} \leq & -\beta^2 \|x(t)\|_2^2 + \gamma^2 \|w(t)\|_2^2 - x^T(k)Nx(k) + 4 \left( \frac{\mu_0(x(k))}{\alpha} (e^{\alpha(t-\delta_k)} - 1) \right)^2 \\ & + 4 \left( \int_{\delta_k}^t e^{\alpha(t-s)} \|\sqrt{M}B_2\|_2 \|w(s)\|_2 ds \right)^2, \end{aligned} \quad (6.48)$$

for all  $t \in [\delta_k, \delta_{k+1})$ . For notational convenience, let

$$\mathcal{I}(t) = \int_{\delta_k}^t e^{\alpha(t-s)} \|\sqrt{M}B_2\|_2 \|w(s)\|_2 ds. \quad (6.49)$$

Integrating both sides of (6.48) for all  $t \in [\delta_k, \delta_{k+1})$ ,

$$\begin{aligned} \int_{\delta_k}^{\delta_{k+1}} \dot{V} dt \leq & -\beta^2 \int_{\delta_k}^{\delta_{k+1}} \|x(t)\|_2^2 dt + \gamma^2 \int_{\delta_k}^{\delta_{k+1}} \|w(t)\|_2^2 dt - \int_{\delta_k}^{\delta_{k+1}} x^T(k)Nx(k) dt \\ & + \int_{\delta_k}^{\delta_{k+1}} 4\mathcal{I}(t)^2 dt + \int_{\delta_k}^{\delta_{k+1}} 4 \left( \frac{\mu_0(x(k))}{\alpha} (e^{\alpha(t-\delta_k)} - 1) \right)^2 dt. \end{aligned} \quad (6.50)$$

Evaluating the last term, we get

$$\begin{aligned}
& \int_{\delta_k}^{\delta_{k+1}} 4 \left( \frac{\mu_0(x(k))}{\alpha} (e^{\alpha(t-\delta_k)} - 1) \right)^2 dt \\
&= \frac{2\mu_0^2}{\alpha^3} [2\alpha(\delta_{k+1} - \delta_k) - 4e^{\alpha(\delta_{k+1}-\delta_k)} + e^{2\alpha(\delta_{k+1}-\delta_k)} + 3] \leq \int_{\delta_k}^{\delta_{k+1}} x^T(k) N x(k) dt,
\end{aligned} \tag{6.51}$$

where the inequality is obtained from (6.38) which is enforced by the choice of  $\delta_{k+1}$ . Substituting (6.51) into (6.50),

$$\int_{\delta_k}^{\delta_{k+1}} \dot{V} dt \leq -\beta^2 \int_{\delta_k}^{\delta_{k+1}} \|x(t)\|_2^2 dt + \gamma^2 \int_{\delta_k}^{\delta_{k+1}} \|w(t)\|_2^2 dt + \int_{\delta_k}^{\delta_{k+1}} 4\mathcal{I}(t)^2 dt. \tag{6.52}$$

Using Cauchy-Schwarz inequality

$$\left( \int_a^b X(t)Y(t)dt \right)^2 \leq \left( \int_a^b X^2(t)dt \right) \left( \int_a^b Y^2(t)dt \right), \tag{6.53}$$

to bound the integral in the last term of (6.52), we get

$$\int_{\delta_k}^{\delta_{k+1}} 4\mathcal{I}(t)^2 dt \leq \frac{4\|\sqrt{M}B_2\|_2^2}{\alpha^2} (e^{\alpha(\delta_{k+1}-\delta_k)} - 1)^2 \int_{\delta_k}^{\delta_{k+1}} \|w(s)\|_2^2 ds. \tag{6.54}$$

Applying the bounds given in (6.37), the upper and lower bounds on (6.52) are obtained as

$$\begin{aligned}
& -\beta^2 \int_{\delta_k}^{\delta_{k+1}} \|x(t)\|_2^2 dt + \left[ \gamma^2 + \frac{4\|\sqrt{M}B_2\|_2^2}{\alpha^2} (e^{\alpha \underline{\tau}} - 1)^2 \right] \int_{\delta_k}^{\delta_{k+1}} \|w(s)\|_2^2 ds \leq \int_{\delta_k}^{\delta_{k+1}} \dot{V} dt \leq \\
& -\beta^2 \int_{\delta_k}^{\delta_{k+1}} \|x(t)\|_2^2 dt + \left[ \gamma^2 + \frac{4\|\sqrt{M}B_2\|_2^2}{\alpha^2} (e^{\alpha \bar{\tau}} - 1)^2 \right] \int_{\delta_k}^{\delta_{k+1}} \|w(s)\|_2^2 ds.
\end{aligned} \tag{6.55}$$

Summing the above inequality for all  $k \in \mathbb{Z}^+$ , we get

$$\begin{aligned} -\beta^2 \int_0^\infty \|x(t)\|_2^2 dt + \underline{\Gamma}^2 \int_0^\infty \|w(s)\|_2^2 ds &\leq \int_0^\infty \dot{V} dt \leq \\ -\beta^2 \int_0^\infty \|x(t)\|_2^2 dt + \bar{\Gamma}^2 \int_0^\infty \|w(s)\|_2^2 ds, \end{aligned} \quad (6.56)$$

where  $\underline{\Gamma}$  and  $\bar{\Gamma}$  are defined in (6.40). Inequality (6.56) shows that sampled-data system (6.24) is finite-gain  $\mathcal{L}_2$  stable from  $w$  to  $x$  with an induced gain bounded between  $\underline{\Gamma}$  and  $\bar{\Gamma}$ .

**Case 2:** Following the similar analysis as in case 1, squaring both sides of (6.32), we get

$$\begin{aligned} \|\sqrt{M}e_t^k\|_2^2 &\leq 4 \left( \frac{\mu_0(x(k))}{\alpha} (e^{\alpha(t-\delta_k)} - 1) \right)^2 + 4 \left( \int_{\delta_{k+1}^c}^t e^{\alpha(t-s)} \|\sqrt{M}B_2\|_2 \|w(s)\|_2 ds \right)^2 \\ &\quad + 4 \left( e^{\alpha(t-\delta_{k+1}^c)} \int_{\delta_k}^{\delta_{k+1}^c} e^{\alpha(\delta_{k+1}^c-s)} \|\sqrt{M}B_2\|_2 \|w(s)\|_2 ds \right)^2. \end{aligned} \quad (6.57)$$

Substituting (6.57) in (6.27), we get

$$\begin{aligned} \dot{V} &\leq -\beta^2 \|x(t)\|_2^2 + \gamma^2 \|w(t)\|_2^2 - x^T(k)Nx(k) + 4 \left( \frac{\mu_0(x(k))}{\alpha} (e^{\alpha(t-\delta_k)} - 1) \right)^2 \\ &\quad + 4 \left( \int_{\delta_{k+1}^c}^t e^{\alpha(t-s)} \|\sqrt{M}B_2\|_2 \|w(s)\|_2 ds \right)^2 \\ &\quad + 4e^{2\alpha(t-\delta_{k+1}^c)} \left( \int_{\delta_k}^{\delta_{k+1}^c} e^{\alpha(\delta_{k+1}^c-s)} \|\sqrt{M}B_2\|_2 \|w(s)\|_2 ds \right)^2, \end{aligned} \quad (6.58)$$



for all  $t \in [\delta_{k+1}^c, \delta_{k+1}^a]$ . For notational convenience, let

$$\mathcal{I}_1(t) = \int_{\delta_{k+1}^c}^t e^{\alpha(t-s)} \|\sqrt{M}B_2\|_2 \|w(s)\|_2 ds; \quad \mathcal{I}_2(t) = \int_{\delta_k}^{\delta_{k+1}^c} e^{\alpha(\delta_{k+1}^c-s)} \|\sqrt{M}B_2\|_2 \|w(s)\|_2 ds. \quad (6.59)$$

Integrating both sides of (6.58) for all  $t \in [\delta_{k+1}^c, \delta_{k+1}^a]$

$$\begin{aligned} \int_{\delta_{k+1}^c}^{\delta_{k+1}^a} \dot{V} dt &\leq -\beta^2 \int_{\delta_{k+1}^c}^{\delta_{k+1}^a} \|x(t)\|_2^2 dt + \gamma^2 \int_{\delta_{k+1}^c}^{\delta_{k+1}^a} \|w(t)\|_2^2 dt - \int_{\delta_{k+1}^c}^{\delta_{k+1}^a} x^T(k) N x(k) dt \\ &+ \int_{\delta_{k+1}^c}^{\delta_{k+1}^a} 4\mathcal{I}_1(t)^2 dt + \int_{\delta_{k+1}^c}^{\delta_{k+1}^a} 4 \left( \frac{\mu_0(x(k))}{\alpha} (e^{\alpha(t-\delta_k)} - 1) \right)^2 dt + \int_{\delta_{k+1}^c}^{\delta_{k+1}^a} 4e^{2\alpha(t-\delta_{k+1}^c)} \mathcal{I}_2(t)^2 dt. \end{aligned} \quad (6.60)$$

Evaluating the fifth term, we get

$$\begin{aligned} &\int_{\delta_{k+1}^c}^{\delta_{k+1}^a} 4 \left( \frac{\mu_0(x(k))}{\alpha} (e^{\alpha(t-\delta_k)} - 1) \right)^2 dt \\ &= \frac{2\mu_0^2}{\alpha^3} [2\alpha(\delta_{k+1}^a - \delta_{k+1}^c) + e^{-2\alpha\delta_k} (e^{\alpha\delta_{k+1}^a} - e^{\alpha\delta_{k+1}^c}) (e^{\alpha\delta_{k+1}^a} + e^{\alpha\delta_{k+1}^c} - 4e^{\alpha\delta_k})]. \end{aligned} \quad (6.61)$$

Using Taylor series expansion  $e^\delta = 1 + \delta + \mathcal{O}$ , where  $\mathcal{O}$  represents the higher order terms (negligible for small values of  $\delta$ ), we can rewrite (6.61) as

$$\begin{aligned} &\int_{\delta_{k+1}^c}^{\delta_{k+1}^a} 4 \left( \frac{\mu_0(x(k))}{\alpha} (e^{\alpha(t-\delta_k)} - 1) \right)^2 dt \\ &= \frac{4\mu_0^2}{\alpha^2} (\delta_{k+1}^a - \delta_{k+1}^c) + \frac{2\mu_0^2}{\alpha^2} (1 - 2\alpha\delta_k + \mathcal{O})(\delta_{k+1}^a - \delta_{k+1}^c + \mathcal{O})(e^{\alpha\delta_{k+1}^a} + e^{\alpha\delta_{k+1}^c} - 4e^{\alpha\delta_k}) \\ &= \frac{4\mu_0^2}{\alpha^2} (\delta_{k+1}^a - \delta_{k+1}^c) \\ &+ \frac{2\mu_0^2}{\alpha^2} [(\delta_{k+1}^a - \delta_{k+1}^c) + \mathcal{O} - 2\alpha\delta_k(\delta_{k+1}^a - \delta_{k+1}^c) - 2\alpha\delta_k\mathcal{O} + (\delta_{k+1}^a - \delta_{k+1}^c)\mathcal{O} + \mathcal{O}] \\ &\quad (e^{\alpha\delta_{k+1}^a} + e^{\alpha\delta_{k+1}^c} - 4e^{\alpha\delta_k}) \end{aligned}$$

$$\begin{aligned}
&= \frac{4\mu_0^2}{\alpha^2}(\delta_{k+1}^a - \delta_{k+1}^c) \\
&+ \frac{2\mu_0^2}{\alpha^2}(\delta_{k+1}^a - \delta_{k+1}^c)[1 + \mathcal{O} - 2\alpha\delta_k - 2\alpha\delta_k\mathcal{O} + \mathcal{O}](e^{\alpha\delta_{k+1}^a} + e^{\alpha\delta_{k+1}^c} - 4e^{\alpha\delta_k}) \quad (6.62) \\
&= (\delta_{k+1}^a - \delta_{k+1}^c) \left[ \frac{4\mu_0^2}{\alpha^2} + \frac{2\mu_0^2}{\alpha^2} \mathcal{O} \right].
\end{aligned}$$

where, with a slight abuse of notation, we regard the result of all operations on the higher order terms as  $\mathcal{O}$ , and  $\mu_0(x(k))$  is represented as  $\mu_0$ . Evaluating  $\mu_0^2(x(k))$  using (6.30) gives,

$$\begin{aligned}
\mu_0^2(x(k)) &= x^T(k)\bar{A}^T\sqrt{M}^T\sqrt{M}\bar{A}x(k) \leq x^T(k)A^T\sqrt{M}^T\sqrt{M}Ax(k) \\
&\quad (\because \bar{A} = A - B_1B_1^TP \Rightarrow \bar{A} \leq A) \\
&\leq x^T(k)\sqrt{M}^T\sqrt{M}^{-T}A^T\sqrt{M}^T\sqrt{M}A\sqrt{M}^{-1}\sqrt{M}x(k) \\
&\leq \alpha^2x^T(k)Mx(k) \quad (\because \alpha^2 = \sqrt{M}^{-T}A^T\sqrt{M}^T\sqrt{M}A\sqrt{M}^{-1}) \\
&\leq 2\alpha^2x^T(k)Nx(k) \quad (\because M = 2N - PB_1B_1^TP \Rightarrow M \leq 2N; \text{ see(6.28)}) \\
&\leq 2\alpha^2x^T(k)Nx(k).
\end{aligned}$$

Substituting this into (6.62), gives

$$\begin{aligned}
\int_{\delta_{k+1}^c}^{\delta_{k+1}^a} 4 \left( \frac{\mu_0(x(k))}{\alpha} (e^{\alpha(t-\delta_k)} - 1) \right)^2 dt &\leq (\delta_{k+1}^a - \delta_{k+1}^c)[x^T(k)Nx(k) + \xi_k] \\
&\leq \int_{\delta_{k+1}^c}^{\delta_{k+1}^a} x^T(k)Nx(k)dt + \xi_k(\delta_{k+1}^a - \delta_{k+1}^c). \quad (6.63)
\end{aligned}$$

*Remark 44* Note that the higher order terms  $\mathcal{O}$  are lumped in the bounded constant  $\xi_k$ .

Substituting (6.63) into (6.60) and applying the bound given in assumption 7, we

get

$$\begin{aligned} \int_{\delta_{k+1}^c}^{\delta_{k+1}^a} \dot{V} dt &\leq -\beta^2 \int_{\delta_{k+1}^c}^{\delta_{k+1}^a} \|x(t)\|_2^2 dt + \gamma^2 \int_{\delta_{k+1}^c}^{\delta_{k+1}^a} \|w(t)\|_2^2 dt \\ &+ \int_{\delta_{k+1}^c}^{\delta_{k+1}^a} 4\mathcal{I}_1(t)^2 dt + \int_{\delta_{k+1}^c}^{\delta_{k+1}^a} 4e^{2\alpha(t-\delta_{k+1}^c)} \mathcal{I}_2(t)^2 dt + \xi_k \tau'. \end{aligned} \quad (6.64)$$

Using (6.53) and applying bounds given in assumption 7 on the last two integrals, we get

$$\int_{\delta_{k+1}^c}^{\delta_{k+1}^a} \dot{V} dt \leq -\beta^2 \int_{\delta_{k+1}^c}^{\delta_{k+1}^a} \|x(t)\|_2^2 dt + \xi_k \tau' + \Psi^2 \int_{\delta_{k+1}^c}^{\delta_{k+1}^a} \|w(t)\|_2^2 dt + \psi^2. \quad (6.65)$$

where  $\Psi$  and  $\psi$  are defined in (6.45) and (6.46), respectively. Since the terms  $\psi^2$  and  $\xi_k \tau'$  are bounded, the inequality (6.65) is sufficient to show that the sampled-data system (6.24) is finite-gain  $\mathcal{L}_2$  stable from  $w$  to  $x$  with an induced gain less than  $\Psi$ . █

*Remark 45* Additional term  $\psi$  is a result of the error accumulated during  $[\delta_k, \delta_{k+1}^c)$ , as depicted in the last term of (6.32). This additional term and  $\xi_k \tau'$  are bounded and just add to the upper-bound on  $\dot{V}$  in  $\mathcal{L}_2$  gain inequality.

### 6.4.1 Triggering time computation

The computation is based on the idea to find the time period  $\tau_k$ , which satisfies inequality (6.29), i.e.,

$$\|\sqrt{M}e_{k+1}^k\|_2 = \mu(x(k)). \quad (6.66)$$

Based on this idea, the theorem is now presented, which gives  $\tau_k : \mathbb{R}^n \rightarrow \mathbb{R}^+$  as a function of the state  $x(k)$ , i.e., the ST scheme which guarantees finite-gain  $\mathcal{L}_2$  stability from  $w$  to  $x$  for sampled-data system (6.24).

**Theorem 6.4** *Consider sampled-data system (6.24) with Assumptions 6 and 7.*

*Let*

- $\beta \in (0, 1]$  be such that  $M$  (defined in (6.28)) has full rank, and
- the bounded constants  $\sigma \in (0, 1]$ ,  $\underline{\tau}$ ,  $\bar{\tau} \in \mathbb{R}^+$ .

*If for any  $k \in \mathbb{Z}^+$*

- *the initial condition is  $\delta_0 = 0$ , and*
- *$(k + 1)^{\text{th}}$  release time satisfies*

$$\delta_{k+1} = \delta_k + \max\{\underline{\tau}, \min\{\bar{\tau}, \sigma\tau_k(x(k))\}\}, \quad (6.67)$$

*where  $\tau_k(x(k)) : \mathbb{R}^n \rightarrow \mathbb{R}^+$  is defined as*

$$\tau_k(x(k)) = \begin{cases} \frac{1}{\alpha} \ln \left( 1 + \frac{\alpha\mu(x(k))}{2\mu_0(x(k))} \right) & x(k) \neq 0 \\ \infty & x(k) = 0, \end{cases} \quad (6.68)$$

*then system (6.24) is finite-gain  $\mathcal{L}_2$  stable from  $w$  to  $x$ .*

**Proof.** As mentioned in the proof of Theorem 6.3, the choice of triggering time guarantees  $\mathcal{L}_2$  stability. It will be shown now that ST scheme given by (6.67) indeed satisfies (6.36)–(6.38).

Since the triggering time is lower bounded by  $\underline{\tau}$ , inequality (6.36) is satisfied. Furthermore, the upper and lower bounds *enforced* in (6.67) show that (6.37) is also satisfied. For the third inequality i.e., (6.38), we will show that the expression for  $\tau_k(x(k))$  satisfies the  $\mathcal{L}_2$  stability condition. Specifically, we evaluate the expression  $4 \left( \frac{\mu_0(x(k))}{\alpha} (e^{\alpha(t-\delta_k)} - 1) \right)^2$  at  $t = \delta_{k+1}$ , which is the deterministic part of squared error bound (6.47). Taking square root and substituting  $t = \delta_{k+1}$  from (6.67), we get

$$2 \left( \frac{\mu_0(x(k))}{\alpha} (e^{\alpha(\delta_{k+1}-\delta_k)} - 1) \right) = \mu(x(k)),$$

which shows that the choice of  $\tau_k(x(k))$  renders sampled data system (6.24) finite-gain  $\mathcal{L}_2$  stable for all  $t \in [\delta_k, \delta_{k+1})$ . ■

*Remark 46 Adaptive  $\sigma$  multiplier can also be considered which depends on the amount of disturbance in previously sampled states.*

## 6.4.2 System's Overall State Indicator (SOSI)

As mentioned earlier, the first level controller is responsible for sending next triggering time and SOSI to the second level controller (NM) for PBS. The factors affecting the selection of SOSI are:

- Denied transmission requests,
- Distance of trajectories from set-point or equilibrium  $\|x(k) - x_e(k)\|_2$ , where  $x_e(k)$  is the equilibrium-point state at  $k$ , and

- Magnitude of the disturbance, which can be estimated by a disturbance observer/estimator.

Let  $\mathcal{A}_k^j$ , denoting the SOSI of  $j^{\text{th}}$  system where  $j \in \{1, \dots, N\}$ , be given as

$$\mathcal{A}_k^j = m^j \times (\|x^j(k) - x_e^j(k)\|_2), \quad (6.69)$$

where  $m^j$  is the appropriate weight used to set the priority of  $j^{\text{th}}$  system. For instance, the monitoring nodes in the network can be assigned low weights relative to the sensing nodes (control loops). Also, the systems which are expected to face disturbance or those which need more attention can be assigned higher weights.

This information, along with the next sampling time, is sent to the NM which computes the *relative* SOSI ( $\mathcal{R}_k^j$ ) of each control loop as

$$\mathcal{R}_k^j = \frac{\mathcal{A}_k^j}{\sum_{q=1}^N \mathcal{A}_k^q} + F_m^j, \quad (6.70)$$

where,  $F_m^j$  denotes the flag indicating previously missed transmission, given as

$$F_m^j = \begin{cases} 0 & \text{if transmission was allowed} \\ 1 & \text{if transmission was denied.} \end{cases} \quad (6.71)$$

Note that the third factor, i.e., magnitude of the disturbance, is not included in the calculation of  $\mathcal{A}_k^j$ , because it demands a disturbance observer which translates into more computational cost. Instead by using the distance of state trajectories from their set-points, disturbance can be accounted for because more disturbance

results in larger difference between the actual state and its equilibrium value.

## 6.5 Second Level: Network Manager

The slotted mode of IEEE 802.15.4 wireless networking protocol with modified NM and superframe structures is considered. Details of the said protocol are left out due to limited space and can be found in [9]. The motivation for the modifications comes mainly from the use of ST strategy, which does not require the controllers to “contend” for transmission slot due to the predicted triggering times, hence eliminating the need for Contention Access Period (CAP). This knowledge allows the scheduler to pre-schedule the transmission slots for the next superframe. In addition, as it will be seen in the forthcoming text and simulation results, significant energy savings can be achieved at the battery-powered sensor nodes at the expense of slightly increased computational load at the mains powered NM.

### 6.5.1 Superframe

In the modified superframe structure, as shown in Fig. 6.10, the CAP is eliminated and the active and inactive portions are distributed. This allows the systems to get their states at any time during the beacon interval, unlike “fixed” time slots placed in the Contention Free Period (CFP). A superframe can allow at most  $N_{max}$  transmissions each of duration  $\Delta_s$ .

The constraints that govern the choice of  $\underline{\tau}$  and  $\bar{\tau}$  are imposed by the physical layer of the protocol and plant dynamics. Specifically,

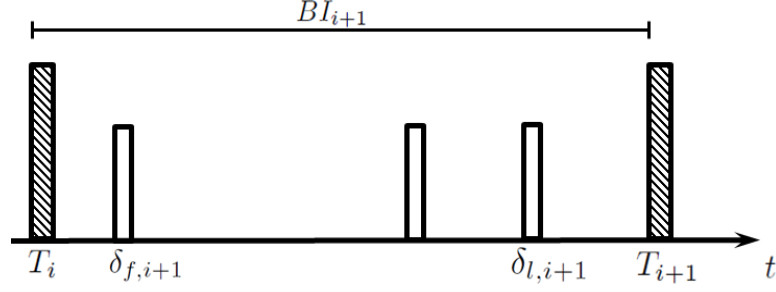


Figure 6.10: Modified superframe structure. The duration is denoted as  $BI_{i+1}$ . Active period includes a beacon packet and three slots for transmission; remaining time constitutes the inactive period. Each slot is of duration  $\Delta_s$ .

- $\min BI \leq \tau \leq \frac{1}{5\lambda_{min}}$ ,
- $\min BI \leq BI \leq \max BI$ ,
- $\bar{\tau} \leq \max BI$ ,

where  $\lambda_{min}$  denotes the dominant pole of the fastest plant among the participating systems, the upper-bound on  $\alpha$ , i.e.,  $\frac{1}{5\lambda_{min}}$  is chosen using the rule-of-thumb, and  $\min BI$  and  $\max BI$  represent the minimum and maximum values of BI corresponding to the constraint  $0 \leq \text{BeconOrder (macBO)} \leq 14$  imposed by the original protocol [9] as

$$BI = aBaseSFDuration \times 2^{\text{macBO}}, \quad (6.72)$$

with  $aBaseSFDuration \triangleq SFD \equiv \frac{\text{No. of symbols}}{\text{Symbol rate}}$ .



## 6.5.2 Network Manager

The NM has wired connection with the ST controllers and communicates over a wireless link with the sensor nodes. The proposed NM structure appends a scheduler module with the Personal Area Network (PAN) coordinator as shown in Fig. 6.11. The coordinator broadcasts beacon packets that contain the assigned trans-

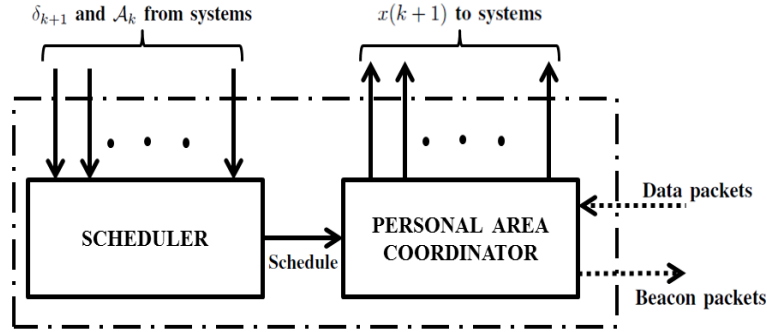


Figure 6.11: Modified structure of the Network Manager. Solid line: wired connections; dotted line: wireless link.

mission time/slot for each sensor node and the beacon interval. This enables each sensor node to sleep until its transmission time is due, transmit the state information in the assigned slot, and sleep again until the next beacon transmission. After sampling the states of their systems in the assigned slots, the sensor nodes transmit this information over the wireless network to the coordinator, which delivers this information to respective controllers. Each controller computes  $\delta_{k+1}$  and  $\mathcal{A}_k$  (only necessary if  $N > N_{max}$  to determine the priority of transmissions), and sends this information to the scheduler over the wired connection. The scheduler keeps storing this information in a buffer until it receives from all the controllers scheduled for that particular beacon interval, and then starts the scheduling algorithm. The NM performs following tasks:

- Ensures that no two transmissions overlap in the next superframe.
- If  $N > N_{max}$ , then implements PBS algorithm.
- Keeps track of the slow systems and places their transmission slots in appropriate superframe. This way, the need to sample every system in each superframe is eliminated.
- Provides the coordinator with a transmission schedule.

*Remark 47 To avoid overlap of transmissions in case two systems require the same slot, the NM schedules the sampling times in consecutive slots. This does not have a significant effect on stability, owing to a very small duration of the slot (typically around 1 msec) as compared to the sampling time which is typically many times larger than the slot duration.*

After getting the scheduling information, the coordinator forms a beacon packet and broadcasts it to the sensors.

**Assumption 8** *It is assumed that,*

- *all the controllers have knowledge of the initial state,  $x(0)$ , of their respective systems,*
- *the scheduler takes  $\varsigma \leq \bar{\varsigma} \in \mathbb{R}^+$  units of time for all computations during a superframe,*
- *a sensor node requires only one slot duration to transmit the whole state information,*

- *beacon packet requires only one slot duration, and*
- $\Delta_s$  *includes inter-frame spacing (IFS) (see [9]).*

### 6.5.3 Modified Protocol

Given the predicted triggering time of each system, the length of the next SF is computed as  $BI_{i+1} = \delta_{f,i+1} - T_i - \Delta_s + N_{max}\Delta_s + IaP$ , where  $\delta_{f,i+1}$  is the first system which will transmit in the next SF, and  $IaP$  denotes the inactive period which will allow the scheduler ample time to construct the next SF and economize energy. In order to ensure schedulability of the first system in the next SF in the worst-case scenario, the duration  $N_{max}\Delta_s + IaP = \underline{\tau} - \Delta_s$ . This results in

$$BI_{i+1} = \delta_{f,i+1} - T_i - 2\Delta_s + \underline{\tau} \triangleq b. \quad (6.73)$$

The proposed protocol has two parts, depending upon the number of attached nodes. If the number of nodes is not more than the maximum number of available slots, i.e.,  $N \leq N_{max}$ , then the NM does not require PBS algorithm. Initially, all the controllers use initial states to compute the next triggering times. This information is used by the scheduler to schedule the first superframe starting at  $T_0 = 0$ , and compute its duration following (6.73) as,  $BI_1 = \delta_{f,1} - T_0 - 2\Delta_s + \underline{\tau}$ , where  $\delta_{f,1}$  denotes the first system which will transmit in the first superframe. The coordinator broadcasts the first beacon packet at  $T_0$ , which contains triggering times for all the nodes and the beacon interval  $BI_1$ . For any superframe  $i$ , the

scheduler computes

$$\delta_{l,i+1} - T_i + \Delta_s \triangleq a, \quad (6.74)$$

besides  $b$ , where  $\delta_{l,i+1}$  denotes the last system which will transmit in the next superframe. The scheduler then compares  $a$  and  $b$ ; if  $a \leq b$  then all the nodes are allowed to transmit in the next superframe, otherwise the nodes for which the next triggering time falls in the next superframe duration are allowed to transmit, and the remaining nodes' slots are placed in the appropriate future superframe. The algorithm is given as follows:

**Algorithm 2** For  $N \leq N_{max}$ :

Initialization

1.  $i = 0$  and  $k = 0$ .

End Initialization

2. At  $\delta_k^j$  in  $i$ -th superframe, scheduler gets  $\delta_{k+1}^j$  for those systems which transmit in  $BI_i$ ;

3. Wait until  $\delta_{l,i}$ ;

4. Compute (6.73) and (6.74);

If  $a \leq b$  then

5. All the nodes are allowed transmission in  $BI_{i+1}$ ;

6. Increment  $i$  and  $k$  by one;

```

7.      GOTO 2;

      else

8.      The nodes with  $\delta_{k+1} \in [T_i + \Delta_s, T_{i+1})$  are allowed transmission
      in  $BI_{i+1}$ ;

9.      Increment  $i$ ;

10.     Increment  $k$  for those systems which transmit in  $BI_{i+1}$ ;

11.     GOTO 2;

      end

end

```

Since the algorithm only ensures optimal usage of communication resources while assigning transmission slots to the systems according to their computed triggering times, all the systems will be finite-gain  $\mathcal{L}_2$  stable.

In case the number of systems exceeds the maximum number of transmission slots, i.e.,  $N > N_{max}$ , the scheduler is provided with  $\mathcal{A}_k$  (6.69) from each controller besides  $\delta_{k+1}$ . The scheduler then uses this information to schedule the transmission slots according to PBS. In PBS, the priorities are assigned according to  $\mathcal{R}_k$  (6.70) of each system such that the system with highest  $\mathcal{R}_k$  is guaranteed a transmission slot in the next superframe. The remaining nodes for which the transmission is denied are assigned *new* triggering times as

$$\delta_{new} = \delta_{l,k+1} + \Delta_s + \mathcal{I}, \quad (6.75)$$

and their missed-superframe flags  $F_m$  (6.71) are also incremented. Note that the value of  $F_m$  reveals the number of consecutively missed superframes of respective system. A sketch of the algorithm is given as follows:

**Algorithm 3** For  $N > N_{max}$ :

Initialization

1.  $i = 0$  and  $k = 0$ ;
2. Clear all flags i.e.,  $F_m^j = 0$ .

End Initialization

3. At  $\delta_k^j$  in  $i$ -th superframe, scheduler gets  $\delta_{k+1}^j$  and  $\mathcal{A}_k^j$  for those systems which transmit in  $BI_i$ ;
4. Wait until  $\delta_{l,i}$ ;
5. Call PBS function;
6. Compute (6.73) and (6.74);
  - If  $a \leq b$  then
7. The first  $N_{max}$  nodes with highest  $\mathcal{R}_k^j$  values transmit in  $BI_{i+1}$ ;
8. Increment  $i$ ;
9. Increment  $k$  for those systems which transmit in  $BI_{i+1}$ ;

```

10.     GOTO 3;

       else

11.     The nodes with  $\delta_{k+1} \in [T_i + \Delta_s, T_{i+1})$  transmit in  $BI_{i+1}$ ;

12.     Increment  $i$ ;

13.     Increment  $k$  for those systems which transmit in  $BI_{i+1}$ ;

14.     GOTO 3;

       end

Function:  PBS

15. Compute (6.70);

16. The first  $N_{max}$  nodes with highest  $\mathcal{R}_k^j$  values are allowed
    transmission in  $BI_{i+1}$ ;

17. Clear  $F_m$  for systems which will transmit in  $BI_{i+1}$ ;

18. The remaining nodes are assigned consecutive transmission
    slots starting from (6.75);

19. Increment  $F_m$  for the remaining nodes;

20. Return;

     end

```

*Remark 48* For this chapter,  $N \leq N_{max} + 1$  is considered. A detailed analysis of the bound on  $N$  will be considered in future work.

**Theorem 6.5** Consider  $N$  sampled-data systems represented by (6.24), with Assumptions 6 and 7, which share a common wireless communication medium, under Assumption 8, to close their feedback loops; with the inequalities and constants defined in Theorem 6.3. The communication medium has limited number of transmission slots  $N_{max}$  and  $N > N_{max}$ . If the communication protocol applies Algorithm 3, then all the control loops are finite-gain  $\mathcal{L}_2$  stable from  $w$  to  $x$  with a bounded induced gain.

**Proof.** For those  $N_{max}$  systems which are assigned their demanded triggering times, the stability is given in Theorem 6.3. The remaining systems which are assigned consecutive time slots starting from (6.75), the stability is given as follows:

The systems which were not allotted time slots in the next  $BI$ , are now scheduled according to (6.75), which results in their assigned times being:

$$\delta_{k+1}^a = \delta_{l,k+1} + \Delta_s + \underline{\tau}. \quad (6.76)$$

The difference between the assigned time in (6.76) and the one demanded by the system ( $\delta_{k+1}^e$ ) will be bounded since the right hand side of (6.76) is constant considering  $\delta_{l,k+1}$ , which is a fixed time instant corresponding to the last system to transmit in the next  $BI$ . Hence Assumption 7 holds, and the stability follows directly from Theorem 6.3, Case 2. █



## 6.6 Simulation Results and Discussion

Simulation results of the application of the above defined scheme are now presented for three identical inverted pendulum over a moving cart systems represented by (6.24), with state vector  $x = [y \ \dot{y} \ \theta \ \dot{\theta}]^T$ , where  $y$  and  $\theta$  denote the cart's position and bob's angle, respectively. The system matrices are given as

$$A = \begin{bmatrix} 0 & 1 & 0 & 0 \\ 0 & 0 & -\frac{m_b g}{M_c} & 0 \\ 0 & 0 & 0 & 1 \\ 0 & 0 & \frac{g}{l} & 0 \end{bmatrix}; B_1 = \begin{bmatrix} 0 \\ \frac{1}{M_c} \\ 0 \\ -\frac{1}{M_c l} \end{bmatrix}; B_2 = \begin{bmatrix} 1 \\ 1 \\ 1 \\ 1 \end{bmatrix}, \quad (6.77)$$

where  $m_b$  is bob's mass,  $M_c$  denotes cart's mass,  $l$  is the length of the pendulum, and  $g$  is gravitational acceleration. The values of  $N_{max} = 4$  for Algorithm 2 and  $N_{max} = 2$  for Algorithm 3.  $\Delta_s = (\text{Number of symbols in one slot})/(\text{Symbol rate})$ , where the values given in Tables 51 and 66 of [9] are 60 symbols per slot and 40 *ksymbols/sec* (for 915 MHz band), respectively. The values of all the parameters are given in Table 6.1. The choice of weights for (6.69) is made such that the system experiencing disturbance gets high priority. In this simulation, systems 2 and 3 experience  $w(t)$  as

$$\begin{aligned} \text{System 2 : } w(t) &= 0.1 \operatorname{sgn}(\sin t), & 0 \leq t < 10, \\ &= 0, & \text{otherwise.} \end{aligned}$$

$$\begin{aligned} \textbf{System 3} : w(t) &= 0.3 (\sin 5t), & 0 \leq t < 4, \\ &= 0, & \text{otherwise.} \end{aligned}$$

Table 6.1: Parameters for simulation.

| Parameter           | Value                         |
|---------------------|-------------------------------|
| $m_b$               | 1                             |
| $M_c$               | 10                            |
| $l$                 | 3                             |
| $x_o$               | $[0.98 \ 0 \ 0.2 \ 0]^T$      |
| $\beta$ eq. (6.28)  | 0.3                           |
| $\gamma$ eq. (6.23) | 200                           |
| $\sigma$ eq. (6.67) | 1                             |
| $\lambda_{min}$     | 1.8257                        |
| $\underline{\tau}$  | 0.106                         |
| $\bar{\tau}$        | 0.45                          |
| $m$ eq. (6.69)      | 1 (Sys1); 12 (Sys2); 5 (Sys3) |

In order to compare the schemes, two separate measures of duty cycle are introduced. The first one indicates transmission time (i.e.,  $\Delta_s$ ), and the second gives listening period of the sensor nodes. The reason for this is the difference in power consumed by the sensor nodes in transmission and reception modes, which is also indicated in [8]. The expressions are given as,  $DC_{tx} = (\text{No. of transmissions in } BI_i \times \Delta_s) / (BI_i)$  and  $DC_{rx} = (\Delta_s) / (BI_i)$ , where  $\Delta_s$  denotes the time duration of transmission slot or beacon packet, because it is assumed that each transmission from the sensor nodes, and beacon packet transmission take one slot to complete (Assumption 8).

**Algorithm 2:** Results of Algorithm 2 are compared with the periodic implementation of the same systems over the *original* IEEE 802.15.4 protocol for which  $BO = 4$  and  $\tau = 0.192sec$  for all the systems, which are assigned consecutive

GTs in every superframe, and  $N_{max} = 4$ . The results are given in figs. 6.12 to 6.14. All the systems are stabilized within 20 seconds.

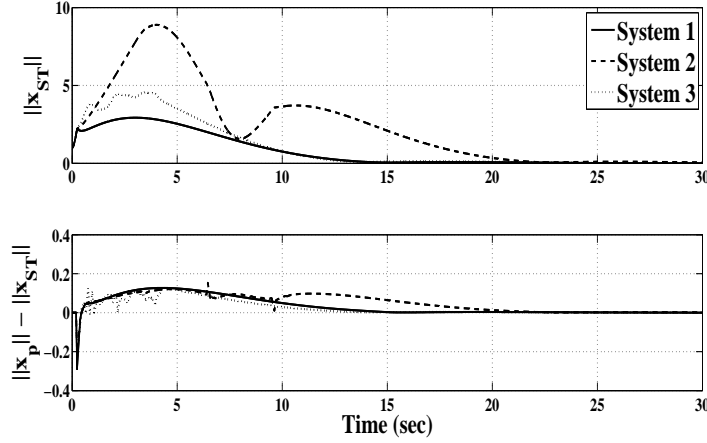


Figure 6.12: System states. Top:  $\|x_{ST}(t)\|$  for Algorithm 2; bottom:  $\|x_p(t)\| - \|x_{ST}(t)\|$ , where  $x_p(t)$  denotes states for periodic implementation.

Fig. 6.13 shows that the ST scheme adjusts triggering times according to the disturbance encountered by the system. Moreover, the assigned triggering times to all the systems follow the bounds  $\underline{\tau}$  and  $\bar{\tau}$ . A snapshot of the transmissions is shown in Fig. 6.14, which demonstrates the generation of superframes with variable duration, and transmission from the systems. It can be seen that some of the superframes do not contain transmissions from all three systems, which supports the communication-saving claim of the proposed algorithm. In addition, the operation of the scheduler is also shown which starts its execution after the last transmission in each superframe.

As reported in Table 6.2, the periodic scheme demands more transmissions, translating into greater bandwidth and energy usage as compared with the proposed ST implementation in Algorithm 2. The results indicate a 68% decrease in average  $DC_{tx}$  and 9.5% increase in average  $DC_{rx}$ , which show that despite a

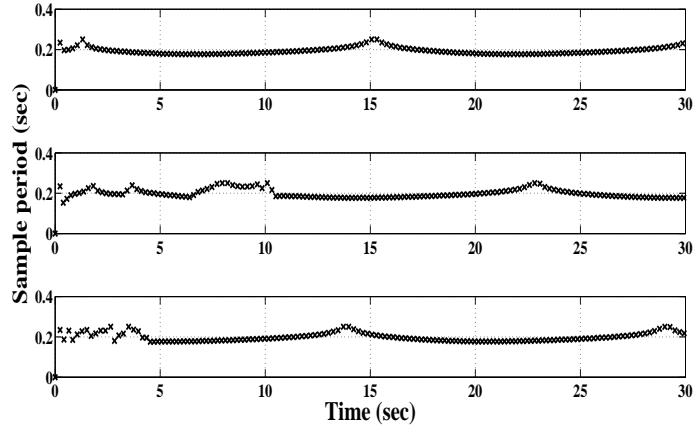


Figure 6.13: ST events. Top: System 1, middle: System 2, bottom: System 3.

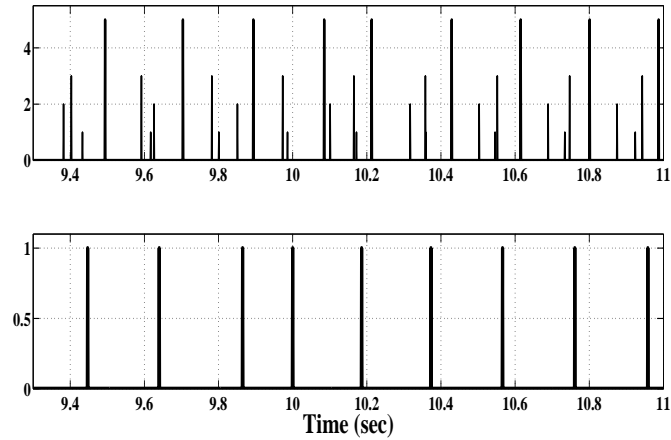


Figure 6.14: Snapshot of transmissions,  $N_{max} = 4$ . Top: beacon packets and transmissions for systems 1, 2, and 3 are scaled as 5, 1, 2, and 3, respectively; bottom: duty cycle of the scheduler.

slight increase in the listening period of the nodes, the transmission duration has decreased significantly.

**Algorithm 3:** Now the results of Algorithm 3 and Algorithm 2 are compared.

Fig. 6.15 (top) shows more variations in the transient periods of systems 1 and 3 as compared with system 2. Also, the difference in states for both algorithms (bottom) shows variations only for systems 1 and 3. This is due to the choice of weights (table 6.1) for PBS algorithm which give highest priority to system 2 as compared with systems 1 and 3.

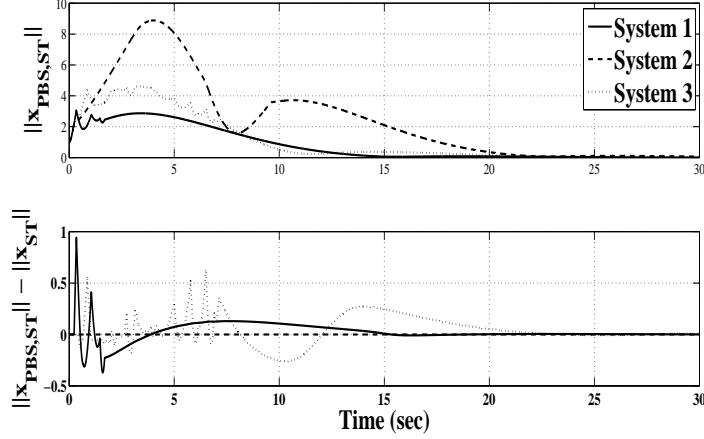


Figure 6.15: System states. Top:  $\|x_{PBS,ST}(t)\|$  for Algorithm 3; bottom:  $\|x_{PBS,ST}(t)\| - \|x_{ST}(t)\|$ , where  $\|x_{PBS,ST}(t)\|$  denotes the states due to PBS algorithm.

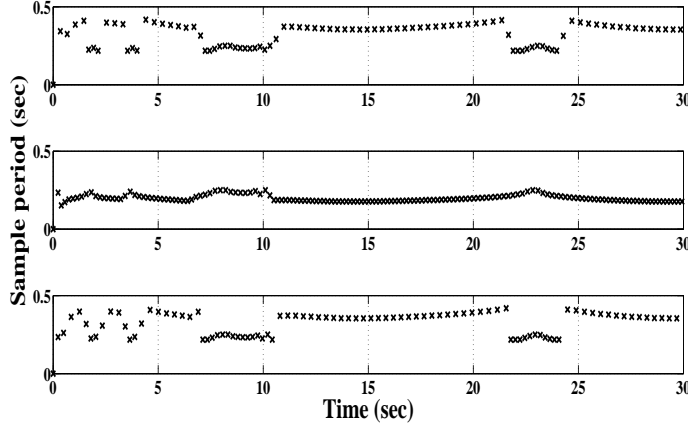


Figure 6.16: ST events. Top: System 1, middle: System 2, bottom: System 3.

Due to same reason, Fig. 6.16 shows that the event times for system 2 are in the range of 0.15 to 0.25sec and that for systems 1 and 3 are in the range of 0.2 to 0.45sec, i.e., system 2 is given more attention as compared with systems 1 and 3. Table 6.2 reveals the same fact where the number of ST events reduces from 150 and 152 to 93 for systems 1 and 3, respectively. Also, a significant decrease of 25% in  $DC_{tx}$  as compared with Algorithm 2 can be observed at the expense of a slight increase of 6.4% in  $DC_{rx}$ .

Note that the event times assigned by NM to systems 1 and 3 are larger than  $\bar{\tau}$

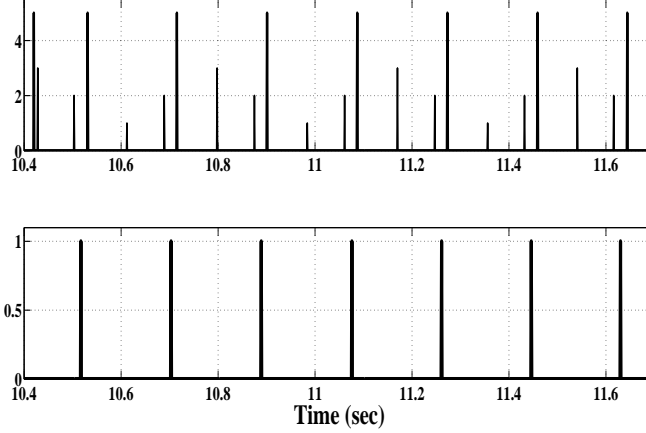


Figure 6.17: Snapshot of transmissions,  $N_{max} = 2$ . Top: beacon packets and transmissions for systems 1, 2 and 3 are scaled as 5, 1, 2, and 3, respectively, bottom: duty cycle of the scheduler.

due to limited number of transmission slots, and these systems are still stable with increased variation in state trajectories, which conforms with the results of theorem 6.3. Additionally, Fig. 6.16 shows that when system 2 demands less number of samples, the other two systems are allowed to have more frequent transmissions, for instance between 6 and 11 seconds. This shows that PBS algorithm works as intended and accommodates the systems according to the assigned priorities and transmission requirements.

Fig. 6.17 shows more frequent transmissions of system 2, variable beacon intervals, and a maximum of two transmissions allowed in each superframe.

Table 6.2: Comparison of three implementations for simulation time of 30sec. The periodic scheme uses  $BO = 4$  and  $\tau = 0.192$ . Tx  $j$ : number of transmissions from  $j$ -th system; SF: number of superframes.

| Imp.     | Tx1 | Tx2 | Tx3 | SF  | Av. $DC_{tx}$ | Av. $DC_{rx}$ |
|----------|-----|-----|-----|-----|---------------|---------------|
| Periodic | 474 | 474 | 474 | 158 | 14.22 %       | 1.58 %        |
| Algo.2   | 150 | 152 | 152 | 173 | 4.54 %        | 1.73 %        |
| Algo.3   | 93  | 153 | 93  | 184 | 3.39 %        | 1.84 %        |

## 6.7 Conclusion

A two-level design for NCSs is presented by employing ST mechanism over the modified IEEE 802.15.4 protocol. The idea behind splitting the problem into two levels is to upper-bound the transmission rate. First level is composed of ST based  $\mathcal{H}_\infty$  controller for each system, which guarantees finite-gain  $\mathcal{L}_2$  stability, and second level comprises of the modified IEEE protocol. This methodology ensures optimal usage of the network bandwidth, while reducing energy consumption of the wireless sensor nodes. Additionally, the proposed methodology requires less computational power as compared with [10], because it pre-schedules the next beacon interval without computing the disturbance estimate and two-steps ahead triggering time. Two algorithms are given depending upon the number of systems and maximum number of transmission slots. The results demonstrate optimized bandwidth usage, and the provision of attaching to the network more systems as compared with the available transmission slots. Specifically, the simulations for Algorithm 2 indicate a 68% decrease in the average transmission duty cycle of the sensor nodes against periodic implementation over the original IEEE protocol, with a slight increase of 9.5% in the average reception duty cycle. PBS based Algorithm 3 shows a 25% decrease in average transmission duty cycle as compared with the first algorithm, with an increase of 6.4% in the reception duty cycle.

*Adaptive* weights,  $m^j$  for SOSI, which adjust according to the disturbance experienced by the system, can be considered as a topic of future research.

## CHAPTER 7

# CONCLUSION AND FUTURE WORK

In this work, a special case of NCSs was dealt with, namely wireless NCS or WNCS. The main objective was to present a framework for the optimization of control, communication, and computational ( $\mathcal{C}^3$ ) resources in a setting with multiple control loops sharing a common communication network for SC link. Specifically, asynchronous LQG controller was used to compensate for the delays and aperiodic nature of the transmissions, while optimizing the control cost. A novel ST technique based on the trade-off optimization between control cost and communication bandwidth usage was introduced and results showed that the novel methodology outperformed ST LQR reported in the literature [1]. IEEE 802.15.4 protocol was modified to enhance the energy efficiency in ST controller setting. Moreover, a ST  $\mathcal{H}_\infty$  controller was presented and it was demonstrated that the communication protocol can accommodate more number of control loops than the



number of available communication slots. The specific contributions of this work are stated as follows:

- A comprehensive literature review of the existing works in the area of aperiodically triggered NCSs,
- Consideration of computational and network-induced delays,
- Decoupled design of control gain and aperiodic triggering mechanism (ET or ST) which eases the design and analysis,
- Efficient utilization of computational resources besides control and communication costs,
- Design of ST sampler which causes higher sampling frequency in transient phase as compared with a lower frequency when the plant is regulated,
- Two-level design method for WNCSs where multiple control-loops a common communication medium for SC link,
- Modifications in IEEE 802.15.4 protocol for enhanced energy efficiency,
- Integration of PBS mechanism in the modified protocol which accommodates more systems as compared with the number of available communication slots.

Conclusively, we highlight the following important findings of this thesis:

- Besides the sampling frequency, it is also important *when* the state information is collected. In the particular case of inverted-pendulum system in

Chapter 5, it was seen that the proposed scheme was able to stabilize the system, while the controller due to [1] failed to achieve stability. This is because of a high sampling frequency, resulting from the proposed ST sampler, in the transient phase when the system required more state information.

- With a recent thrust towards CPSs, it is vital to the design of NCSs that the computational efficiency be also included in the optimization of control and communication costs.
- The ET methodology is not suitable for applications involving wireless sensor nodes. On the other hand, ST scheme is more conservative in terms of sampling frequency and less robust to disturbances. As a solution to these drawbacks, recently hybrid triggering methodology has been proposed in the literature, whereby the system runs using ST scheme in normal conditions and as soon as the disturbance occurs, an ET mechanism at the sensor node is activated.

This work can be extended to the case of non-linear systems. Furthermore, the consideration of packet-dropouts, output feedback, optimization of  $\gamma$  for ET condition in Chapter 3, and determination of maximum number of systems that can be accommodated in the methodology of Chapter 6 are deemed as the direction for future work. Most importantly, experimental validation of simulation results would make a significant contribution and a step towards replacing the periodic schemes in industry.

# REFERENCES

- [1] T. Gommans, D. Antunes, T. Donkers, P. Tabuada, and M. Heemels, “Self-triggered linear quadratic control,” *Automatica*, vol. 50, no. 4, pp. 1279–1287, 2014.
- [2] B. Demirel, Z. Zou, P. Soldati, and M. Johansson, “Modular design of jointly optimal controllers and forwarding policies for wireless control,” 2012.
- [3] M. Björkbom, S. Nethi, L. M. Eriksson, and R. Jäntti, “Wireless control system design and co-simulation,” *Control Engineering Practice*, vol. 19, no. 9, pp. 1075–1086, 2011.
- [4] M. S. Mahmoud and A. M. Memon, “Aperiodic triggering mechanisms for networked control systems,” *Information Sciences*, vol. 296, pp. 282–306, 2015.
- [5] D. E. Quevedo, V. Gupta, W.-J. Ma, and S. Yuksel, “Stochastic stability of event-triggered anytime control,” *IEEE Transactions on Automatic Control*, vol. 59, pp. 3373–3379, 2014.

- [6] D. Antunes and W. Heemels, “Rollout event-triggered control: Beyond periodic control performance,” *Automatic Control, IEEE Transactions on*, vol. 59, no. 12, pp. 3296–3311, Dec 2014.
- [7] M. Velasco, J. Fuertes, and P. Marti, “The self triggered task model for real-time control systems,” in *Work-in-Progress Session of the 24th IEEE Real-Time Systems Symposium (RTSS03)*, vol. 384, 2003.
- [8] J. Araújo, M. Mazo, A. Anta, P. Tabuada, and K. H. Johansson, “System architectures, protocols and algorithms for aperiodic wireless control systems,” *Industrial Informatics, IEEE Transactions on*, vol. 10, no. 1, pp. 175–184, 2014.
- [9] “Ieee 802.15.4 standard: Wireless medium access control (mac) and physical layer (phy) specifications for low-rate wireless personal area networks (wpans),” 2006. [Online]. Available: <http://www.ieee802.org/15/pub/TG4.html>
- [10] U. Tiberi, C. Fischione, K. H. Johansson, and M. D. Di Benedetto, “Energy-efficient sampling of networked control systems over ieee 802.15. 4 wireless networks,” *Automatica*, vol. 49, no. 3, pp. 712–724, 2013.
- [11] V. Vasyutynskyy and K. Kabitzsch, “Event-based control: Overview and generic model,” in *Factory Communication Systems (WFCS), 2010 8th IEEE International Workshop on*. IEEE, 2010, pp. 271–279.

- [12] K. J. Aström, *Event based control, Analysis and design of nonlinear control systems*. Springer Berlin Heidelberg, 2008.
- [13] W. Heemels, J. Sandee, and P. Van Den Bosch, “Analysis of event-driven controllers for linear systems,” *International journal of control*, vol. 81, no. 4, pp. 571–590, 2008.
- [14] W. Heemels, M. Donkers, and A. R. Teel, “Periodic event-triggered control based on state feedback,” in *Decision and Control and European Control Conference (CDC-ECC), 2011 50th IEEE Conference on*. IEEE, 2011, pp. 2571–2576.
- [15] L. Grüne, S. Jerg, O. Junge, D. Lehmann, J. Lunze, F. Müller, and M. Post, “Two complementary approaches to event-based control zwei komplementäre zugänge zur ereignisbasierten regelung,” *at-Automatisierungstechnik Methoden und Anwendungen der Steuerungs-, Regelungs- und Informationstechnik*, vol. 58, no. 4, pp. 173–182, 2010.
- [16] R. Postoyan, A. Anta, D. Nesic, and P. Tabuada, “A unifying lyapunov-based framework for the event-triggered control of nonlinear systems,” in *Decision and Control and European Control Conference (CDC-ECC), 2011 50th IEEE Conference on*. IEEE, 2011, pp. 2559–2564.
- [17] X. Meng and T. Chen, “Event-based stabilization over networks with transmission delays,” *Journal of Control Science and Engineering*, vol. 2012, p. 2, 2012.

- [18] P. Tabuada, “Event-triggered real-time scheduling of stabilizing control tasks,” *Automatic Control, IEEE Transactions on*, vol. 52, no. 9, pp. 1680–1685, 2007.
- [19] S. Hu and D. Yue, “L2-gain analysis of event-triggered networked control systems: a discontinuous lyapunov functional approach,” *International Journal of Robust and Nonlinear Control*, vol. 23, no. 11, pp. 1277–1300, 2013.
- [20] N. Marchand, S. Durand, and J. F. G. Castellanos, “A general formula for event-based stabilization of nonlinear systems,” *Automatic Control, IEEE Transactions on*, vol. 58, no. 5, pp. 1332–1337, 2013.
- [21] Y. Lin, Q.-L. Han, and F. Yang, “Event-triggered control for networked systems based on network dynamics,” in *Industrial Electronics (ISIE), 2013 IEEE International Symposium on*. IEEE, 2013, pp. 1–6.
- [22] P. Tallapragada and J. Cortés, “Event-triggered stabilization of linear systems under bounded bit rates,” *arXiv preprint arXiv:1405.6196*, 2014.
- [23] X. Wang and M. Lemmon, “On event design in event-triggered feedback systems,” *Automatica*, vol. 47, no. 10, pp. 2319–2322, 2011.
- [24] N. Marchand, J. J. M. Molina, S. Durand, and F. Guerrero-Castellanos, “Lyapunov event-triggered control: a new event strategy based on the control,” in *9th IFAC Symposium on Nonlinear Control Systems (NOLCOS 2013)*, 2013.

- [25] S. Durand, J. F. G. Castellanos, N. Marchand, and W. F. G. Sanchez, “Event-based control of the inverted pendulum: Swing up and stabilization,” *Journal of Control Engineering and Applied Informatics*, vol. 15, no. 3, pp. 96–104, 2013.
- [26] D. Yue, E. Tian, and Q.-L. Han, “A delay system method for designing event-triggered controllers of networked control systems,” *Automatic Control, IEEE Transactions on*, vol. 58, no. 2, pp. 475–481, 2013.
- [27] C. Peng and T. C. Yang, “Event-triggered communication and h<sub>∞</sub> control co-design for networked control systems,” *Automatica*, vol. 49, no. 5, pp. 1326–1332, 2013.
- [28] J. Yépez, M. Velasco, P. Marti, E. Martin, and J. M. Fuertes, “One-step finite horizon boundary with varying control gain for event-driven networked control systems,” in *IECON 2011-37th Annual Conference on IEEE Industrial Electronics Society*. IEEE, 2011, pp. 2606–2611.
- [29] A. Molin and S. Hirche, “Suboptimal event-triggered control for networked control systems,” *ZAMM-Journal of Applied Mathematics and Mechanics/Zeitschrift für Angewandte Mathematik und Mechanik*, vol. 94, no. 4, pp. 277–289, 2014.
- [30] S. Hu and D. Yue, “Event-triggered control design of linear networked systems with quantizations,” *ISA transactions*, vol. 51, no. 1, pp. 153–162, 2012.

- [31] B. Demirel, V. Gupta, and M. Johansson, “On the trade-off between control performance and communication cost for event-triggered control over lossy networks,” in *Control Conference (ECC), 2013 European*. IEEE, 2013, pp. 1168–1174.
- [32] A. Molin and S. Hirche, “Optimal event-triggered control under costly observations,” in *Proceedings of the 19th international symposium on mathematical theory of networks and systems*, 2010.
- [33] A. Molin, H. Tischer, and S. Hirche, “Order reduction in optimal event-triggered control design for linear stochastic systems,” in *American Control Conference (ACC), 2011*. IEEE, 2011, pp. 2222–2227.
- [34] A. Molin and S. Hirche, “Adaptive event-triggered control over a shared network.” in *CDC*, 2012, pp. 6591–6596.
- [35] —, “On the optimality of certainty equivalence for event-triggered control systems,” *Automatic Control, IEEE Transactions on*, vol. 58, no. 2, pp. 470–474, 2013.
- [36] —, “A bi-level approach for the design of event-triggered control systems over a shared network,” *Discrete Event Dynamic Systems*, vol. 24, no. 2, pp. 153–171, 2014.
- [37] M. Lemmon, “Event-triggered feedback in control, estimation, and optimization,” in *Networked Control Systems*. Springer, 2010, pp. 293–358.



- [38] J. Lunze and D. Lehmann, “A state-feedback approach to event-based control,” *Automatica*, vol. 46, no. 1, pp. 211–215, 2010.
- [39] D. Lehmann and J. Lunze, “Event-based control with communication delays,” in *Proceedings of the 18th IFAC world congress*, 2011, pp. 982–987.
- [40] —, “Extension and experimental evaluation of an event-based state-feedback approach,” *Control Engineering Practice*, vol. 19, no. 2, pp. 101–112, 2011.
- [41] E. Kofman and J. H. Braslavsky, “Level crossing sampling in feedback stabilization under data-rate constraints,” in *Decision and Control, 2006 45th IEEE Conference on*. IEEE, 2006, pp. 4423–4428.
- [42] M. Donkers and W. Heemels, “Output-based event-triggered control with guaranteed l8-gain and improved event-triggering,” in *Decision and Control (CDC), 2010 49th IEEE Conference on*. IEEE, 2010, pp. 3246–3251.
- [43] —, “Output-based event-triggered control with guaranteed-gain and improved and decentralized event-triggering,” *Automatic Control, IEEE Transactions on*, vol. 57, no. 6, pp. 1362–1376, 2012.
- [44] L. Li and M. Lemmon, “Event-triggered output feedback control of finite horizon discrete-time multi-dimensional linear processes,” in *Decision and Control (CDC), 2010 49th IEEE Conference on*. IEEE, 2010, pp. 3221–3226.

- [45] D. Lehmann and J. Lunze, “Event-based output-feedback control,” in *Control & Automation (MED), 2011 19th Mediterranean Conference on*. IEEE, 2011, pp. 982–987.
- [46] L. Jetto and V. Orsini, “A new event-driven output-based discrete-time control for the sporadic mimo tracking problem,” *International Journal of Robust and Nonlinear Control*, vol. 24, no. 5, pp. 859–875, 2014.
- [47] H. Yu and P. J. Antsaklis, “Event-triggered output feedback control for networked control systems using passivity: Achieving  $l_2$  stability in the presence of communication delays and signal quantization,” *Automatica*, vol. 49, no. 1, pp. 30–38, 2013.
- [48] L. Li and M. Lemmon, “Weakly coupled event triggered output feedback control in wireless networked control systems,” in *Communication, Control, and Computing (Allerton), 2011 49th Annual Allerton Conference on*. IEEE, 2011, pp. 572–579.
- [49] X.-M. Zhang and Q.-L. Han, “Event-triggered dynamic output feedback control for networked control systems,” *IET Control Theory & Applications*, vol. 8, no. 4, pp. 226–234, 2014.
- [50] R. Cogill, S. Lall, and J. P. Hespanha, “A constant factor approximation algorithm for event-based sampling,” in *American Control Conference, 2007. ACC’07*. IEEE, 2007, pp. 305–311.

- [51] J. Sijs, M. Lazar, and W. Heemels, “On integration of event-based estimation and robust mpc in a feedback loop,” in *Proceedings of the 13th ACM international conference on Hybrid systems: computation and control*. ACM, 2010, pp. 31–40.
- [52] L. Li, M. Lemmon, and X. Wang, “Event-triggered state estimation in vector linear processes,” in *American Control Conference (ACC), 2010*. IEEE, 2010, pp. 2138–2143.
- [53] J. Weimer, J. Araújo, and K. H. Johansson, “Distributed event-triggered estimation in networked systems,” in *Analysis and Design of Hybrid Systems*, 2012, pp. 178–185.
- [54] J. Wu, Q.-S. Jia, K. H. Johansson, and L. Shi, “Event-based sensor data scheduling: Trade-off between communication rate and estimation quality,” *Automatic Control, IEEE Transactions on*, vol. 58, no. 4, pp. 1041–1046, 2013.
- [55] D. Shi, T. Chen, and L. Shi, “Event-based state estimation of linear dynamical systems: Communication rate analysis,” in *American Control Conference (ACC), 2014*. IEEE, 2014, pp. 4665–4670.
- [56] D. Han, Y. Mo, J. Wu, S. Weerakkody, B. Sinopoli, and L. Shi, “Stochastic event-triggered sensor schedule for remote state estimation,” *arXiv preprint arXiv:1402.0599*, 2014.

- [57] W. Heemels, M. Donkers, and A. R. Teel, “Periodic event-triggered control for linear systems,” *Automatic Control, IEEE Transactions on*, vol. 58, no. 4, pp. 847–861, 2013.
- [58] D. Antunes, W. Heemels, and P. Tabuada, “Dynamic programming formulation of periodic event-triggered control: Performance guarantees and co-design.” in *51st IEEE Conf. on Decision and Control*, 2012, pp. 7212–7217.
- [59] R. Yang, P. Shi, G.-P. Liu, and H. Gao, “Network-based feedback control for systems with mixed delays based on quantization and dropout compensation,” *Automatica*, vol. 47, no. 12, pp. 2805–2809, 2011.
- [60] M. Lemmon, “Efficiently attentive event-triggered control systems with limited bandwidth.” [Online]. Available: <http://www3.nd.edu/lemmon/projects/NSF-05-1518/Publications/efficient-attentiveness.pdf>
- [61] R. Yang, G.-P. Liu, P. Shi, C. Thomas, and M. V. Basin, “Predictive output feedback control for networked control systems,” *Industrial Electronics, IEEE Transactions on*, vol. 61, no. 1, pp. 512–520, 2014.
- [62] S. Jerg, O. Junge, and M. Post, “Global optimal feedbacks for stochastic quantized nonlinear event systems,” 2013.
- [63] L. Li, X. Wang, and M. Lemmon, “Stabilizing bit-rates in quantized event triggered control systems,” in *Proceedings of the 15th ACM international*

- conference on Hybrid Systems: Computation and Control*. ACM, 2012, pp. 245–254.
- [64] M. Mazo and P. Tabuada, “Decentralized event-triggered control over wireless sensor/actuator networks,” *Automatic Control, IEEE Transactions on*, vol. 56, no. 10, pp. 2456–2461, 2011.
- [65] E. Garcia and P. J. Antsaklis, “Decentralized model-based event-triggered control of networked systems,” in *American Control Conference (ACC), 2012*. IEEE, 2012, pp. 6485–6490.
- [66] X. Wang and M. D. Lemmon, “Event-triggered broadcasting across distributed networked control systems,” in *American Control Conference, 2008*. IEEE, 2008, pp. 3139–3144.
- [67] M. Guinaldo, D. V. Dimarogonas, K. H. Johansson, J. Sánchez, and S. Dormido, “Distributed event-based control strategies for interconnected linear systems,” *Control Theory & Applications, IET*, vol. 7, no. 6, pp. 877–886, 2013.
- [68] M. Mazo and M. Cao, “Asynchronous decentralized event-triggered control,” *Automatica*, vol. 50, no. 12, pp. 3197–3203, 2014.
- [69] X. Wang, Y. Sun, and N. Hovakimyan, “Asynchronous task execution in networked control systems using decentralized event-triggering,” *Systems & Control Letters*, vol. 61, no. 9, pp. 936–944, 2012.

- [70] X. Wang and M. D. Lemmon, “Event-triggering in distributed networked systems with data dropouts and delays,” in *Hybrid systems: Computation and control*. Springer, 2009, pp. 366–380.
- [71] —, “Event-triggering in distributed networked control systems,” *Automatic Control, IEEE Transactions on*, vol. 56, no. 3, pp. 586–601, 2011.
- [72] C. De Persis, R. Sailer, and F. Wirth, “Parsimonious event-triggered distributed control: A zeno free approach,” *Automatica*, vol. 49, no. 7, pp. 2116–2124, 2013.
- [73] M. Guinaldo, D. V. Dimarogonas, K. H. Johansson, J. Sánchez, and S. Dormido, “Distributed event-based control for interconnected linear systems,” in *Decision and Control and European Control Conference (CDC-ECC), 2011 50th IEEE Conference on*. IEEE, 2011, pp. 2553–2558.
- [74] M. Guinaldo, D. Lehmann, J. Sánchez, S. Dormido, and K. H. Johansson, “Distributed event-triggered control with network delays and packet losses.” in *CDC*, 2012, pp. 1–6.
- [75] P. Wan and M. D. Lemmon, “Distributed network utility maximization using event-triggered barrier methods,” in *Proc. European Control Conf.(ECC)*, 2009.
- [76] —, “Distributed network utility maximization using event-triggered augmented lagrangian methods,” in *American Control Conference, 2009. ACC’09*. IEEE, 2009, pp. 3298–3303.

- [77] —, “Event-triggered distributed optimization in sensor networks,” in *Information Processing in Sensor Networks, 2009. IPSN 2009. International Conference on*. IEEE, 2009, pp. 49–60.
- [78] T. Liu, M. Cao, C. De Persis, J. M. Hendrickx *et al.*, “Distributed event-triggered control for synchronization of dynamical networks with estimators?” in *IFAC Workshop on Distributed Estimation and Control in Networked Systems, Koblenz, Germany, 2013*, pp. 116–121.
- [79] X. Wang and N. Hovakimyan, “L 1 adaptive control of event-triggered networked systems,” in *American Control Conference (ACC), 2010*. IEEE, 2010, pp. 2458–2463.
- [80] X. Wang, E. Kharisov, and N. Hovakimyan, “Real-time l1 adaptive control algorithm in uncertain networked control systems,” *submitted to IEEE Transactions on Automatic Control*, 2011.
- [81] A. Sahoo, “Adaptive state feedback event-triggered control of affine nonlinear discrete time systems,” in *Proc. 7th Ann. ISC Graduate Research Symp.(ISC-GRS), Rolla, Missouri, 2013*.
- [82] A. Sahoo, H. Xu, and S. Jagannathan, “Adaptive event-triggered control of a uncertain linear discrete time system using measured input and output data,” in *American Control Conference (ACC), 2013*. IEEE, 2013, pp. 5672–5677.

- [83] E. Garcia and P. J. Antsaklis, “Model-based event-triggered control for systems with quantization and time-varying network delays,” *Automatic Control, IEEE Transactions on*, vol. 58, no. 2, pp. 422–434, 2013.
- [84] W. Heemels and M. Donkers, “Model-based periodic event-triggered control for linear systems,” *Automatica*, vol. 49, no. 3, pp. 698–711, 2013.
- [85] J. Verhaegh, T. Gommans, and W. Heemels, “Extension and evaluation of model-based periodic event-triggered control,” in *Control Conference (ECC), 2013 European*. IEEE, 2013, pp. 1138–1144.
- [86] Y. Iino, T. Hatanaka, and M. Fujita, “Event-predictive control for energy saving of wireless networked control system,” in *American Control Conference, 2009. ACC’09*. IEEE, 2009, pp. 2236–2242.
- [87] P. Varutti, B. Kern, T. Faulwasser, and R. Findeisen, “Event-based model predictive control for networked control systems,” in *Decision and Control, 2009 held jointly with the 2009 28th Chinese Control Conference. CDC/CCC 2009. Proceedings of the 48th IEEE Conference on*. IEEE, 2009, pp. 567–572.
- [88] A. Eqtami, D. V. Dimarogonas, and K. J. Kyriakopoulos, “Event-triggered control for discrete-time systems,” in *American Control Conference (ACC), 2010*. IEEE, 2010, pp. 4719–4724.



- [89] —, “Novel event-triggered strategies for model predictive controllers,” in *Decision and Control and European Control Conference (CDC-ECC), 2011 50th IEEE Conference on*. IEEE, 2011, pp. 3392–3397.
- [90] V. Veselý, D. Rosinova, and T. Quang, “Networked output feedback robust predictive controller design,” *Int. J. Innov. Comput. I*, vol. 9, no. 10, pp. 3941–3953, 2013.
- [91] H. Li and Y. Shi, “Event-triggered robust model predictive control of continuous-time nonlinear systems,” *Automatica*, vol. 50, no. 5, pp. 1507–1513, 2014.
- [92] G. A. Kiener, D. Lehmann, and K. H. Johansson, “Actuator saturation and anti-windup compensation in event-triggered control,” *Discrete event dynamic systems*, vol. 24, no. 2, pp. 173–197, 2014.
- [93] U. Tiberi, J. Araujo, and K. H. Johansson, “On event-based pi control of first-order processes,” in *IFAC Proceedings Volumes (IFAC-PapersOnline) v2, part 1*, 2012, pp. 448–453.
- [94] M. Rabi and K. H. Johansson, “Scheduling packets for event-triggered control,” in *Proceedings of 10th European Control Conference*, 2009, pp. 3779–3784.
- [95] X. Wang and M. Lemmon, “Attentively efficient controllers for event-triggered feedback systems,” in *Decision and Control and European Control*

- Conference (CDC-ECC), 2011 50th IEEE Conference on.* IEEE, 2011, pp. 4698–4703.
- [96] L. Li, B. Hu, and M. D. Lemmon, “Resilient event triggered systems with limited communication.” in *CDC*, 2012, pp. 6577–6582.
- [97] H. Bentez-Prez and A. Bentez-Prez, “Networked control systems design considering scheduling restrictions and local faults using local state estimation,” *International Journal of Innovative Computing, Information & Control*, vol. 9, no. 8, pp. 3225–3239, 2013.
- [98] X.-C. Jia, X.-B. Chi, Q.-L. Han, and N.-N. Zheng, “Event-triggered fuzzy  $\mathcal{H}_\infty$  control for a class of nonlinear networked control systems using the deviation bounds of asynchronous normalized membership functions,” *Information Sciences*, vol. 259, pp. 100–117, 2014.
- [99] D. Nešić and A. R. Teel, “Input-to-state stability of networked control systems,” *Automatica*, vol. 40, no. 12, pp. 2121–2128, 2004.
- [100] M. Mazo and P. Tabuada, “Input-to-state stability of self-triggered control systems,” in *Decision and Control, 2009 held jointly with the 2009 28th Chinese Control Conference. CDC/CCC 2009. Proceedings of the 48th IEEE Conference on.* IEEE, 2009, pp. 928–933.
- [101] M. Lemmon, T. Chantem, X. S. Hu, and M. Zyskowski, “On self-triggered full-information h-infinity controllers,” in *Hybrid Systems: computation and control.* Springer, 2007, pp. 371–384.

- [102] X. Wang and M. D. Lemmon, “Self-triggering under state-independent disturbances,” *Automatic Control, IEEE Transactions on*, vol. 55, no. 6, pp. 1494–1500, 2010.
- [103] —, “Self-triggered feedback control systems with finite-gain stability,” *Automatic Control, IEEE Transactions on*, vol. 54, no. 3, pp. 452–467, 2009.
- [104] M. Mazo, A. Anta, and P. Tabuada, “On self-triggered control for linear systems: Guarantees and complexity,” in *European Control Conf.*, 2009.
- [105] J. Araújo, H. Fawzi, M. M. Jr, P. Tabuada, and K. H. Johansson, “An improved self-triggered implementation for linear controllers.” in *3rd IFAC Workshop on Distributed Estimation and Control in Networked Syst. (Nec-Sys)*, 2012.
- [106] S. Durand, J.-F. Guerrero-Castellanos, and R. Lozano-Leal, “Self-triggered control for the stabilization of linear systems.” in *CCE*, 2012, pp. 1–6.
- [107] J. Almeida, C. Silvestre, and A. Pascoal, “Self-triggered output feedback control of linear plants,” in *American Control Conference (ACC), 2011*, June 2011, pp. 2831–2836.
- [108] —, “Observer based self-triggered control of linear plants with unknown disturbances,” in *American Control Conference (ACC), 2012*, June 2012, pp. 5688–5693.
- [109] —, “Observer based self-triggered control of an acyclic interconnection of linear plants.” in *CDC*, 2012, pp. 7553–7558.

- [110] A. Anta and P. Tabuada, “To sample or not to sample: Self-triggered control for nonlinear systems,” *Automatic Control, IEEE Transactions on*, vol. 55, no. 9, pp. 2030–2042, 2010.
- [111] —, “Exploiting isochrony in self-triggered control,” *Automatic Control, IEEE Transactions on*, vol. 57, no. 4, pp. 950–962, 2012.
- [112] U. Tiberi and K. H. Johansson, “A simple self-triggered sampler for perturbed nonlinear systems,” *Nonlinear Analysis: Hybrid Systems*, vol. 10, pp. 126–140, 2013.
- [113] D. Tolic, R. G. Sanfelice, and R. Fierro, “Self-triggering in nonlinear systems: A small gain theorem approach,” in *Control and Automation (MED), 2012 20th Mediterranean Conference on*. IEEE, 2012, pp. 941–947.
- [114] R. W. Brockett, “Minimum attention control,” in *Decision and Control, 1997., Proceedings of the 36th IEEE Conference on*, vol. 3. IEEE, 1997, pp. 2628–2632.
- [115] D. Chakraborty, *Need-based feedback: An optimization approach*, 2007, vol. 68, no. 09.
- [116] A. Anta and P. Tabuada, “On the minimum attention and anytime attention problems for nonlinear systems,” in *Decision and Control (CDC), 2010 49th IEEE Conference on*. IEEE, 2010, pp. 3234–3239.
- [117] M. Donkers, P. Tabuada, and W. Heemels, “On the minimum attention control problem for linear systems: A linear programming approach,” in

*Decision and Control and European Control Conference (CDC-ECC), 2011*  
*50th IEEE Conference on.* IEEE, 2011, pp. 4717–4722.

- [118] U. Tiberi, C.-F. Lindberg, and A. J. Isaksson, “Dead-band self-triggered pi control for processes with dead-time,” in *Advances in PID Control*, vol. 2, no. 1, 2012, pp. 442–447.
- [119] R. P. Anderson, D. Milutinovic, and D. V. Dimarogonas, “Self-triggered stabilization of continuous stochastic state-feedback controlled systems,” in *Control Conference (ECC), 2013 European.* IEEE, 2013, pp. 1151–1155.
- [120] M. Souza, G. S. Deaecto, J. C. Geromel, and J. Daafouz, “Self-triggered linear quadratic networked control,” *Optimal Control Applications and Methods*, vol. 35, no. 5, pp. 524–538, 2014.
- [121] M. F. Sångfors and H. T. Toivonen, “H<sub>8</sub> and lqg control of asynchronous sampled-data systems,” *Automatica*, vol. 33, no. 9, pp. 1663–1668, 1997.
- [122] S. K. Mazumder, K. Acharya, and M. Tahir, “Joint optimization of control performance and network resource utilization in homogeneous power networks,” *Industrial Electronics, IEEE Transactions on*, vol. 56, no. 5, pp. 1736–1745, 2009.
- [123] X. Cao, P. Cheng, J. Chen, and Y. Sun, “An online optimization approach for control and communication codesign in networked cyber-physical systems,” *Industrial Informatics, IEEE Transactions on*, vol. 9, no. 1, pp. 439–450, 2013.

- [124] Y. Niu, X. Wu, H. Yang, and H. Zhang, “Co-design of discrete linear quadratic regulator and resource scheduling for priority-driven networked control systems,” in *Computational Science and Computational Intelligence (CSCI), 2014 International Conference on*, vol. 1. IEEE, 2014, pp. 15–20.
- [125] A. Molin and S. Hirche, “A bi-level approach for the design of event-triggered control systems over a shared network,” *Discrete Event Dynamic Systems*, vol. 24, no. 2, pp. 153–171, 2014.
- [126] M. Guinaldo, D. Lehmann, J. Sanchez, S. Dormido, and K. H. Johansson, “Distributed event-triggered control for non-reliable networks,” *Journal of the Franklin Institute*, vol. 351, no. 12, pp. 5250–5273, 2014.
- [127] X. Luan, P. Shi, and C.-L. Liu, “Stabilization of networked control systems with random delays,” *Industrial Electronics, IEEE Transactions on*, vol. 58, no. 9, pp. 4323–4330, 2011.
- [128] A. Onat, T. Naskali, E. Parlakay, and O. Mutluer, “Control over imperfect networks: model-based predictive networked control systems,” *Industrial Electronics, IEEE Transactions on*, vol. 58, no. 3, pp. 905–913, 2011.
- [129] P. Park, J. Araújo, and K. H. Johansson, “Wireless networked control system co-design,” in *Networking, Sensing and Control (ICNSC), 2011 IEEE International Conference on*. IEEE, 2011, pp. 486–491.

- [130] P. Park, C. Fischione, and K. H. Johansson, “Modeling and stability analysis of hybrid multiple access in the iee 802.15. 4 protocol,” *ACM Transactions on Sensor Networks (TOSN)*, vol. 9, no. 2, p. 13, 2013.
- [131] Y. Sadi, S. Ergen, and P. Park, “Minimum energy data transmission for wireless networked control systems,” *Wireless Communications, IEEE Transactions on*, vol. 13, no. 4, pp. 2163–2175, April 2014.
- [132] M. Mazo and P. Tabuada, “On event-triggered and self-triggered control over sensor/actuator networks,” in *Decision and Control, 2008. CDC 2008. 47th IEEE Conference on*. IEEE, 2008, pp. 435–440.
- [133] A. Cervin, D. Henriksson, B. Lincoln, J. Eker, and K.-E. Årzén, “How does control timing affect performance?” *IEEE control systems magazine*, vol. 23, no. 3, pp. 16–30, 2003.
- [134] M. Souza, G. S. Deaecto, J. C. Geromel, and J. Daafouz, “Self-triggered linear quadratic networked control,” *Optimal Control Applications and Methods*, vol. 35, no. 5, pp. 524–538, 2014.
- [135] M. Souza and J. C. Geromel, “H2 self-triggered dynamic output feedback for networked control,” in *Decision and Control (CDC), 2013 IEEE 52nd Annual Conference on*. IEEE, 2013, pp. 4736–4741.
- [136] E. Henriksson, D. E. Quevedo, H. Sandberg, and K. H. Johansson, “Self-triggered model predictive control for network scheduling and control,” in *8th IFAC Symposium on Advanced Control of Chemical Processes*, 2012.

- [137] D. Seto, J. P. Lehoczky, L. Sha, and K. G. Shin, “On task schedulability in real-time control systems,” in *Real-Time Systems Symposium, 1996., 17th IEEE*. IEEE, 1996, pp. 13–21.
- [138] A. Saifullah, C. Wu, P. B. Tiwari, Y. Xu, Y. Fu, C. Lu, and Y. Chen, “Near optimal rate selection for wireless control systems,” *ACM Transactions on Embedded Computing Systems (TECS)*, vol. 13, no. 4s, pp. 128:1–128:25, 2014.
- [139] M. Grebeck, “A comparison of controllers for the quadruple tank system,” *Department of Automatic Control, Lund Institute of Technology, Lund, Sweden, Tech. Rep*, 1998.



# Vitae

- Name: Azhar Mehmood Memon
- Nationality: Pakistan
- Date of Birth: June 17, 1987
- Email: *m3mon.azhar@gmail.com*

## Education

- M.Sc.: Automation and Control Engineering,  
National University of Singapore (NUS), Singapore.
- B.E.: Electronics Engineering,  
National University of Sciences and Technology (NUST), Pakistan.

# Publications

## Published:

- **Azhar M. Memon** and Magdi S. Mahmoud, “An Evaluation of Novel Self-Triggering Method for Optimization of Communication and Control,” *IET Control Theory and Applications*, DOI: 10.1049/iet-cta.2015.0780.
- **Azhar M. Memon** and Magdi S. Mahmoud, “Two-Level design for aperiodic networked control systems,” *Signal Processing*, vol. 120, pp. 43-55, Mar., 2016.
- Magdi S. Mahmoud and **Azhar M. Memon**, “Aperiodic triggering mechanisms for networked control systems,” *Information Sciences*, vol. 296, pp. 282–306, Mar., 2015.

## Submitted:

- **Azhar M. Memon** and Magdi S. Mahmoud, “Self-Triggered Linear Quadratic Control of Multiple Systems Sharing IEEE 802.15.4 Network,” submitted to *IEEE Transactions on Cybernetics*.